30(1-2)

30(1-2)

気象庁欧文海洋報告

第30巻 第1-2号

THE OCEANOGRAPHICAL MAGAZINE

Vol. 30 Nos. 1-2

LIBRARY
SEP 7 1979
FISH & WILDLIFE SERVICE

CONTENTS

SHUTO, K.: The flow conditions of the Kuroshio in the vicinity of Cape Shionomisaki 1

KONAGA, S., K. NISHIYAMA, A. WATANABE and H. SAITO: Short term fluctuations of current velocities near Oshima Island, Izu District, Japan 15

ISOZAKI, I.: On the seiches of Habu-harbor 31

SANO, A., N. SATOH and N. KUBO: Floating particulate petroleum residues, tar balls, in the western Pacific 47

SUZUOKI, T. and K. SHIRAKAWA: Visual observation on the floating pollutants in open ocean 55

SHIGEHARA, K., K. KIMURA, J. OHOYAMA and N. KUBO: Fluorescing materials in marine environment and petroleum pollution. I. Analytical method and preliminary report of the result 61

Note

Oceanography Division, Japan Meteorological Agency: The normals of monthly mean sea surface temperature in the western North Pacific 75

Published by the Japan Meteorological Agency

March, 1979

投稿規定

1　資　格

原則として，気象庁職員に限る。ただし，気象庁職員との連名の場合は，この限りでない。

2　論文及び報文（以下「論文等」という。）の内容

未発表の原稿で，海洋（物理・化学・生物・地質など）及び海上気象（波浪・海氷・海気相互関係など）に関する論文並びに気象庁における海洋・海上気象業務の活動，そのために開発された測器及び方法に関する報文など。

3　書き方

(1) 用語は，欧文（原則として英文）とする。

(2) 論文等には，英文（300語以内）及び和文（800字以内）の要約を付ける。要約は，方法・測器・実験・観測の結果・仮定・理論などの中味が読みとれるように留意し，なるべく指定の長さで簡潔に書く。

(3) 論文等の始めには，題名・著者名及所属機関名を明記する。和文の要約にも同様のことを明記する。

(4) 原稿は，厚手の用紙にダブルスペースでタイプする。

(5) 図は，白紙又は青方眼紙に墨入れし，図及び図中の文字の大きさは，印刷の際の縮小率を考えて作成する。特に重要な図は，投稿者が大きさを指定する（印刷の都合上，希望どおりにならないこともある。）

(6) 図（写真を含む。）及び表には，必ず説明を付ける。図の説明文は，別紙にタイプする。折り込みの図及び表は，なるべく避ける。図及び表のそう入箇所を本文の欄外に記入する。

(7) 数式は，2行取りに書き，数式の文字及び記号をはっきりと説明する。

(8) 論文等の中に文献を引用する場合は，「ALLEN (1927)」又は「(ALLEN, 1927)」のように書く。

(9) 引用文献は，最後にまとめて付け，著者名のアルファベット順に並べる。書き方は次のようにする。

ALLEN, W.E. (1927): Surface catches of marine diatoms and dinoflagellates made by U.S.A. Pioneer in Alaskan waters in 1923. *Bull. Scripps Inst. Occanogr., Tech. Ser.* 1(4), 39–48.

BUDYKO, M. I. (1956): *The heat balance of the earth's surface.* Hydrometeorogical Publishing House, Leningrad, pp. 254.

VERONINS, G. and H. STOMMEL (1956): The action of a variable wind stress on a stratified ocean. *J. Mar. Res.*, 15(1), 43–75.

4　提出方法

投稿票を付け，本稿のほかにコピー（図及び表を含む。）2部を添える。

5　締切り

毎年気象庁公報により公示する。

6　送付先

気象庁海洋気象部海洋課

（原則として，書留便で送付する。）

7　その他

論文等1編につき別刷り50部を著者に無料で送付する。

Oceanographical Magazine

編集委員長　Editor

半　沢　　正　男，M. HANZAWA

編集委員　Editorial Board

飯　田　　隼　人，H. IIDA*
磯　崎　　一　郎，I. ISOZAKI**
窪　田　　　将，M. KUBOTA***
松　崎　　正　夫，M. MATSUZAKI*
杉　村　　行　勇，Y. SUGIMURA**
石　黒　　昭　次，S. ISHIGURO*
小　長　　俊　二，S. KONAGA**
長　坂　　昂　一，K. NAGASAKA*
重　原　　好　次，K. SHIGEHARA*

* 気　象　庁　JAPAN METEOROLOGICAL AGENCY

** 気象研究所　METEOROLOGICAL RESEARCH INSTITUTE

*** 気象大学校　METEOROLOGICAL COLLEGE

The Oceanographical Magazine
Vol. 30, Nos. 1-2, pp. 1 to 14, March 1979

The flow conditions of the Kuroshio in the vicinity of Cape Shionomisaki

Kenzo SHUTO
Maizuru Marine Observatory

(Received November 9, 1977; revised June 15, 1978; accepted January 11, 1979)

Abstract: It has been revealed that the surface current velocity and the water temperature of the Kuroshio change discontinuously between the offing of the Kii Channel west of Cape Shionomisaki and the offing of the sea of Kumanonada or Enshunada east of the cape. The BT and GEK observations of the Kuroshio were made in the sea adjacent to the cape in May, 1975 in order to investigate the discontinuity of velocity. The effects of the bottom topography on the Kuroshio was recognized as follows:—

(1) When the Kuroshio flows across the ridge of the continental slope in the vicinity of Cape Shionomisaki, the surface current velocity of the Kuroshio is maximized at the top of it.

(2) The current meanders slightly as it passes over the ridge and the form of the meander resembles the path of the flow calculated from the theory of slope current affected by bottom topography.

(3) In a vertical section along the current axis, isotherms are disturbed to rise abruptly just behind the top of the ridge.

(4) In another vertical sections along the current, isotherms are undulatory over a trough.

1. Introduction

Hydrographic surveys for the monitoring the Kuroshio have been intensively made in the south of Honshu by various institutes. Kobe Marine Observatory has also been engaged in active surveys on board the R/V Shumpu Maru.

Among several hydrographic sections across the Kuroshio, the meridional sections at 135°15′E west of Cape Shionomisaki and at 137°30′E south of Lake Hamanako are named G and U line, respectively. Those sections are aimed not only to obtain typical cross-sections of the Kuroshio but also to monitor the cold water region in the sea of Enshunada. The hydrographic observations along these sections are made four times a year namely, once in each season.

KONAGA and SHUTO (1969) pointed out that the geostrophic velocity and volume transport of the Kuroshio are generally larger at the U line than that at the G line, and this feature is also remarkable with respect to the surface current velocity measured

with GEK. KONAGA *et al.* (1966 a, b) and KONAGA (1971) discussed the discontinuity of the surface current velocity which are based on the observations made during from 1966 to 1970 on board the R/V Shumpu Maru. During the period, the discontinuity of the surface current velocity and water temperature of the Kuroshio in the offing of Cape Shionomisaki was strongest in May, 1967.

This remarkable discontinuity seems to be mainly due to the formation of cold water belt (10–15°C at the 200 m depth) along the northern edge of the Kuroshio to the east of the cape. Although the general feature of the oceanographic conditions has been revealed by the ordinary hydrographic casts as mentioned above, the distance between the G line and the U line, more than 100 miles, is too broad to clarify the mechanism of the discontinuity. In May, 1975, BT and GEK observations were carried out in this area more closely than that of the ordinary survey intending to study the detailed mechanism of the velocity discontinuity of the Kuroshio.

2. Observations

In the present survey much efforts have been made to observe the Kuroshio as rapid in time and as close in space as possible off Cape Shionomisaki. The BT and GEK were used to determine the thermal structure in the subsurface layers and the sea surface current. The stations are occupied as shown in Fig. 1. The observation was started from St. 75–115 in the morning of May 20th, 1975. Initially it was planned to take six meridional sections across the Kuroshio from upstream to downstream. However, we gave up to take the section along 135°30′E owing to strong wind and the meridional survey was started along 135°50′E. 135°40′E was taken finally in this observation.

The five sections were completed during about 27 hours.

SHOJI and NITANI (1966) stated that the east component of the Kuroshio stream off the sea of Kumanonada was 3 knots on average and its diurnal variation was predominant with the amplitude of 0.5 knot in October of 1964 and semi-diurnal fluctuations excelled in October of 1965.

From October to November in 1967, a co-operative survey of the Kuroshio was carried out by the five research vessels of JMA off the sea of Kumanonada.

MASUZAWA (1968) and KONAGA (1970) pointed out the presence of short-term fluctuation in the Kuroshio such as the variation of the velocity nearly with the period of inertia motion of which amplitude is between 1.0 knot and 1.5 knots and the variation having the period of four or five days with the amplitude of about 0.6 knot.

Thus, the diurnal fluctuation of the Kuroshio in that region is considerable large, but in the following study the author was forced to treat the results of the observation as quasi-stationary in one day or so, because the observation was made only once.

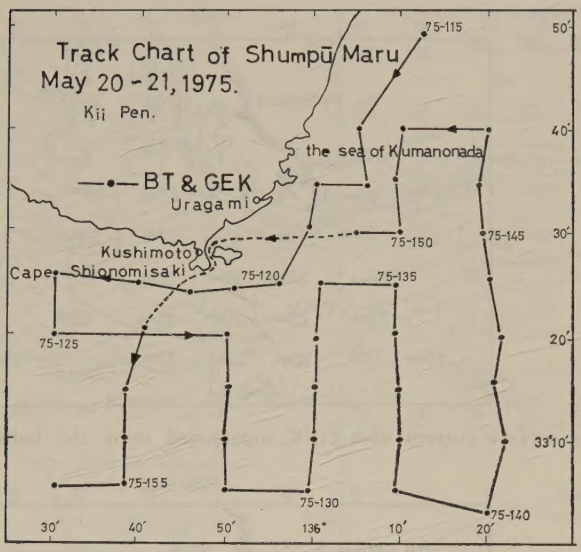

Fig. 1. Track chart of the R/V Shumpu Maru, May 20-21, 1975.

Fig. 2 shows the surface current with GEK on a bathymetric chart. The Kuroshio flowed nearly eastward spreading over at least between 33°05′N and 33°25′N in the offing of Cape Shionomisaki. The northern edge and the current axis of the Kuroshio were positioned along 33°25′N and 33°20′N respectively and they were across the ridge of the continental slope around the Kii Peninsula off Cape Shionomisaki. The velocity of the Kuroshio increased and its direction was deflected slightly southward near the top of the ridge. The current was accelerated when it flowed above a trough near 33°05′N–33°10′N, 136°00′E and when it passed through the neighbourhood of 136°20′E.

The Kuroshio seems to meander slightly northward between 135°30′E and 135°40′E and northward at the trough between 136°00′E and 136°10′E. The surface current flowed southward in almost all region of the sea of Kumanonada converging to the Kuroshio. The distribution of current speed is summarized in Fig. 3, in which the current axis and the acceleration of the velocity at the top of the ridge and near 33°20′N, 136°20′E are well revealed. Fig. 4 indicates the horizontal divergence of the sea surface current measured with GEK. The acceleration of current speed at the top of the ridge of the continental slope in the offing of Cape Shionomisaki brings about divergence above the rise of the ridge and convergence above the fall of it. The area of divergence due to acceleration along the current axis spreads out

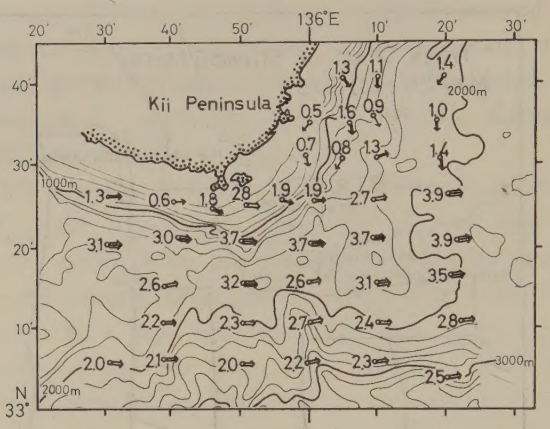

Fig. 2. Sea surface current with GEK superposed upon the bathymetric chart.

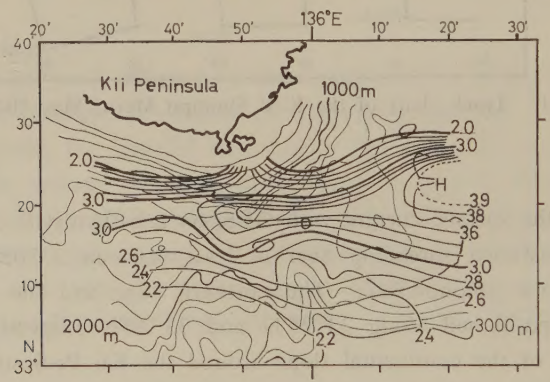

Fig. 3. Distribution of the speed of the sea surface current of the Kuroshio (knot).

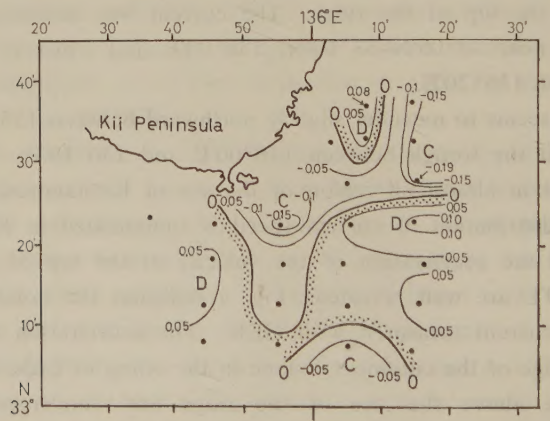

Fig. 4. Horizontal divergence of the sea surface current (hour^{-1}).

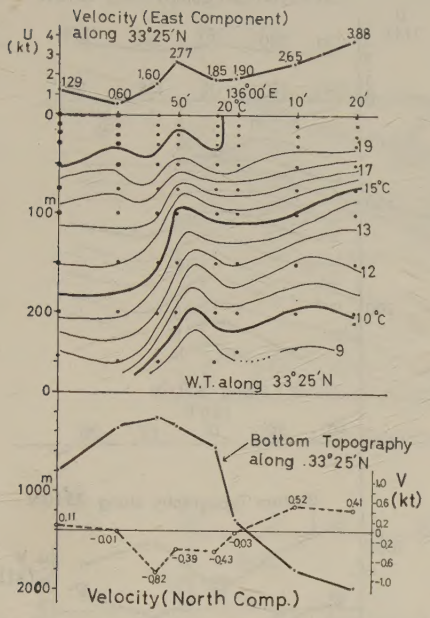

Fig. 5. Distribution of water temperature, velocity and depth along 33°25′N.

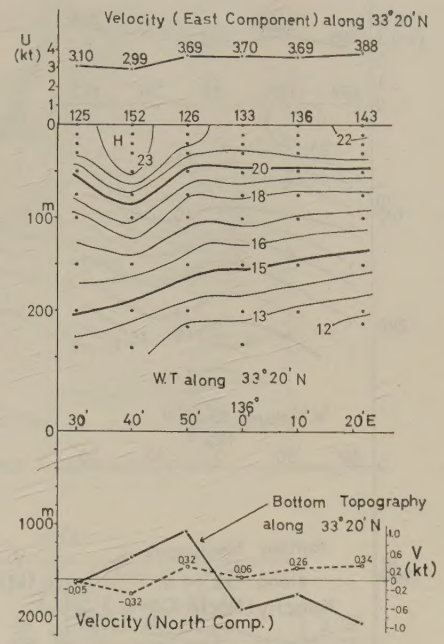

Fig. 6. Distribution of water temperature, velocity and depth along 33°20′N.

around 136°20′E and convergence is also observed in the southeast of the sea valley near 136°E.

There is a rise of isotherms near 135°50′E just behind the top of the ridge in the section along 33°25′N parallel to the stream (Fig. 5). This disturbance does not seem to be similar to the one caused by a lee wave over a mountain because in a lee wave disturbances occur in such a way as the streamlines or the boundary surface of two layers discend along the down slope of a mountain.

It is also not to be similar to the case of a hydraulic jump which takes place in an open channel with an obstacle set on the bottom of it. For example, if we choose 0.55 m/s as the mean velocity v and 1,200 m as the mean depth H for the flow between St. 75–124 and St. 75–125, we obtain 35 m as the critical depth H_c and 19 m/s as the critical velocity v_c. H_c and v_c are given by

$$H_c=\left[\frac{1}{g}\left(\frac{Q}{B}\right)^2\right]^{1/3} \quad \text{and} \quad v_c=\sqrt{gH_c}$$

where B is the width of an open channel and Q is the volume transport of the flow and $Q=vHB$. In fact, the depth is about 200 m and the velocity is about 0.9 m/s

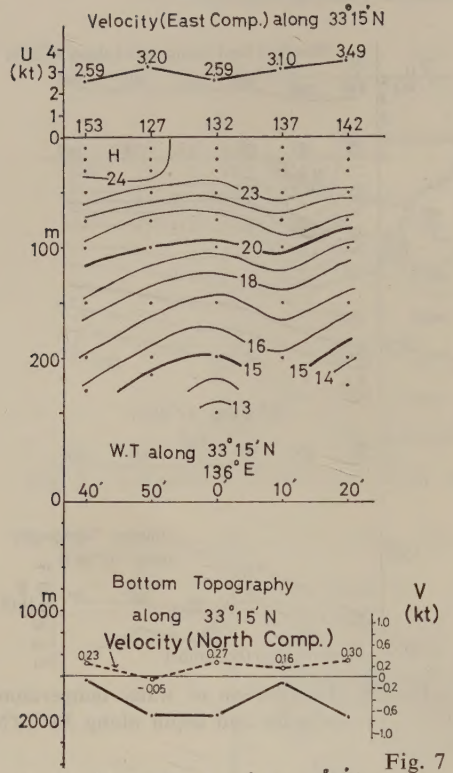

Fig. 7

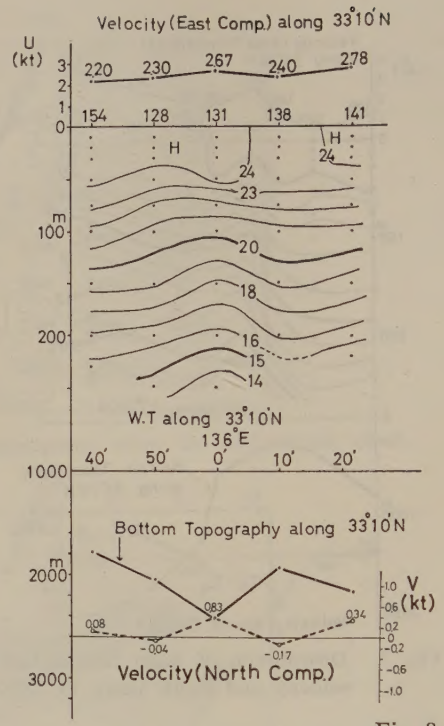

Fig. 8

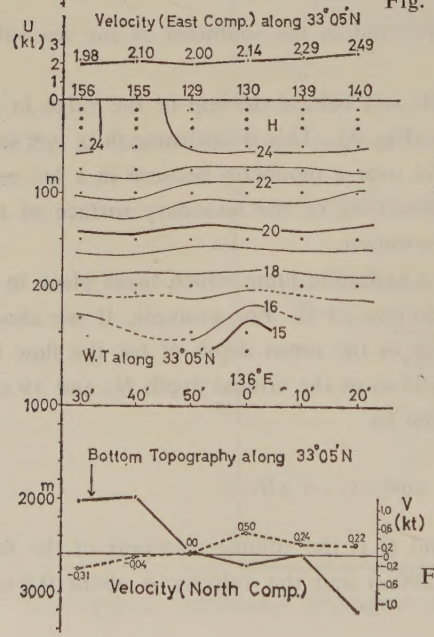

Fig. 9

Fig. 7. Distribution of water temperature, velocity and depth along 33°15′N.

Fig. 8. Distribution of water temperature, velocity and depth along 33°10′N.

Fig. 9. Distribution of water temperature, velocity and depth along 33°05′N.

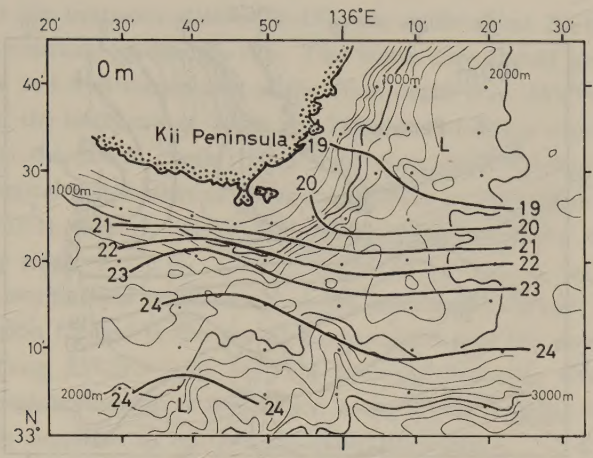

Fig. 10. Sea surface temperature (°C).

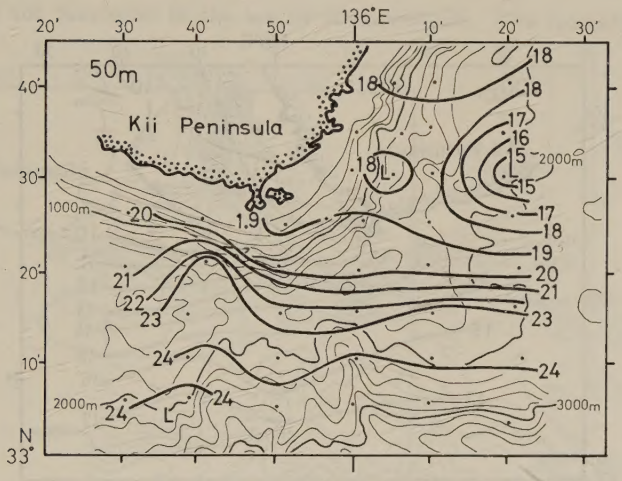

Fig. 11. Water temperature at the 50 m depth (°C).

in the vicinity of the top of the ridge. Thus, the velocity is far smaller and the depth is far larger than corresponding values of the assumed hydraulic jump.

Though details of the dynamical mechanism of the bottom topography effects in connection with the deformation of isotherms as shown in Fig. 5 is unknown, it is possible that the upwelling due to horizontal divergence occurs there and the rise of the bottom topography also contributes to the upwelling. So, this rise of isotherms brings about the disconnection of isotherms near Cape Shionomisaki in the horizontal

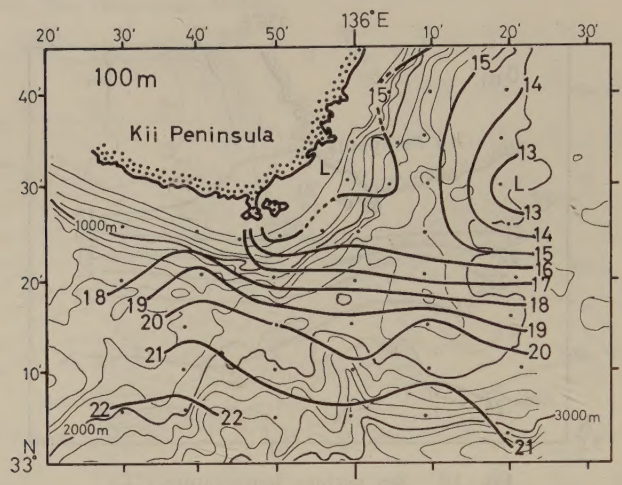

Fig. 12. Water temperature at the 100 m depth (°C).

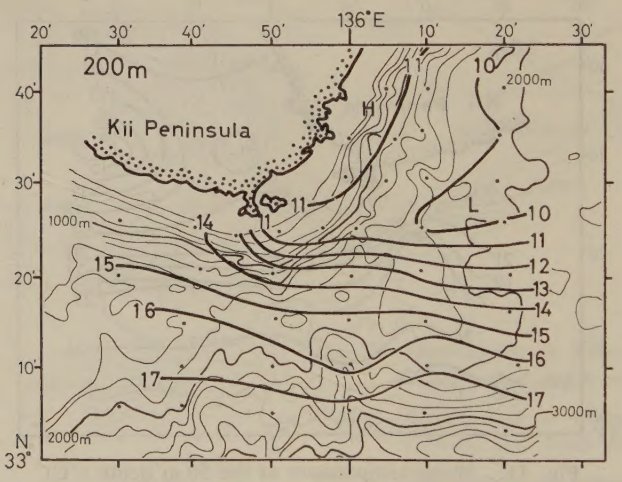

Fig. 13. Water temperature at the 200 m depth (°C).

distribution of water temperature in the layer between the 50 m and the 200 m depth (Fig. 11, 12, 13).

A warm core exists around 135°40′E in the section along 33°20′N parallel to the axis of the Kuroshio (Fig. 6).

The distribution of isotherms in this section is well related to the horizontal divergence or convergence of the sea surface current. Here, it should be noted that

the observation at the upstream station 75–152 was made about 20 hours later than the one at the downstream station 75–126. This warm core should generate the anti-cyclonic curvature and it is remarkable at the 50 m depth (Fig. 11).

The meander of the isotherms of 20°C and 21°C at the 100 m depth (Fig. 12) and 16°C and 17°C at the 200 m depth (Fig. 13) between 136°00′E and 136°10′E corresponds to the vertical distribution of water temperature in the section along 33°10′N (Fig. 8) and 33°15′N (Fig. 7) where the isotherms ascend above the trough and descend above the ridge.

It corresponds to the local acceleration of the geostrophic current velocity due to the cold water region formed in the sea of Kumanonada that the depth of isotherms in the sections along 33°20′N and 33°25′N becomes shallower downstream. The isotherms are almost horizontal in the section along 33°05′N (Fig. 9) and the geostrophic velocity is supposed to be uniform along the current.

Fig. 14 shows the distribution of the surface salinity. As inferred by SHUTO *et al.* (1976), the low salinity water from the coast of Kii Peninsula is found along the northern edge of the Kuroshio in the sea of Kumanonada. The iso-haline of 34.4‰

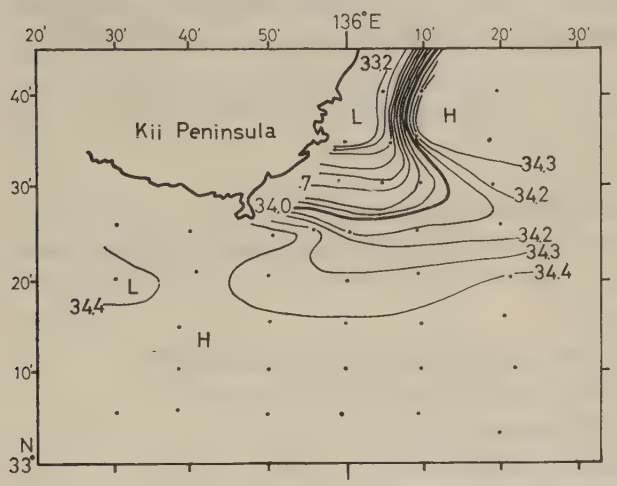

Fig. 14. Sea surface salinity (‰). ↑

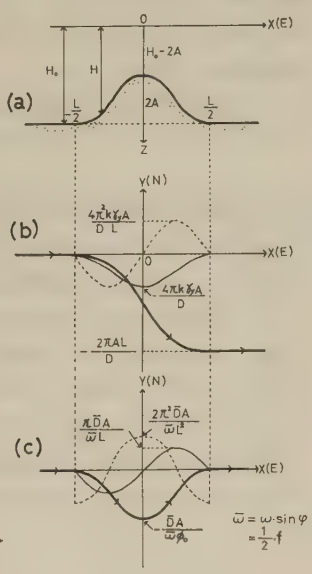

Fig. 15

Fig. 15. (a) A model of bottom topography of a ridge.→
(b) The path of a flow (thick solid line) and its north component of velocity obtained from the Ekman's theory (thin solid line).
(c) The path of a flow (thick solid line) and its north component of vertical mean velocity obtained from the Stockman's theory (thin solid line). Broken lines indicate $\partial v/\partial x$. ($v=G_y$ or ϕ_y)

was separated near 135°40′E in the main current of the Kuroshio.

3. Theoretical consideration on the flow pattern at a ridge

On the case that the uniform eastward current flows over a ridge, the author performed some calculation based on the theories of Ekman and Stockman (SHULEIKIN, 1968). The topography of the ridge is given as the equations (1) and (2), and is shown in Fig. 15(a). The path of the flow and the north component of its velocity across the ridge obtained from the calculation are also shown in Fig. 15(b) and Fig. 15(c).

Let us take the coordinates x and y eastward and northward respectively.

$$H=H_0 \text{ (constant)} \qquad \left(|x| \geqq \frac{L}{2}\right) \tag{1}$$

$$H=H_0-A\left(1+\cos\frac{2\pi}{L}x\right) \quad \left(|x| \leqq \frac{L}{2}\right) \tag{2}$$

Notations are summarized in appendix. In both theories the relation existing among curl of velocity, vertical friction, the effects of bottom topography, the wind stress and the rotation of the earth on its axis are taken on the steady state. The density of water is assumed as homogeneous in Ekman's theory but nonhomogeneous in Stockman's theory.

In the theory of Stockman, not only the vertical friction but also lateral friction are taken into considerations.

(A) An example of calculation by Ekman's theory

Here a slope current $\vec{G}(G_x, G_y)$ with the sea surface inclination $\vec{\gamma}(\gamma_x, \gamma_y)$ is treated. Under following conditions:

(i) Wind stress is constant,

(ii) The depth H is independent upon the coordinate $y(\partial H/\partial y=0)$,

(iii) The y component of the sea surface inclination is constant $(\partial\zeta/\partial y \equiv -\gamma_y = -G_x/k = \text{constant})$,

(iv) The Colioli's parameter f is assumed to be constant,

the vorticity equation of the current becomes

$$\frac{d^2\zeta}{dx^2}=\frac{2\pi}{h}\cdot\gamma_y\cdot\frac{dH}{dx}\,. \tag{3}$$

Integrating this equation with respect to x and using the relation

$$\frac{\partial\zeta}{\partial x}\equiv-\gamma_x=\frac{G_y}{k} \quad \text{and} \quad \frac{dy}{dx}=G_y/G_x=-\gamma_x/\gamma_y\,,$$

we get the following equation concerning the path of the current.

$$\frac{dy}{dx}=\frac{2\pi}{h}(H-H_0) \tag{4}$$

From equations (2) and (4), the path of the current, y and the north component of the velocity, G_y for the region $|x|\leqq L/2$ are given as follows.

$$y=-\frac{2\pi}{h}A\left(x+\frac{L}{2}+\frac{L}{2\pi}\sin\frac{2\pi}{L}x\right)+y_0 \tag{5}$$

$$G_y=-k\gamma_x=-\frac{2\pi}{h}k\gamma_y A\left(1+\cos\frac{2\pi}{L}x\right) \tag{6}$$

These are shown in Fig. 15(b).

(B) An example of calculation by Stockman's theory

Under the following conditions:

(i) Wind stress is constant,

(ii) $|\nabla_L{}^2\bar{\rho}|\ll|\nabla_L{}^2(H\bar{D})|$,

(iii) $\bar{D}$ does not change along the coordinate x,

(iv) $\bar{D}$ is a linear function of y,

(v) The depth H does not change along the coordinate y,

the vertically integrated vorticity equation becomes

$$\bar{D}\frac{d^2H}{dx^2}=f\left(\frac{\partial\phi_y}{\partial x}-\frac{\partial\phi_x}{\partial y}\right). \tag{7}$$

Supposing $\phi_x=\phi_0$ (constant) and using the relation $dy/dx=\phi_y/\phi_x$, we get the path of the current, y and the north component of volume transport ϕ_y (proportional to the north component of vertical mean velocity) from the equations (2) and (7) as follows.

$$y=-\frac{\bar{D}A}{f\phi_0}\left(\cos\frac{2\pi}{L}x+1\right)+y_0 \tag{8}$$

$$\phi_y=\frac{\bar{D}A}{f}\cdot\frac{2\pi}{L}\sin\frac{2\pi}{L}x \tag{9}$$

These are shown in Fig. 15(c).

4. Remarks and conclusion

In the region of the Kuroshio, water temperature makes a greater contribution to the change of water density than salinity does. It is generally known that the current axis of the Kuroshio corresponds to the isotherms of from 15°C to 17°C at the 200 m depth off the southern coast of Japan. Comparing the surface current in Fig. 2 with the horizontal distribution of water temperature at each depth, it seems that the path

of the flow over the ridge of the continental slope off Cape Shionomisaki corresponds to the isotherms of from 21°C to 23°C at the sea surface (Fig. 10) and the path above the trough near 136°E corresponds to the isotherms of 16°C or 17°C at the 200 m depth (Fig. 13).

It is found that the flow pattern over the ridge off Cape Shionomisaki resembles the path calculated from the Ekman's theory rather than from the Stockman's theory.

If the results of observations of the Kuroshio obtained during 27 hours is regarded as quasi-stationary within these variability, the following conclusion will be made about the effect of the bottom topography on the Kuroshio.

(1) The discontinuity and the disturbances of the velocity of the Kuroshio and of the water temperature distribution occur in the vicinity of Cape Shionomisaki and they are related closely to the bottom topography.

(2) The velocity is maximized at the top of the ridge when the Kuroshio flows in the offing of Cape Shionomisaki.

(3) The disturbance is found that isotherms in the vertical section along the current axis rise abruptly just behind the top of the ridge. This disturbance may be caused by the upwelling on the rise of the ridge where horizontal divergence of the surface current takes place and the upwelling may be forced also by the rise of the bottom.

(4) The acceleration of velocity, the meander of the path and the vertical undulation of the isotherms are found above a trough of about 2,400 m depth, and it is inferred that the bottom topography affects the current there.

(5) The distribution of isotherms which seems to correspond to the path of the Kuroshio, and the distribution of the cross-stream component (north component) of the surface current velocity over the ridge near Cape Shionomisaki resemble those of Ekman's theory rather than those of the Stockman's theory.

Acknowledgements

The author wishes to express his hearty thanks for the cooperation of collaborators in the observation, and to the officers and crew on board the R/V Shumpu Maru.

Dr. Masamori MIYAZAKI and Mr. Takeo TSUCHIDA are also acknowledged for their advice and careful reading of this manuscript.

(Appendex)

H : depth, $H=H(x)$

$2A$: height of the ridge

L : width of the ridge

$\vec{G}(G_x, G_y)$: velocity of a gradient current, $G_x=k\gamma_y$, $G_y=-k\gamma_x$

$\vec{\gamma}(\gamma_x,\gamma_y)$: vector of the sea surface inclination

ζ : elevation of the sea surface

h : frictional depth, $h=\pi\sqrt{\frac{\mu}{\rho\omega\sin\varphi}}$ (μ is the coefficient of eddy viscosity.)

$\bar{\rho}$: vertical mean density of sea water, $\bar{\rho}=\frac{1}{H}\int_0^H \rho\, dz$

$\bar{D}$: vertical mean dynamic depth, $\bar{D}=\frac{1}{H}\int_0^H D\, dz$, $D=\int_0^p \frac{1}{\rho}\, dp$

$\vec{\phi}(\phi_x,\phi_y)$: vector of the volume transport of a flow, $\phi_x=\int_0^H u\, dz$, $\phi_y=\int_0^H v\, dz$

f : Corilis' parameter, $f=2\omega\sin\varphi$

y_0 : an arbitrary constant

References

KONAGA, S. *et al.* (1967a): On the relation between Kuroshio strong currents and the water temperature of 200 m depth (in Japanese), Umi To Sora, **42** (3-4), 1-5.

KONAGA, S. *et al.* (1967b): On the relation between Kuroshio strong currents and the water temperature of 200 m depth (II) (in Japanese), Umi To Sora, **43** (2), 10-15.

KONAGA, S. and K. SHUTO (1969): On the relation between strong geostrophic currents and the water temperature of 200 m depth (in Japanese), Umi To Sora, **44** (4), 29-32.

KONAGA, S. (1970): On the short period fluctuation of Kuroshio (in Japanese), Bulletin of Kobe Marine Observatory, **183**, 83-95.

KONAGA, S. (1971): On the relation between Kuroshio strong currents and the water temperature of 200 m depth (III) (in Japanese), Umi To Sora, **46** (3-4), 11-19.

MASUZAWA, J. (1968): Cruise report on multi-ship study of short-term fluctuations of the Kuroshio in October to November, 1967, Oceanogr. Mag., **20** (1), 91-96.

MASUZAWA, J. (1969): Data on the characteristics of the zone of the Kuroshio strong current (in Japanese), J. Oceanogr. Soc. of Jap., **25** (5), 37-38.

SHOJI, D. and H. NITANI (1969): On the variability of the velocity of the Kuroshio—I, J. Oceanogr. Soc. of Jap., **22** (5), 10-14.

SHULEIKIN, V. V. (1968): Physics of the Sea, 84-92, 108-114 (in Russian), Publishing House of Science, Moscow, pp. 1083.

SHUTO, K,. K. OHNISHI and H. MINAMI (1976): Thermal microstructures and distribution of surface water temperature, salinity and current velocity in the Kuroshio main current off Kumanonada (in Japanese), Bulletin of Kobe Marine Observatory, **192**, 24-41.

潮岬付近における黒潮主流の流動状況について

周 東 健 三

(舞鶴海洋気象台)

従来，各層観測や追跡観測により，黒潮主流の流速及び水温分布において潮岬の西側の紀伊水道沖と東側の熊野灘ないし遠州灘沖との間に不連続があることが知られていた。

その不連続の潮岬付近における局所的な構造を調べるために，1975年5月潮岬近傍で BT 及び GEK を用いて黒潮主流の観測を行なった。その結果，次の点において黒潮主流に対する海底地形の影響が認められた。

（1） 黒潮主流が潮岬近傍の大陸棚斜面を越えるとき，斜面の頂上で流速が極大になっている。

（2） 主流が上記の斜面を通過するとき小さな蛇行をしており，その蛇行の形は Ekman 理論にもとづいて計算した流線に似ている。これは，その付近では鉛直摩擦が水平摩擦よりも卓越していることを示しているように思われる。

（3） 流軸に沿った鉛直断面内で，上記の斜面の頂上を通過した直後，等温線が急上昇し，攪乱を受けている。

（4） 主流が沖合の海底谷上を流れるときも，等温線が鉛直面内で波状を呈している。

The Oceanographical Magazine
Vol. 30, Nos. 1-2, pp. 15 to 29, March 1979

Short term fluctuations of current velocities near Oshima Island, Izu District, Japan

Shunji KONAGA, Katsunobu NISHIYAMA and Akira WATANABE
(*Meteorological Research Institute*)
Hitoshi SAITO
(*Yokosuka Electrical Communication Laboratory*)
(Received July 8, 1978; accepted January 11, 1979)

Abstract: A current meter measurement at the shelf edge on the south-west of Oshima Island with suspended current meter from one of the moornig chains of the Telecommunication Relay Float (hereafter designated only the Float), Yokosuka Electrical Communication Laboratory, N.T.T.P.C., was carried out from 1 July to 26 August 1975. Together with the sea surface temperature from the ship, coastal observation stations and the Float and with coastal tidal records, these current records are analysed to study a short term fluctuation of the Kuroshio.

Tidal amplitudes of the current was varied not only with the moon age, but with the variation of the intensity of the mean current speed. Lower frequency fluctuations had considerably large amplitude and might correspond to varying the Kuroshio flow path, and were coherent with the mean sea level difference between Minami Izu and Kozushima and with the fluctuation of the surface water temperature near the Float. Higher frequency fluctuations also exist, probably caused by the higher harmonics of tides, direct atmospheric forcing and some topographic influences at the shelf edge.

1. Introduction

As is well known, the Kuroshio current fluctuates by the period of tidal, inertial and several to ten and several days, which have been observed by the surface current with GEK and subsurface thermal structure (Konaga, 1970; Shoji, 1972). But continuously observed subsurface current data are rarely found in the region, although current measurements have recently been occupied frequently in the open or deep sea area where being no intense current.

On the other hand, there have been many observations of currents in the Straits of Florida on moored systems. Especially, 1970's intensive observations yield the fruitful results relevant to the fluctuations of the Florida current. There were prominent tidal (baroclinic semidiurnal and barotropic diurnal oscillations), inertial and sub-inertial lower frequencies (two days to two weeks). The lower frequency oscillations are generated by the direct atmospheric forcing, shelf waves excited

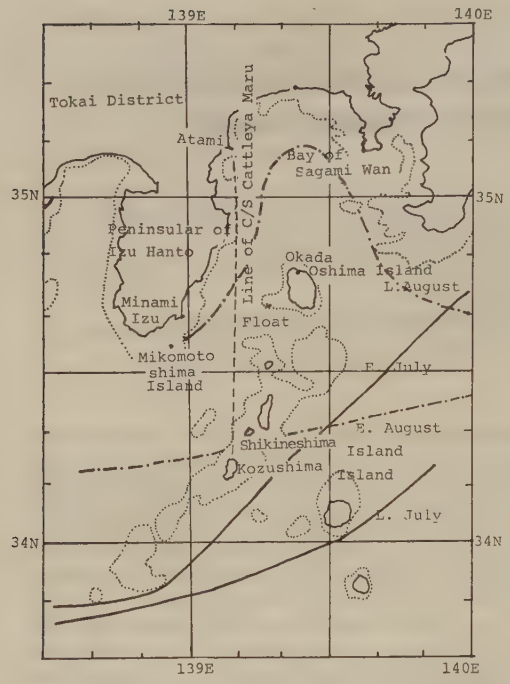

Fig. 1. Geographical map near the observation station; dotted lines indicate 200 m bathymetric contours, dashed lines, course of Cattleya Maru, and flow paths of the Kuroshio branch (13°C isotherm in 200 m layer) in each period.

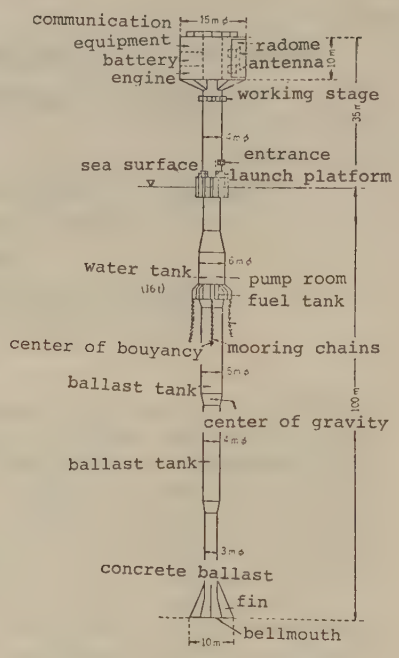

Fig. 2. Schematic description of the Telecommunication Relay Float.

by the moving weather systems and others (Webster 1968; Kielman *et al.* 1974; Niiler 1968; Düing *et al.* 1977; Lee 1977 and so on).

In this paper we will describe current meter records measured with suspended current meter from the Float on the south west of Oshima Island during 57 consecutive days from 1 July to 26 August 1975, consisting of the prominent tidal and sub-inertial fluctuations.

Observation station will be seen in figure 1, together with the flow path of the Kuroshio Branch (13°C isotherm in 200 m layer), and the course line of the commercial ship of Cattleya Maru, Tokai Ship Line, K.K. Dotted line shows 200 m isobath.

2. Measurements

The Float has been set at the shelf edge (180 m deep) to the southwest of Oshima

Island (34°40′48.0″N, 139°18′55.3″E) with four mooring chains by the Yokosuka Electrical Communication Laboratory, N.T.T.P.C., in order to test various effects of the oceanic and atmospheric phenomena to the electrical communication by the use of such a Float. As shown in figure 2, the Float is 135 m long and about 6 m in diameter, and submerged in water lower 100 m to stabilize the vertical situation. Current measurements were made to confirm how affect the currents on the inclination, excursion and skewing motion of the Float. A current meter, MTCM-V2 manufactured by Tsurumi Seiki Co. Ltd., was suspended from one of the mooring chains at the depth of 50 m (about 130 m above the sea float). A measured data were transmitted to Yokosuka Electrical Communication Laboratory and recorded in analog form once a minute. As the suspended cable from the chain was so short and magnitudes of the excursion of the Float is so small (about 180 m in horizontal and a few meters in vertical in maximum) that an error induced by these motions was negligibly small, **i.e.,** maximum speed of the horizontal excursion was only about 0.5 cm s^{-1}.

Current records which read out once an hour during 57 consecutive days from 1 July to 26 August 1975 are now used to make an analysis of the fluctuation of the currents and the oceanographic condition. Decomposing to N-S and E-W components the time series of the currents are depicted in figure 3. At the first glance, the semi-diurnal fluctuation excels throughout the period and lower and higher frequencies are superposed on it. Amplitude of semi-diurnal oscillation seems to suffer greatly day by day variation, depending on moon age, that is to say, in new moon it has considerably large amplitude but in full moon it has rather small and between them (during young and waning moon), it has small amplitude. A smallness of the amplitude in full moon is partly due to a the retardation of the eastward current (in late July) and partly due to a large disturbance excited by the severe storm (passage of Typhoon 7506, 21–23 August). The former implies, in our speculation, that the event is probably due to the internal tide, which is generated in or near the thermocline whose depth and intensity are varied accompanying with a change of the flow path, which also changes the mean flow speed, though we could not confirm that with the observation of the subsurface thermal structure. The latter is unable to explain explicitly, however, a rather intense wind drift current, reached at the current meter depth, might possibly be excited by the severe storm, or a superposition of some shelf waves generated by the moving Typhoon near the shelf edge affect the current meter records.

3. Oceanographical conditions adjacent sea of Oshima Island

During July to August in 1975, the Kuroshio has happened to meander greatly offing of Tokai District, Japan. Our observation station suffered some influences of

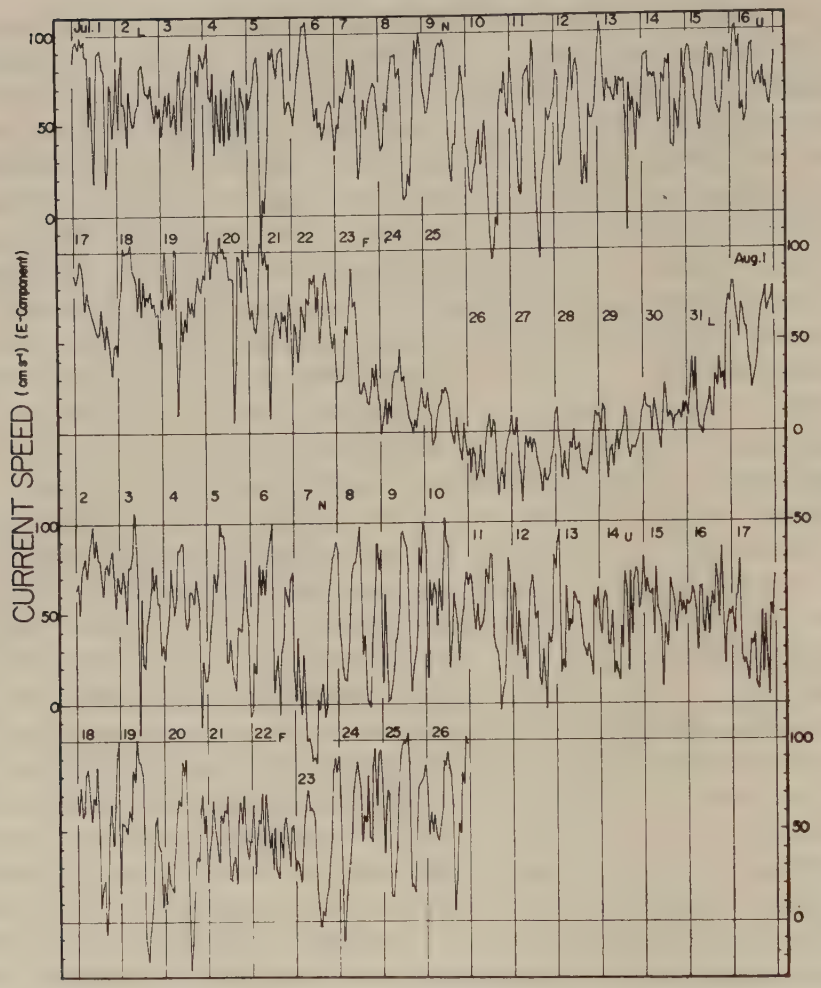

Fig. 3(a)

the varying flow path. Figure 4 shows the flow path of the Kuroshio (indicated by 15°C isotherm in 200 m layer), which shows that the dislocation of the flow path is rather small near Izu District, but it located at farthest offshore in late July. In figure 1, 13°C isotherm in 200 m layer shows more clearly the dislocation of the Kuroshio and/or Kuroshio Branch near Oshima, although the behavior of the Kuroshio branch could not completely be indicated by the isotherm in 200 m layer, because of the shallowness of the sea in the region. But we could appreciate the crude trend which

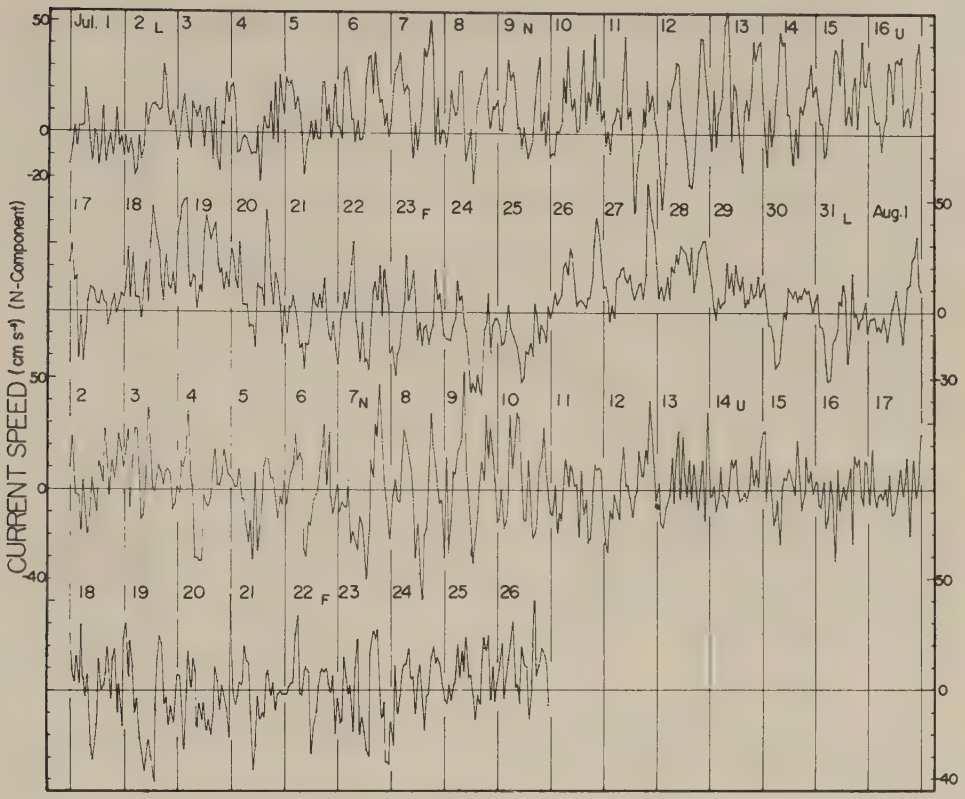

Fig. 3(b)

Fig. 3. Time series of the current record, (a) N-S component and (b) E-W component.

implied the Kuroshio farthest offshore in late July and intrusion into the bay of Sagami Wan in late August.

Sea surface temperature at Mikomoto-shima Is., on the Float and on board Cattleya Maru, Tokai Line K.K., who runs between Atami and Kozu-shima Is., passing through the West Passage of Oshima Straits, are depicted in figure 5. Due to the warm summer climate, a surface manifestation of the change in the oceanographic condition is rather weak, however, the temperature at the station just west of the Float on the course line of Cattleya Maru, shows marked lowering in late July, which is thought to be in connection with going away of the Kuroshio stream axis.

Daily means of the current speed and mean sea levels at Oshima (Okada) and Kozu-shima Is. are shown in figure 6. The shapes of the time series of the E-W component of the currents is very much similar to that of the mean sea level at

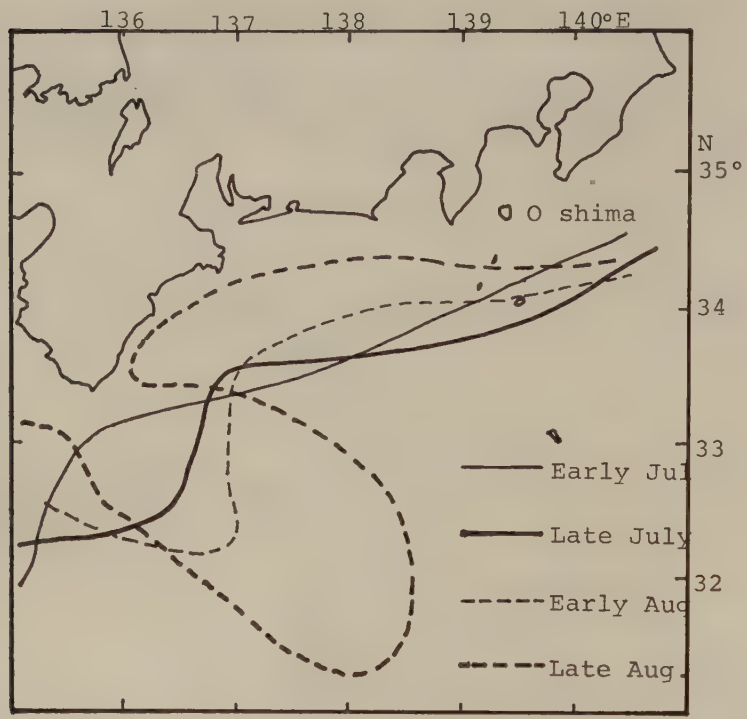

Fig. 4. Flow paths of Kuroshio in each period from early July to late August (15°C isotherms in 200 m layer).

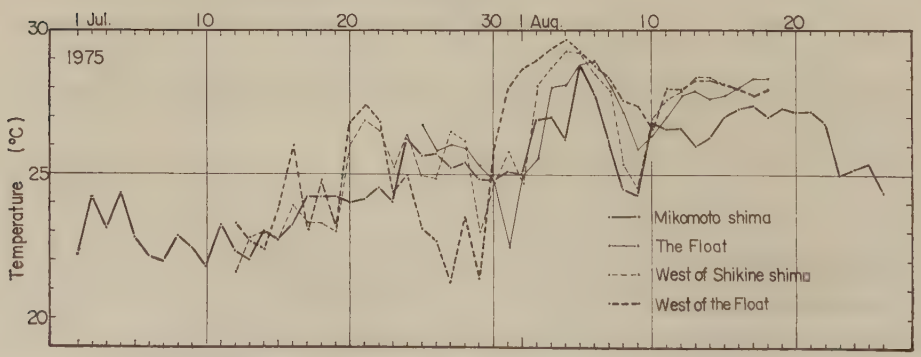

Fig. 5. Time series of surface water temperature at Mikomoto-shima (real thick line), the Float (real thin line), and on the course of Cattleya Maru; to the west of Shikine-shima (dashed thin line) and to the west of the Float (dashed thick line).

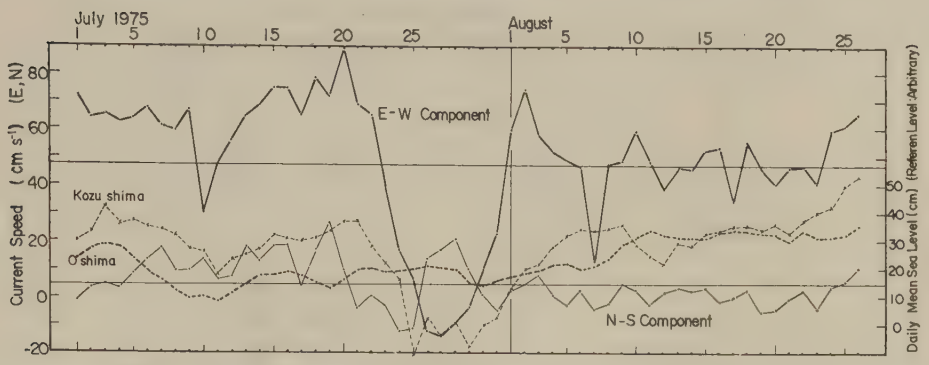

Fig. 6. Daily mean current speed and daily mean sea level at Oshima and Kozu-shima.

Kozu-shima Is., in the first inspection. Several to fortnightly periods seem to be predominant.

Coastal jet, so called Daikyucho, which sometimes occur in the bay of Sagami Wan, was generated in August, probably due to the transient process of the change of the Kuroshio flow path (personal communication from Mr. Y. Matsuyama, Tokyo University of Fishery) which is suggested by the behavior of 13°C isotherm intruded into the bay of Sagami Wan in the period (late August) in figure 1, though our current meter records are insensitive to the event.

4. Estimation of spectral densities

Overall data are devided into two component, N-S and E-W, and estimated the spectral density in each component (not shown). Declination of the curve is slightly steeper in E-W than in N-S component, the former is about $-5/3$, and latter about -1, probably due to the topographic constrain. Spectral density is much more concentrated in semi-diurnal period in E-W than in N-S (a factor of about 20), while for diurnal period, only factor of 2. Inertial and semi-inertial frequencies (about 21 and 42 hours period) are also significant in E-W component.

In figure 7 we depicted the rotary component of the spectra, (Gonella 1972; Mooers 1973), which show the prominent peak at semi-diurnal period. Diurnal, inertial and semi-inertial frequencies have secondary peaks, as stated above in E-W component, at about three days period, when we would anticipated to be some spectral peaks from early study (Konaga 1970), there is a spectral trough and then continuously increase towards lower frequency. At the semi-diurnal period, nearly equal values in anti-clockwise and clockwise components, indicating that the current ellipse is almost uni-direction and slightly anti-clockwise rotation, while at the diurnal period, having much larger value in anti-clockwise than in clockwise, which suggests that

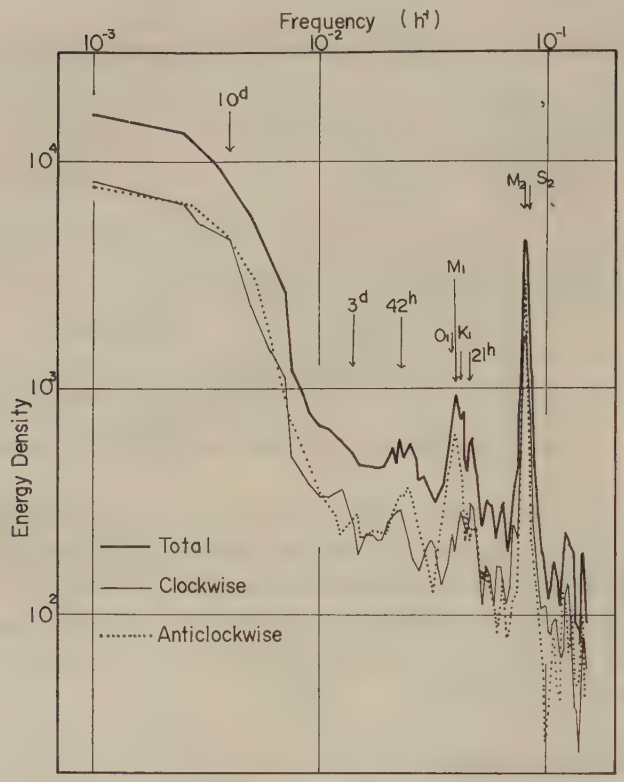

Fig. 7. Rotary component of the spectrum of the current.

the diurnal variation shows almost circularly rotated in anti-clockwise sense. In this sense inertial oscillation is slightly clockwise and semi-inertial's is anti-clockwise, respectively. Moreover lower frequencies are rotating almost linear sense, *i.e.*, the change of the flow path was followed by the E-W component of the current.

To see more clearly the behavior of the lower frequency, we make a spectral estimation with daily means. Figure 8 shows it together with that of the difference of the mean sea level between Kozu-shima and Minami-Izu, and spectral coherence between currents and the difference of the mean sea level. A spectral peak appears at about 20 days, and drops steeply towards higher frequency and slowly decreases towards lower frequency for both spectra. Spectral coherence between them shows very much coherent in the lower frequency portion.

On the other hand, in the higher frequency, some spectral peaks exist where we could consider the higher harmonics of the tide or other locally generated waves, such as internal Poincare wave, by external forcing and topographic influence. In

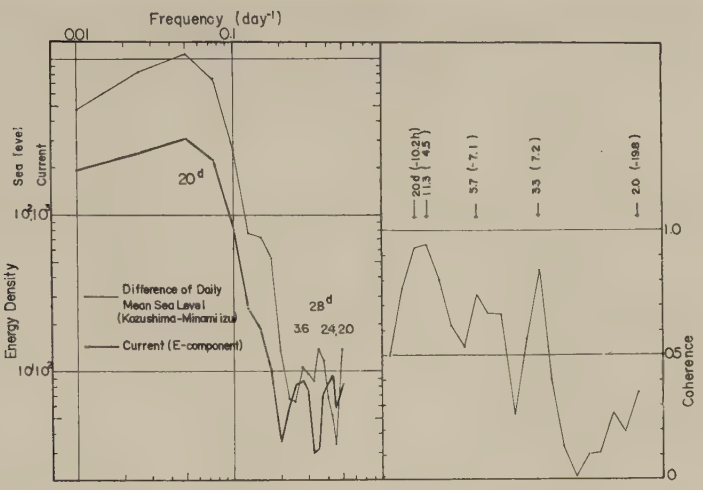

Fig. 8. Left; spectral density of the east component of the current speed (thick line) and difference of daily mean sea level between Kozu-shima and Minami Izu (thin line). Right; spectral coherence of the current and mean sea level difference. Inset numbers are periods (phase) at the spectral peaks.

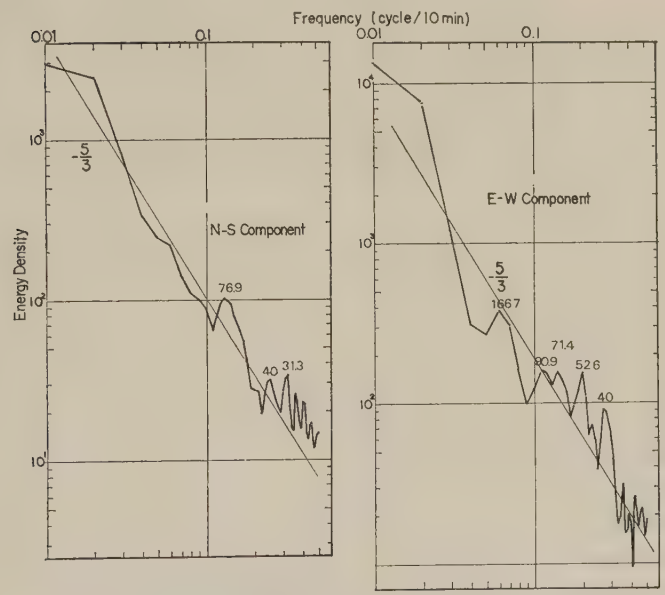

Fig. 9. Spectral density of the current, including a period of severe storm.

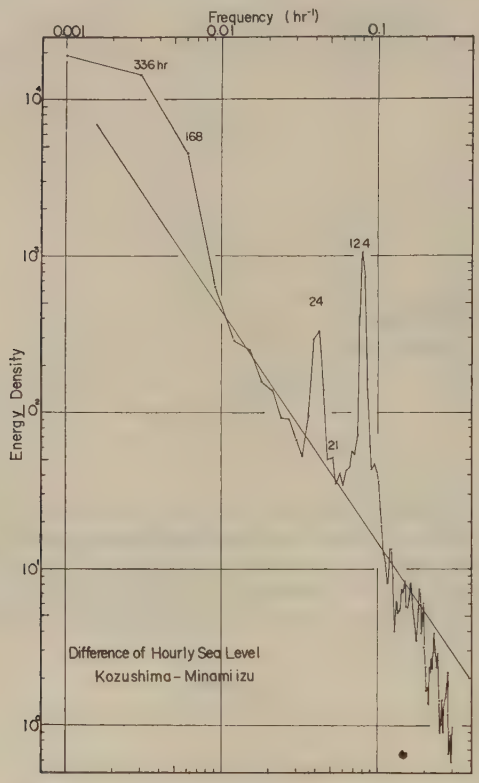

Fig. 10. Spectral density of difference of the mean sea level between Kozu-shima and Minami Izu.

order to see the effect of an external force, spectral estimation is made with every 10 minutes data during from 18 to 26 August, including the period of the passage of Typhoon 7506, which affects marked effect on the sea in the region. Figure 9 shows the behavior of the spectra. A declination of the spectral continuum are inclined along about $-5/3$ for both components and small peaks exist at several ten to two hundred minutes. We could not determine whether those peaks are only noise or edge waves generated by the severe storm.

Energy density spectrum of the difference of the mean sea level between Kozu-shima and Minami-Izu (hourly data) is depicted in figure 10. It shows of course conspicuous peaks in tidal periods and small peaks at inertial and none at semi-inertial's. The declination of the curve is slightly steeper than that of the current, *i.e.* -2. Although we could not interpret well of the unagreement between the spectra of the current and

the sea level, it is probable that it ascribed partly to the worse resolution of the current meter in high frequency and lower speeds. Furthermore, it implies that the semi-inertial oscillation may not be a gravity wave.

5. Harmonic analysis

As we could be seen in earlier section, energy density was concentrated in tidal, inertial and sub-inertial lower frequencies. We divided all of the records into two parts (every 29 days and 29 July is included in both segments) to make harmonic analysis. Then we have amplitudes of currents of five major tidal constituents (O_1, K_1, M_2, S_2 and Mf), together with the inertial oscillation, and with the tidal constituents of Port of Okada and the current in the Straits of Florida observed by Niiler (1969) and Kiilman et al. (1974), as shown in table 1. (Amplitudes of all harmonics in our observation are depicted in figure 11.). Phases of the current fluctuation are defined as zero 0000 JST in the first day of each period and should not be compared with each other. Considerably large amplitude of Mf constituent is resulted by the fluctuation of the Kuroshio during the generation and development of the cold water region offing of Tokai District, Japan in the first period, *i.e.*, in late July, while in the second period, seven days period has large amplitude, which might be considered one of the characteristic frequencies of the fluctuation of the Kuroshio, as shown in early studies of the Kuroshio (*e.g.* Konaga 1970).

In comparing amplitudes of the current for both periods and tidal constituents at Okada, we recognize that it is very similar relation between them which suggest

Table 1. Major constituents of tidal harmonics of the current and inertial component of our data and from the observation on the Florida current, and of Okada's sea level

Period	1–29 July				29 July–26 Aug.				Okada		Straits of Florida 1969 1974	
Component	N		E		N		E				N	
Tidal constituent	[A]	[B]	[A]	[B]	[A]	[B]	[A]	[B]	[A]	[B]	[A]	[B]
O_1	2.3	195	1.3	15	4.4	189	5.2	293	17.6	162.8	5.5	5.8
K_1	2.1	316	6.2	79	4.2	316	4.5	51	22.9	180.5	5.7	5.0
M_2	10.5	337	13.0	59	9.1	295	14.4	36	35.1	149.1	3.4	4.0
S_1	4.1	241	4.4	325	3.9	198	10.4	301	16.7	175.8	2.5	1.2
Mf	4.7	18	27.2	96	2.6	24	3.1	180				
I	2.4	200	3.4	130	1.6	351	5.1	110				

[A]=Amplitude (cm s^{-1}), [B]=Phase degree

Phases in our data are defined zero at 0000JST of initial day in each period. I; inertial oscillation.

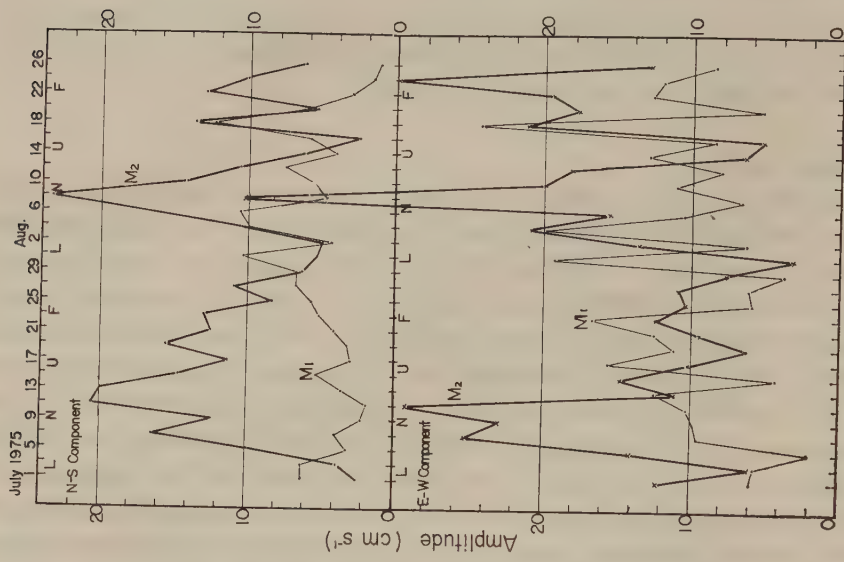

Fig. 12. Amplitudes of M_1 and M_2 constituents of the current speed; upper, N-S and lower, E-W component.

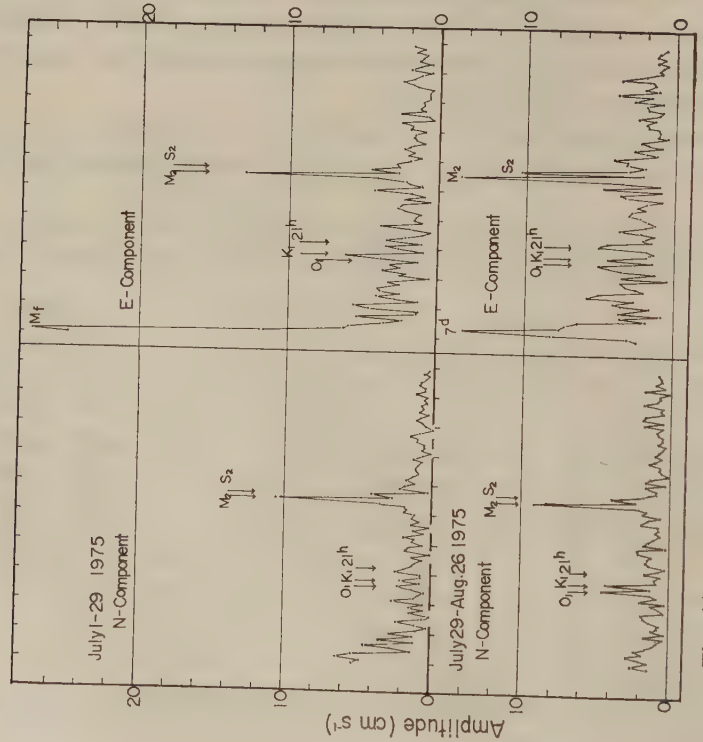

Fig. 11. Amplitudes of all harmonics in both period.

that fluctuations of the current with tidal periods are directly generated by ordinary tide itself, whether barotropic or baroclinic mode. In comparing amplitudes of our observation with in Florida current, semi-diurnal amplitude of ours is larger than in Florida's by the factor of 3 in accord with ordinary tide.

Apparent amplitudes of each constituent, especially semi-diurnal period, vary with day by day, following the moon age as shown in figure 12. It is reasonable to have large amplitude in spring tide and small in neap tide. Furthermore, it seems like to reduce the amplitude during the period in weak mean current speed, as suggested in section 3. It implies that a nonlinear interaction exists between the mean current and a tidal current other than the topographic generation of an internal tide or that if the tidal fluctuation of the current consists of a internal mode, the depth of the thermocline may change with the fluctuation of the Kuroshio flow path, and consequently may affect the amplitude of the tidal current.

It is rather surprising to have an almost same amplitude in inertial oscillations as in diurnal tide. As an inertial oscillation is rather randomly generated by an atmospheric forcing, we should suspect that the harmonic analysis yields a little amplitude. More surprising is semi-inertial oscillation (42 hours) has a significant amplitude, which is anticipated by investigating the fluctuation of the Gulf Stream by Newton (1965).

6. Concluding remarks

Unfortunately, simultaneous observations of temperature and multi-layered current measurements were not taken in this period, so that the vertical profile of the event, *i.e.* whether the vertical mode is of barotropic or baroclinic, are not known. However an information of the current measurement near bottom under the Float in this period, whatever it is false data due to the inclination of the mooring systems by the intense current, was accepted from Mr. Morimitsu (Yokosuka Electrical Communication Laboratory), who shows more intense mean current and similar amplitudes and in phases in the tidal constituents in comparing with our data. We may now suppose that it is only a topographic effect for intensification of the mean current over the bottom topography and events may be barotropic mode, but the retardation of the tidal current with mean flow makes our speculation confusing.

Otherwise, as our observation station located near the shelf edge, various modes trapped in the shelf or the island should be generated by the atmospheric forcing. These waves may have miscellaneous periods from about several hours to several ten days, as shown in the studies on the Florida current (Niiler 1968; Kielmann 1977). Unfortunately, we could not examine the effect from our single current meter records.

We could not detect, however, three to four days period, which is assured to be

prominent period in the Kuroshio in early study (Konaga 1970).

A topographically adjusted buoyancy frequency, $N \times \sin a$, where N is Brunt-Väisälä frequency and a is the inclination of the bottom, is estimated about 200 minutes, minimum frequency for the edge wave, might be limited in the actually observed period (Rhines 1970).

We could conclude from above results that (1) the tidal constituent of the current is rather similar to that of the sea level at Okada, (2) the amplitude of the semi-diurnal period varies not only with moon age but also with the varying mean current speed, (3) in the inertial and semi-inertial frequencies, there are considerably large energy, (4) declinations of the spectral density curves are slightly different in components of the current and in the sea level difference, implying worse resolution of the current meter for higher frequency and lower speed and a difference of a topographic constrain for each component and (5) low frequency variation of the current is coherent to the variation of the oceanographic condition and the mean sea level difference between Kozu-shima and Minami-Izu.

Acknowledgements

We are greatly indebted to Dr. Matsuura and Dr. Morimitsu, Yokosuka Electrical Communication Laboratory, for the data acquisition and useful advise relevant to the motion of the Float.

We also express our hearty thanks to Dr. Nan'niti, Meteorological Research Institute, for his encouragement to accomplish the manuscript.

References

Düing W., C. N. K. Mooers and T. N. Lee (1977): Low frequency variability in the Florida Current and relation to atmospheric forcing from 1972 to 1974. Jour. Mar. Res. **35**, 129-161.

Gonella J., (1972): A rotary component method for analysing meteorological and oceanographic vector time series. Deep-sea Res. **19**, 833-846.

Kielmann J. and W. Düing (1974): Tidal and subinertial fluctuations in the Florida current. Jour. Phys. Oceanogr., **4**, 227-236.

Konaga S. (1970): On the short period fluctuation of Kuroshio. Mem. Kobe Mar. Obs. **183**, 83-95. In Japanese with English abstract.

Lee T. N. and D. A. Mayer (1977): Low frequency current variability and spin-off eddies along the shelf off southeast Florida. Jour. Mar. Res. **35**, 193-220.

Mooers C. N. K. (1973): A technique for the cross spectrum analysis of pairs of complex-valued time series with emphasis of properties of polarized components and rotational invariants. Deep-sea Res. **20**, 1129-1141.

Newton C. W. (1965): Semi-inertial velocity variations along the Gulf Stream axis. Deep-sea Res. **12**, 893-897.

NIILER P. P. (1968): On the internal tidal motions in the Florida straits. Deep-sea Res., **15**, 113-123.
SHOJI D. (1972): Time variation of the Kuroshio south of Japan, in Kuroshio. University of Tokyo Press, pp. 217-233.
RHINES P. (1970): Edge- bottom- and Rossby waves in a rotary stratified fluid. Geophys. Fluid Dyn. **1**, 273-302.
WEBSTER F. (1968): Observations of inertial period motion in the deep sea. Rev. Geophys. **6**, 473-490.

伊豆大島南西沖の電々公社海上中継所で測定した流速の短期変動について

小長俊二・西山勝暢・渡辺　明
（気象研究所）

斉藤　仁
（横須賀電気通信研究所）

伊豆大島南西の陸棚縁辺近くの水深 180 mのところに電々公社，横須賀電気通信研究所の電気通信海洋中継所が設置されている。この実験塔は海洋や気象のさまざまな要素がこの中継所の動揺にどのような影響を与えるかを研究するために，さまざまな要素の測定が行なわれているが，その一つに海面下 50 mで中継所をケイ留した鎖の一つにとりつけて行なった流速測定がある。1975 年 7 月 1 日～8 月 26 日まで，57 日間の有効な測流データが得られたのでこれを解析した。

半日周潮が卓越しているがその振幅は月令だけでなく，平均流の強さや気象力の影響を受けて変動しているように見える。Mf 成分が大きく見えるのは，冷水塊発生に伴なう黒潮流軸の変動と関係がある。後半には 7 日成分が卓越している。

慣性振動やその 1/2 の振動数を持つ振動にもスペクトルピークが見られる。

測定された流れの変動と，神津島と南伊豆の潮位差は非常によく似た変動をしている。

大島西水道の水温変動は，流速の低周波の運動とよく一致している。

数時間より短い周期の変動にもスペクトルピークは見られる。潮汐の高調波か，沿岸に捉えられた固有の波かはよくわからない。

The Oceanographical Magazine
Vol. 30, Nos. 1-2, pp. 31 to 46, March 1979

On the seiches of Habu-harbor

Ichiro Isozaki
Meteorological Research Institute
(Received September 18, 1978; accepted January 11, 1979)

Abstract: In the report, seiches observed in Habu-harbor on Sept. 17, 1976 and Oct. 8, 1977 are explained. These may be caused by swells from Typhoon No. 7619 and Typhoon No. 7714 respectively. The seiches have a predominant period about 10.5 minutes which is not consistent with the one estimated by Merian's formula. So, we examined some characteristics of the bay water oscillations of Habu-harbor by means of a numerical model. The results show that the harbor have proper periods of 10.5 minutes, 2.4 minutes and 1.4 minutes which correspond to the uni-, bi-, and tri-nodal oscillations of the bay respectively. It is confirmed from the theoretical considerations that the seiches of Habu-harbor can be explained by the coupled oscillation of the systems of the harbor part and the canal part.

1. Introduction

During the observations of the long period ocean waves performed in the falls of 1976 and 1977, notable seiches were recorded in Habu-harbor on Sept. 17, 1976 and Oct. 8, 1977. Meteorological conditions around Oshima Island were rather gentle on those days except for the invasion of remarkable swells from southeast. These swells were generated in the gale area of the typhoons No. 7619 and No. 7714 respectively, both of which moved northerly about 800 km far east off Oshima Island, and the seiches might be caused by these swells.

Dominant period of these seiches was 10.5 minutes. It is known generally that the proper periods of bay water oscillations are obtained approximately by applying Merian's formula to a rectangular basin of constant depth by which the bay is approximated. Habu-harbor is approximated by a rectangular bay with the length of 720 m, the width 200 m, and the depth 6.4 m. According to Merian's formula, the proper period of the bay is about 6 minutes which does not agree with the observed period 10.5 minutes. However, it is convinced that a proper period of the bay water oscillations of Habu-harbor is about 10.5 minutes because the mareograms of Habu-harbor have frequently tidal secondary oscillations of about 10 minutes-period.

In this report, some characteristics of the oscillations of Habu-harbor are clarified by means of numerical experiments, and the cause of inconsistency of the observed period with the one estimated by Merian's formula are discussed.

2. Observations

Habu-harbor is a small basin at the southern end of Oshima Island and is connected to the ocean through a mouth opened southeast ward. Geographical location of the harbor is shown in Fig. 1. Fig. 2 shows the configuration of the harbor. The harbor is constructed by a circular harbor part formed by sinking of a volcanic crater and a canal part through which the harbor part is connected with the ocean. The harbor part has a diameter about 270 m, maximum water depth of 17 m and mean water depth of 12 m. The canal part opens toward the ocean with fan shape having the length about 450 m, the mean water depth 3 m and the narrowest width 100 m.

Used long period wave gage is a water pressure type, and the straingage-pressure sensor set up near St. 5 in Fig. 2 is connected to the recorder on land through a cable. The observations were performed in the falls of 1976 and 1977, and notable seiches were recorded from 8^h to 18^h of Sept. 17, 1976 and from 21^h of Oct. 8 to 3^h of Oct. 9, 1977. The highest total amplitudes of them were 84 cm and 53 cm respectively. Fig. 3 shows representative parts of these seiche records. We can see in this figure that the sea level variations are rather complicated but a dominant period of them is about 10 minutes.

Fig. 4 shows the power spectra of sea level variations associated with these seiches. Where the sampling time intervals of sea level records are 1 minute and 0.5 minutes

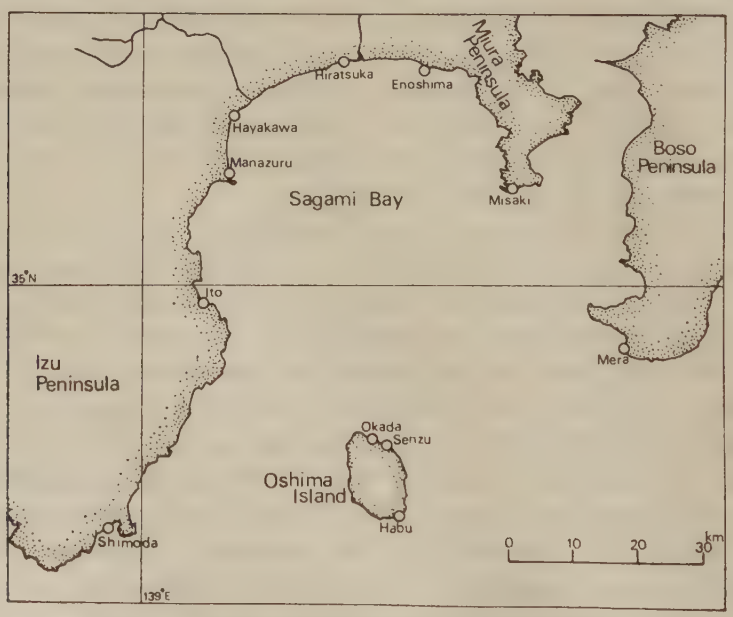

Fig. 1. Geographical location of Habu-harbor.

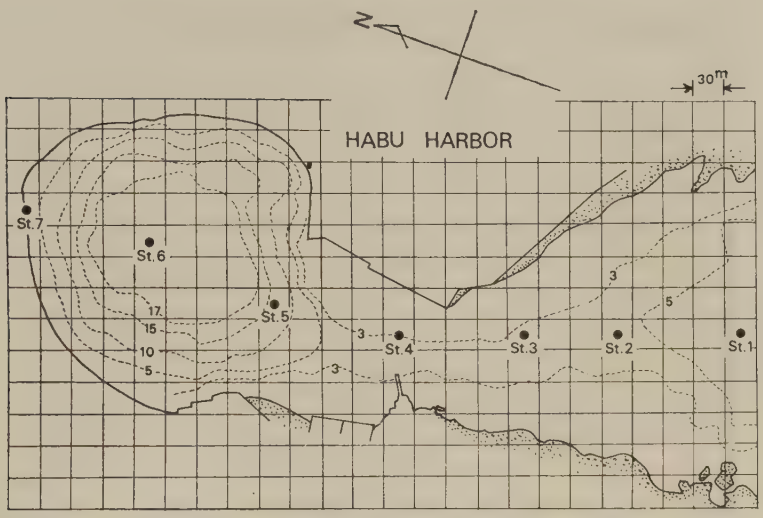

Fig. 2. Configuration of Habu-harbor.

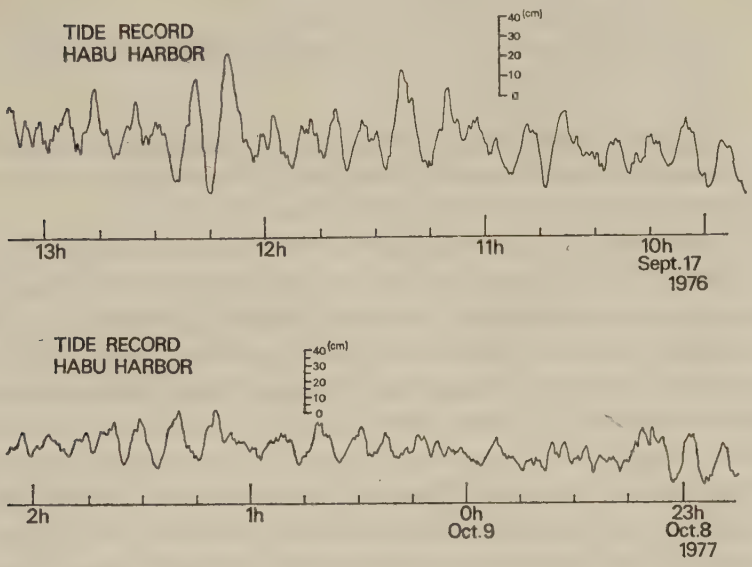

Fig. 3. Records of seiches.

in cases of 1976 and 1977 respectively. The lag number adopted in the spectral analysis is 100. High frequency band of the spectra is omitted in Fig. 4 because of low energy level in this band. Remarkable primary peak is seen in both spectra at about 0.1 cpm (10 minutes-period) which corresponds to the seiche's dominant fre-

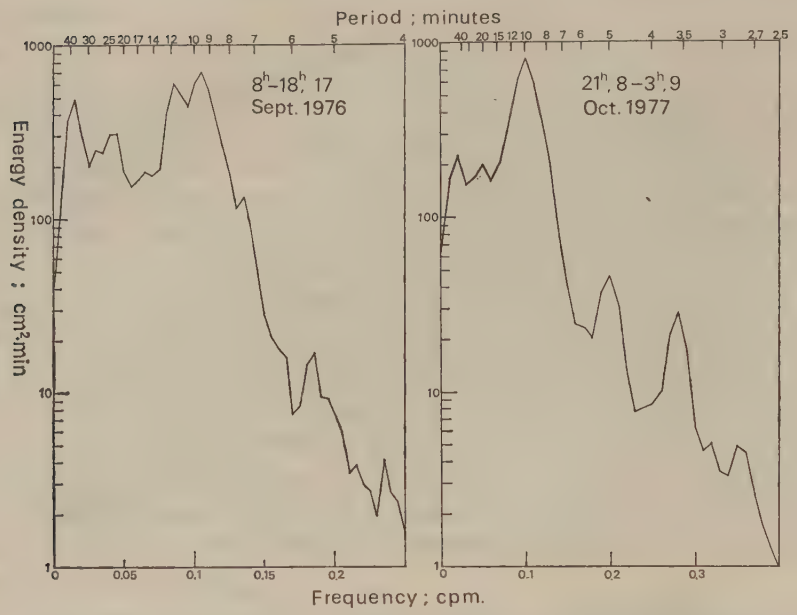

Fig. 4. Power spectra of sea level variations associated with the seiches of Habu-harbor.

quency. The secondary peak seen at about 0.2 cpm (5 minutes-period) will be a higher harmonic component of the primary peak, which is caused by the distortion of the primary wave component from a sinusoidal form.

Fig. 5 shows the tracks of Typhoon No. 7619 and Typhoon No. 7714. In this figure, open circles on the tracks are the typhoon positions at 9^h of respective days and full circles are the successive six hourly positions of the typhoon. The seiches in Habu-harbor began at the time of the nearest approach of these typhoons to Oshima Island. But the meteorological conditions around Oshima Island were not affected by the notable pressure fall, strong winds and heavy rains of these typhoons because the nearest approach of Typhoon No. 7619 was 790 km far east off the island and that of Typhoon No. 7714 was 880 km far east-southeast off. Accordingly, it is not plausible that these seiches were caused by the direct effect of the typhoons.

On the other hand, remarkable swell generated in the gale area of these typhoons had invaded to the sea around Oshima Island. In case of the seiche of 1976, for example, significant wave height was less than 2 meters in Sept. 16 and reached 3 meters on the early morning of Sept. 17 referencing wave gage records off Habu-harbor taken by the Second Port and Harbor Construction Bureau, Japan. The highest waves appeared from 10^h to 16^h of Sept. 17, when the significant wave height

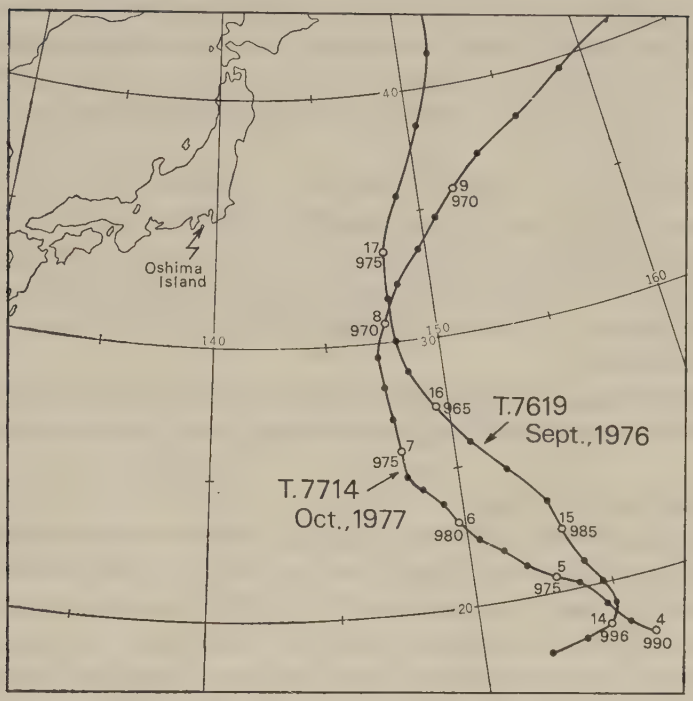

Fig. 5. Tracks of the typhoons No. 7619 and No. 7714. Open circles on the tracks are the typhoon positions at 9^h of respective days, and full circles the successive six hourly positions.

exceeded 4 meters and reached 4.6 meters with period of 13.7 sec at 16^h. The swell decayed gradually after the midnight of Sept. 17. The seiches of Habu-harbor were generated associated with the development of the swell.

The origin of the swell can be estimated by the technique of Barber and Ursell (1948). High wind waves moved and developed with Typhoon No. 7619 from the early morning of Sept. 15 to the early morning of Sept. 16 when the typhoon moved northwesterly increasing its intensity, removed the typhoon area as swell at the morning of Sept. 16, and reached the sea near Oshima Island on Sept. 17. Accordingly, the swell approached Habu-harbor from southeast, and the harbor received the swell influences effectively because its mouth opens southeast-ward.

It is disappointing that we could not get wave records of Oct. 8 and 9, 1977 because of instrumental troubles. But remarkable swell will be expected on these days because the movement of Typhoon No. 7714 is similar to that of Typhoon No. 7619. According to the wind wave analysis in the typhoon area, high wind waves moved and

developed with Typhoon No. 7714 from the morning of Oct. 5 to the morning of Oct. 7 when the typhoon moved northwesterly increasing its intensity, removed the typhoon area as swell at the morning of Oct. 7, and reached the sea near Oshima Island at the midnight of Oct. 8. These situation are similar to the case of Sept. 17, 1976.

Swell development near Oshima Island on the afternoon of Oct. 8, 1977 is also inferred from the fact that the tidal secondary undulations at Mera, southern end of Boso Peninsula, and Okada, northern end of Oshima Island, grew up remarkably from the afternoon of Oct. 8 to the early morning of Oct. 9, 1977 as reported by Isozaki *et al.* (1979). They emphasized that remarkable swell can excite notable tidal secondary undulations.

Apart from the question of the generating mechanism, it will be concluded from above mentioned synoptic situations that the seiches were generated by the swell.

3. Numerical experiments

As stated in the previous sections, the proper period of the oscillations of Habu-harbor is about 10.5 minutes. This is not consistent with the period estimated by Merian's formula. Recently, a number of numerical computations of tides and storm surge have been done by many authors, and their results show fairly good coincidence with observations. So we intend to apply a tidal numerical model developed by Unoki, *et al.* (1964) to the bay of Habu-harbor to know the characteristics of the proper oscillations of the harbor.

3.1 Basic equations and method of computation

In the usual equations of motion and that of continuity, we assume that the pressure is hydrostatic and there is no tangential stress on the sea surface. Integrating them over depth from the surface $z=-\zeta(x, y, t)$ to the bottom $z=h(x, y)$ and neglecting the terms of higher orders and Coriolis force, we have

$$\frac{\partial M_x}{\partial t}=-g(h+\zeta)\frac{\partial \zeta}{\partial x}-\frac{\tau_b{}^{(x)}}{\rho_w}-(h+\zeta)\left\{\frac{\partial \bar{u}^2}{\partial x}+\frac{\partial(\bar{u}\bar{v})}{\partial y}\right\} \tag{1}$$

$$\frac{\partial M_y}{\partial t}=-g(h+\zeta)\frac{\partial \zeta}{\partial y}-\frac{\tau_b{}^{(y)}}{\rho_w}-(h+\zeta)\left\{\frac{\partial(\bar{u}\bar{v})}{\partial x}+\frac{\partial \bar{v}^2}{\partial y}\right\} \tag{2}$$

$$\frac{\partial \zeta}{\partial t}=-\frac{\partial M_x}{\partial x}-\frac{\partial M_y}{\partial y} \tag{3}$$

where x and y are the horizontal rectangular coordinates taken on the undisturbed sea surface, z the vertical coordinate drawn downward, ρ_w the density of sea water, p the pressure, g the acceleration of gravity, ζ the elevation of sea surface, h the depth of basin, $\bar{u}$ and v the components of the mean velocity $\overline{V}$, $\tau_b{}^{(x)}$ and $\tau_b{}^{(y)}$ the

components of bottom friction τ_b. M_x and M_y are the components of the volume transport, being written as

$$M_x=(h+\zeta)\bar{u}=\int_{-\zeta}^{h} u\,dz\,,\quad M_y=(h+\zeta)\bar{v}=\int_{-\zeta}^{h} v\,dz \tag{4}$$

As the bottom friction, we used quadratic formula

$$\tau_b=\rho_w\cdot\gamma_w{}^2\bar{V}|\bar{V}| \tag{5}$$

assuming that the coefficient $\gamma_w{}^2$ is a constant 0.0026. On the coast, we suppose that the current will be parallel to the shore line, then we put

$$M_n=0 \tag{6}$$

where the subscript n means the normal to the coast. Moreover, to complete the calculation, the condition at the open end of the bay must be assigned. This is done to fit the experimental purposes.

In order to solve the differential equations (1), (2) and (3) numerically, we transformed them into finite difference equations with a time difference Δt and a space difference Δs. And then, the flow and the elevation at respective grid points were estimated step by step, using the difference equations of motion and continuity alternatively.

The domain of integration is shown in Fig. 2. The flow was calculated at the center of the line connecting two successive grid points and the surface elevation at the center of each square. For the computation we put $\Delta t=1.5$ sec and $\Delta s=30$ m. St. 1, St. 2,. . . ., St. 7 shown in Fig. 2 are the representative points at which the computed results are output.

3.2 Results of computations

In the first experiment, we shall consider the free oscillations of Habu-harbor. A pulse-like sea level rise with a height 10 cm is given during the first 15 seconds, then the level is maintained undisturbed situation at the bay mouth. Responding to the pulse-like disturbance at the mouth, sea level in the bay will oscillate freely with modes which have a node at the bay mouth.

Fig. 6 shows the computed sea level variations at respective stations through 17 minutes from the initiation of the computation. In this figure, the variations near the bay mouth are rather small because a node is at the mouth. The largest variations are seen at St. 3 and St. 4 which locate at the innermost part of the canal part. The variations of St. 3 are relatively regular and have a period about 2.4 minutes. They are small again in the harbor part.

Fig. 7 shows the computed sea level variations at respective stations from 60

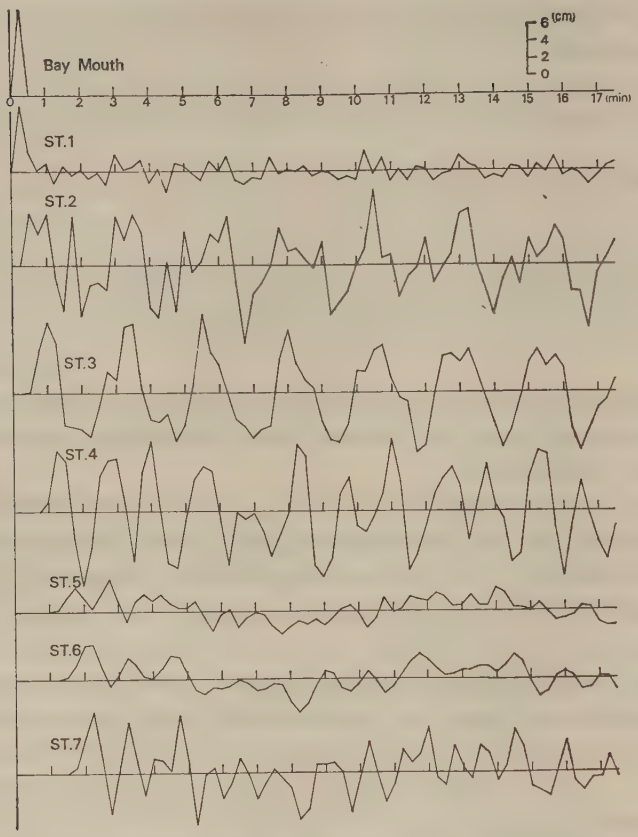

Fig. 6. Computed sea level variations excited by a pulse-like disturbance (first stage).

minutes to 77 minutes after the initiation of the computation. Generally the variations are smaller than in Fig. 6, but the features of them are similar to each other.

Fig. 8a, b show the power spectra of above obtained sea level variations. Fig. 8a contains the spectra for St. 2, St. 3 and St. 4 which are in the canal part, and Fig. 8b the spectra for St. 5, St. 6 and St. 7 which are in the harbor part. Detailed characteristics of these spectra are different, but remarkable peaks of energy level are seen commonly near the frequencies (periods) of 0.1 cpm (10 minutes), 0.4 cpm (2.5 minutes), and 0.7 cpm (1.4 minutes).

The peak near 0.1 cpm is highest at the stations in the harbor part, and decreases its energy level gradually toward the mouth. The peak near 0.4 cpm is highest at St. 3 followed by St. 2 and St. 4. The energy level of this peak in the harbor part is

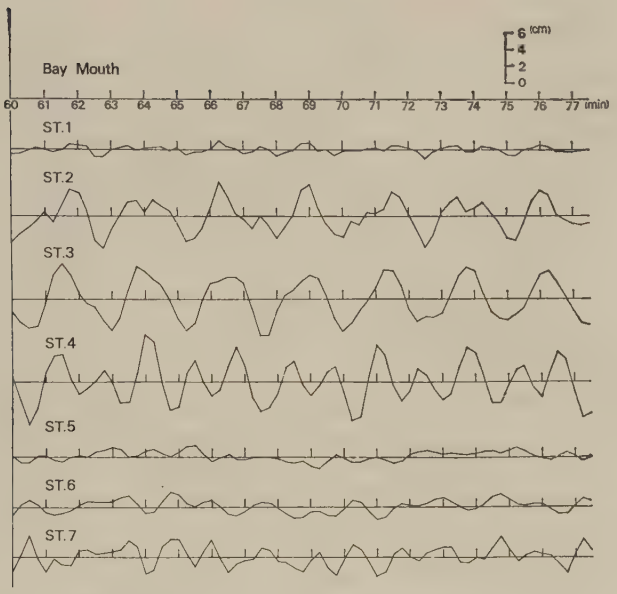

Fig. 7. Computed sea level variations excited by a pulse-like disturbance (60 minutes later stage).

about one order lower than in the canal part, and the lowest peak is at St. 5. Accordingly, the oscillations of 0.4 cpm may have a node near St. 5.

The peak at 0.7 cpm is highest at St. 4 followed by St. 2 and St. 7, and is lowest at St. 3 and St. 5. So, it will be presumed that the sea level oscillations of this frequency may have two nodes near St. 3 and St. 5 in addition to the node at the mouth.

In the next experiment, the response of bay water to the invading disturbance through the mouth is investigated. As the invading disturbance, sinusoidal sea level change with an amplitude of 10 cm and an assigned period is given at the bay mouth. The period of the invading disturbance was selected between 1.2 minutes and 14 minutes, the computation was continued through 8 periods-interval of the disturbance, and the results for the eighth period were output. The continuation of the computation through 8 periods-interval produced nearly steady oscillations for most disturbance periods, but could not reach steady oscillations and showed resonant amplification for some periods.

The computation was done by means of a nonlinear model and a linear model. The bottom stress and the inertia terms were contained in the former but not contained in the latter. The linear model produced a little larger amplitude of sea level

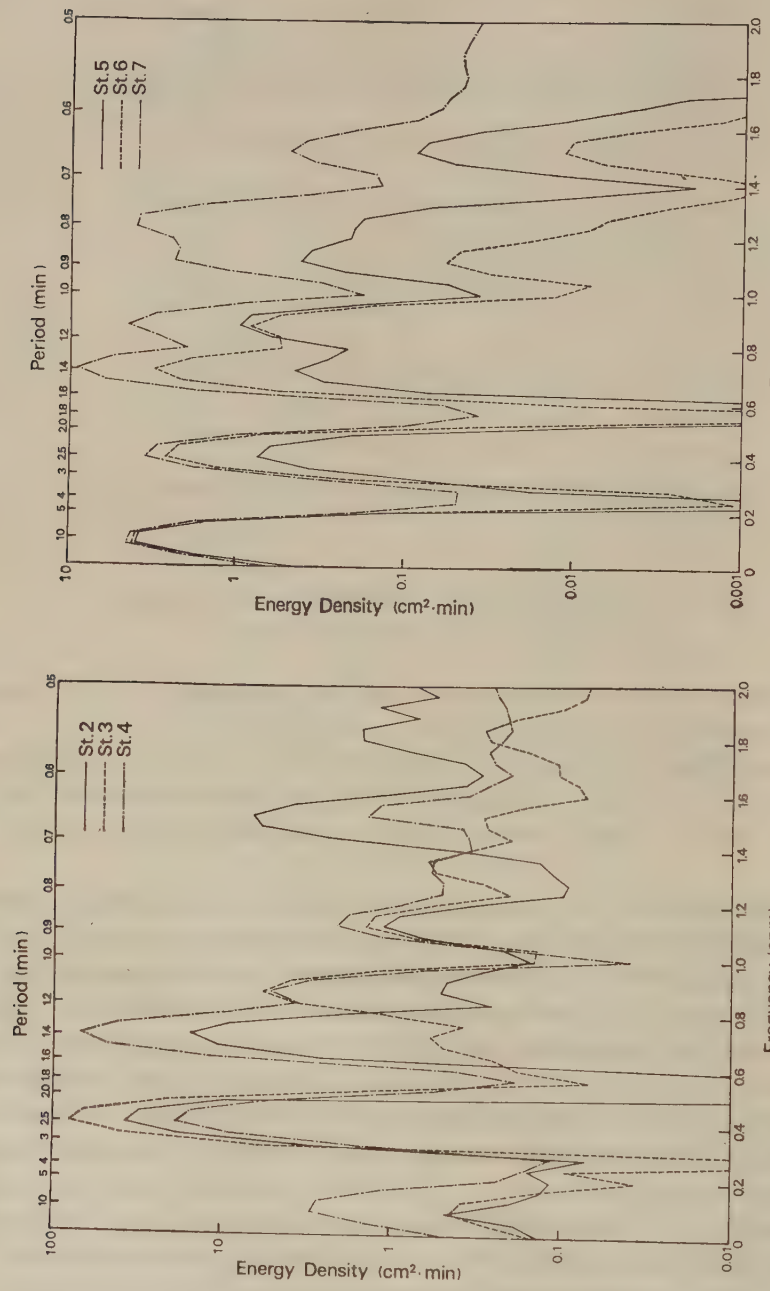

Fig. 8a, b. Power spectra of computed sea level variations excited by a pulse-like disturbance.

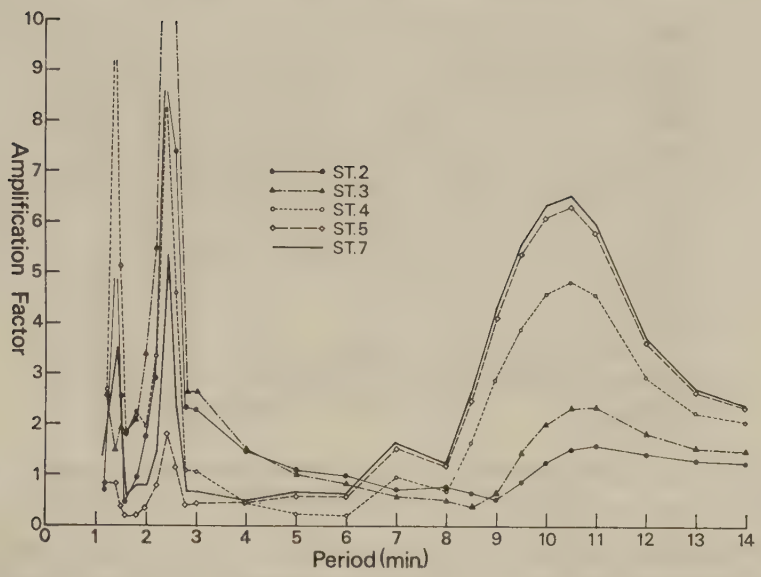

Fig. 9. Estimated amplification factor as a function of the period of disturbance.

oscillations than the nonlinear model, but the differences were not essential. So, we will discuss the results of the nonlinear model.

Fig. 9 shows the amplification factor at respective stations as a function of the disturbance period. Where the amplification factor is defined as the ratio of computed sea level amplitude to the amplitude given at the bay mouth. In this figure, large amplification factor is seen at the period of 10.5 minutes, 2.4 minutes and 1.4 minutes. The factor at 10.5 minutes-period is largest at St. 7 and decreases at successive stations toward the bay mouth. The factor at 2.4 minutes-period is very large except for the small value at St. 5; especially the oscillations at St. 3 and St. 2 showed resonant amplification and could not reach steady oscillations. In case of the oscillations of 1.4 minutes-period, the oscillations at St. 2 and St. 4 amplified continuously with time and could not reach steady state in the present computation. In this case, the factors at St. 3 and St. 5 are noticeably small.

Fig. 10 shows the representative sea level profiles along the bay axis, in explanation of oscillating modes of the characteristic periods, 10.5 minutes, 2.4 minutes and 1.4 minutes obtained in the present experiments. In this figure, the oscillation with a period of 10.5 minutes is the uni-nodal bay water oscillation with a node at the bay mouth. The oscillation with a period of 2.4 minutes is the bi-nodal oscillation with two nodes at the bay mouth and near St. 5, and the sea level variations in the canal

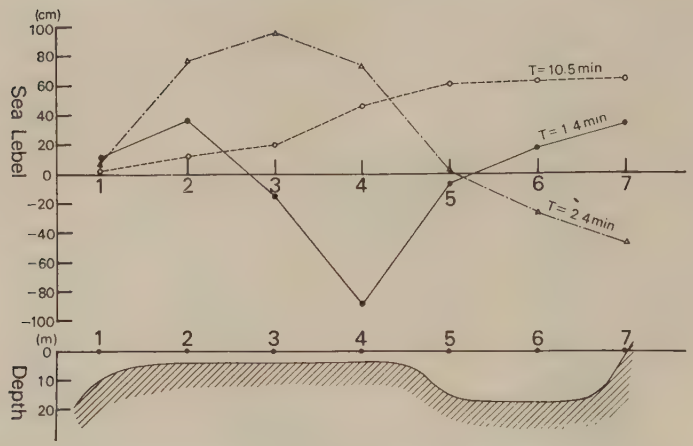

Fig. 10. Representative sea level profiles along the bay axis for the oscillations with periods of 10.5, 2.4, and 1.4 min.

part and the harbor part have reverse phase mutually. The oscillation with a period of 1.4 minutes is tri-nodal oscillations with three nodes at the bay mouth and near St. 3 and St. 5. These are consistent with the features of the free oscillation shown in Figs. 8a and b.

In spite of above mentioned discussion, we cannot detect notable oscillations of the periods of 2.4 minutes and 1.4 minutes on the records in Fig. 3 and on the seiche spectra shown in Fig. 4. As stated in the previous section, the sensor of the long period wave gage was set up near St. 5 near where nodes of 2.4 minutes- and 1.4 minutes-period oscillations are. Accordingly, we can expect that the mareograms contain only negligibly small oscillations of those periods. As to the spectral characteristics, adopted sampling time interval is too large to attain sufficient resolution for these period-band.

4. Theoretical considerations

It is confirmed by numerical experiment that the observed seiches of 10.5 minutes-period are the uni-nodal bay water oscillation of Habu-harbor. Considering smallness of the harbor, the period is too long and not consistent with the common sence of Merian's formula. Such long proper period may be derived from the bay configuration. As clearly seen in Fig. 2, the harbor is constructed by the canal part and the harbor part. Respective part has distinguish contrast in water depth and configurations with each other, and may behave as independent oscillating system. These two parts may cause the coupled oscillation influenced by the disturbances invading through the bay mouth.

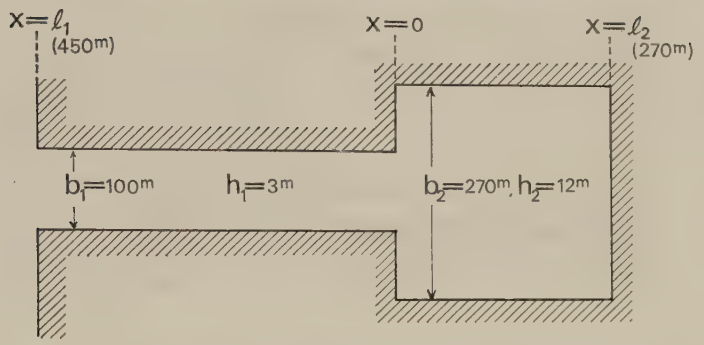

Fig. 11. Model basin which is constructed by a rectangular harbor and a straight canal.

Now consider a bay shown in Fig. 11 in which a harbor part with a length of l_2, a width of b_2 and a depth of h_2 is connected to the outer ocean through a canal part with a length of l_1, a width of b_1 and a depth of h_1. Variables for the canal part and the harbor part are descriminated by suffixes 1 and 2. Then the equations of free oscillation of the canal part and the harbor part are given as follows (Lamb, 1935; p. 264),

$$\frac{\partial^2\zeta_1}{\partial x^2}+\lambda_1^2\zeta_1=0\,;\quad \lambda_1^2=\frac{\sigma^2}{gh_1} \tag{7}$$

$$\frac{\partial^2\zeta_2}{\partial x^2}+\lambda_2^2\zeta_2=0\,;\quad \lambda_2^2=\frac{\sigma^2}{gh_2} \tag{8}$$

where σ is the frequency of the bay water oscillation, and time dependent factors, $\zeta_{1,2}\propto\cos(\sigma t+\epsilon)$, are omitted.

The boundary conditions are

$$\zeta_1=0\,,\qquad \text{at}\quad x=-l_1 \tag{9}$$

$$\frac{d\zeta_2}{dx}=0\,,\qquad \text{at}\quad x=l_2 \tag{10}$$

$$\zeta_1=\zeta_2\,,\qquad \text{at}\quad x=0 \tag{11}$$

$$b_1h_1\frac{d\zeta_1}{dx}=b_2h_2\frac{d\zeta_2}{dx}\qquad \text{at}\quad x=0 \tag{12}$$

The conditions (9) and (10) mean that a node is at the bay mouth and an anti-node is at the bay head respectively. The conditions (11) and (12) represent the continuities of sea level and volume transport at the boundary between the canal part and the harbor part.

Solutions of Eqs. (7) and (8) which satisfy the conditions (9) or (10) are

$$\zeta_1 = A \sin \lambda_1 (x + l_1) \tag{13}$$

$$\zeta_2 = B \cos \lambda_2 (x - l_2) \tag{14}$$

The conditions that the solutions (13) and (14) satisfy the relations (11) and (12) are

$$A \sin \lambda_1 l_1 = B \cos \lambda_2 l_2 \tag{15}$$

$$A\lambda_1 b_1 h_1 \cos \lambda_1 l_1 = B\lambda_2 b_2 h_2 \sin \lambda_2 l_2 \tag{16}$$

Eliminating A and B between (15) and (16),

$$\lambda_1 b_1 h_1 \cos \lambda_1 l_1 \cos \lambda_2 b_2 - \lambda_2 b_2 h_2 \sin \lambda_1 l_1 \sin \lambda_2 l_2 = 0 \tag{17}$$

that is,

$$\frac{b_1 h_1}{c_1} \cos \frac{l_1}{c_1}\sigma \cdot \cos \frac{l_2}{c_2}\sigma - \frac{b_2 h_2}{c_2} \sin \frac{l_1}{c_1}\sigma \cdot \sin \frac{l_2}{c_2}\sigma = 0 \tag{18}$$

or

$$\left(\frac{b_1 h_1}{c_1} + \frac{b_2 h_2}{c_2}\right)\cos\left[\left(\frac{l_1}{c_1} + \frac{l_2}{c_2}\right)\sigma\right] - \left(\frac{b_2 h_2}{c_2} - \frac{b_1 h_1}{c_1}\right)\cos\left[\left(\frac{l_1}{c_1} - \frac{l_2}{c_2}\right)\sigma\right] = 0 \tag{19}$$

where $c_1 = \sqrt{gh_1}$ and $c_2 = \sqrt{gh_2}$. From Eq. (19), we can obtain the proper frequencies of the bay system shown in Fig. 11.

Now approximate Habu-harbor by the model as follows,

$$l_1 = 450 \text{ m},\ l_2 = 270 \text{ m},\ b_1 = 100 \text{ m},\ b_2 = 210 \text{ m},\ h_1 = 3 \text{ m},\ h_2 = 12 \text{ m}$$

and estimate the proper frequencies of the approximated harbor from Eq. (19) numerically. Obtained lowest three values of σ are, in cpm unit,

$$\sigma = 0.082;\ 0.376;\ 0.717$$

and corresponding period is, in minute unit,

$$T = 12.2;\ 2.7;\ 1.4$$

These agree reasonably well with the results obtained by the numerical experiments. Accordingly, it will be concluded that the observed seiche period of 10.5 minutes may be produced by the coupled oscillation of the systems of the canal part and the harbor part.

Now, a ratio of the amplitude factors of the oscillation in the canal part to that in the harbor part is obtained by Eq. (15). For the cases of above obtained three periods they are

$$A/B = 1.49;\ -4.35;\ 5.78$$

then the profiles of relative amplitude along the bay axis are given by Eqs. (13) and (14), as shown in Fig. 12. These profiles agree qualitatively with the profiles in Fig. 10.

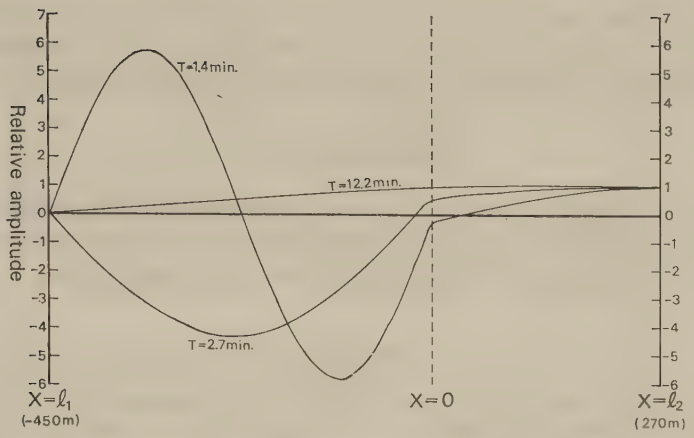

Fig. 12. Profiles of relative amplitude in the model basin shown in Fig. 11.

5. Conclusion

Remarkable seiches were observed in Habu-harbor on Sept. 17, 1976 and Oct. 8, 1977. These seiches were caused under similar meteorological conditions; that is, the weather was rather gentle around Oshima Island except for the invasion of remarkable swell from southeast. The swell was generated in the gale area of Typhoon No. 7619 and Typhoon No. 7714. These typhoons moved northerly about 800 km far east off Oshima Island and not affected to the weather condition around the island. Apart from the question of generating mechanism, it will be concluded by these synoptic situations that the seiches were excited by the swell.

Dominant period of the seiches was 10.5 minutes. It is longer than the one estimated by Merian's formula. So we examined characteristics of the proper oscillations of Habu-harbor by means of a numerical model. The results show that the periods of uni-, bi-, and tri-nodal bay water oscillation are 10.5 minutes, 2.4 minutes and 1.4 minutes respectively. Accordingly, the observed seiches may be the uni-nodal bay water oscillations.

Inconsistency of the proper period of Habu-harbor with the period estimated by Merian's formula may be due to the bay configuration. The harbor consists of the canal part and the harbor part. Respective part has distinguish contrast in water depth and configurations with each other, and will behave as independent oscillating system. These two part may cause the coupled oscillation influenced by the disturbances invading through the bay mouth. It is confirmed by the theoretical considerations that the coupled oscillation will be able to produce bay water oscillations of the periods about 12 minutes, 2.7 minutes and 1.4 minutes in the simplified model of

Habu-harbor. These agree fairly well with the results of the numerical experiments. Accordingly the behavior of the seiche in Habu-harbor can be explained by the coupled oscillation of the systems of the canal part and the harbor part.

Acknowledgements

The author wish to thank Mr. T. Uji who read the manuscript carefully and gave him useful suggestions. This work was supported by the "Investigation of the Long Ocean Waves in Sagami Bay", Science and Technology Agency, Japan.

References

Barber, N. F. and F. Ursell (1948): The generation and propagation of ocean waves and swell. I. Wave periods and velocities. Phil. Trans. Royal Soc., **240** (824), 527-560.

Isozaki, I., K. Kurashige, T. Uji, and T. Konishi (1979): Investigation of the long period ocean waves caused by meteorological and oceanographical disturbances. Tech. Rept. of the Science and Technology Agency, Japan (in press).

Lamb, H. (1935): Hydrodynamics. Cambridge University Press.

Unoki, S., I. Isozaki, and S. Otsuka (1964): Estimation of possible storm surge in the Bay of Tokyo. The Second Port and Harbor Construction Bureau. pp. 125.

波浮港のセイシュについて

磯崎一郎
(気象研究所)

1976年9月17日と1977年10月8日に大島の波浮港において顕著なセイシュを観測した。これらはそれぞれ，台風7619号及び台風7714号からのうねりによって誘発されたものらしい。なお，これらの台風は共に，本邦の東方約800 km の沖合を北上していて，関東近海の気象には直接的な影響を及ぼしていない。

波浮港のセイシュの卓越周期は約10.5分である。これはメリアンの公式で見積られる値より大きい。それで，数値実験によって波浮港の振動特性を調べた。その結果，単節湾振動の周期が約10.5分，2節湾振動で2.4分，3節湾振動では1.4分であることがわかった。従って，観測されたセイシュは単節湾振動である。

観測されたセイシュ周期と，メリアンの公式から見積られる周期の相違は，湾の形状に原因があるらしい。すなわち，波浮港は港湾部分と水路部分に分けられ，それらが独立の振動系であると考えると，湾口から侵入する擾乱に対して，湾水は連成振動を起す。この考えに基づいて周期を概算すると，メリアンの公式の値とは一致せず，観測値とほぼ一致した。すなわち，波浮港のセイシュは連成振動で説明できることがわかった。

The Oceanographical Magazine
Vol. 30, Nos. 1-2, pp. 47 to 54, March 1979

Floating particulate petroleum residues, tar balls, in the western Pacific

Akira SANO, Nobuo SATOH and Naoshi KUBO
Japan Meteorological Agency
(Received January 5, 1979; accepted January 11, 1979)

Abstract: The distribution of particulate petroleum residues, popularly known as floating tar balls, on the surface water in the western Pacific in summer 1977 is presented.

On the waters north of 15°N, concentrations of floating tar on the meridional lines of 137°E and 155°E are found to range from 0.02 to 13.3 mg/m^2 and from 0.01 to 0.18 mg/m^2, respectively. It should be noted that high concentration of 3.0 and 13.3 mg/m^2 were found at the boundaries between coastal water and the Kuroshio, and at the periphery of the eddy which was cut off from the Kuroshio, respectively. These findings indicate that the waters north of 15°N were polluted extensively with floating tar, while the waters south of 15°N show low concentrations ranging from 0.000 to 0.010 mg/m^2.

The JMA type neuston net, used in this survey, is described.

1. Introduction

The amount of crude oil brought to the Far East in supertanker is growing up with increasing of the demands on petroleum as energy source or materials for petrochemical industry.

In the Pacific Ocean, supertanker loading oil is destinated from the Middle East to Japan through the western part of Pacific—the regions of South China Sea, Eastern China Sea, Lombok Str. and the Kuroshio.

It seems that these supertankers made tank cleaning operation on the way back to Middle East or North Africa. During such processes, various kinds of hydrocarbons with petroleum origin, such as tar ball and dissolved/dispersed hydrocarbons, are discharged into marine environment. Petroleum pollution is now spreading from the source of pollution to all over the open oceans and will probably give some impact on marine environment—ecosystem.

One of the main component of petroleum marine pollution is a tar ball (floating petroleum particulate) which, as is well known, soils beaches as well as water along the tanker route.

On floating tar ball, various observations were carried out in the North Atlantic

and the adjacent seas (LEVY & WALTON, 1976). The monitoring of floating tar in the near-shore region of Japan were regularly done by the Maritime Safety Agency (1977) as a part of the Nation's program. ODATE & HAYASHI (1973), KOMAKI & MORIOKA (1975) and MARUMO & KAMATA (1973) also performed the survey on the distribution of floating tar in the waters around and east of Japan. However, the monitoring of floating tar in open ocean such as the western Pacific has never been done before.

Of great importance is to clarify the present level of oil pollution in open ocean to obtain rational basis for preservation and protection of marine environment. In this connection, the present study was carried out.

After more than twenty trials on sample collection on board the R/V Ryofu Maru at the cruises in winter and spring 1977, the regular monitoring of floating tar in the open ocean was started in June–July 1977 on board the R/V Ryofu Maru of Japan Meteorological Agency, in responding to the Marine Pollution (Petroleum) Monitoring Pirot Project (MaPPMoPP) of IGOSS.

2. Sampling

For sampling of floating tar in the routine survey, JMA type neuston net as shown in Fig. 1 was specially designed for the purpose of simplification of sampling procedures described in the operational plan in MaPPMoPP*. In the process of sampling, instruments such as a capstan, roller fair leader and vinylon rope were used instead of the hydrographic winch and wire to avoid contaminations of oil or grease.

Suitable posture of the mouth of net in towing was obtained by adjusting the length of four bridles with turnbuckles, the weights attached to the frame and lengths of the towing rope so as to keep the lower half of the mouth part in the water. The materials with more than 0.35 mm in diameter, which enter in the mouth of net, was filtered and trapped in an inner bag in the porous bucket.

JMA neuston net was towed for one nautical mile at a speed of 4–5 knots to scoop approximately 1,400 m^2 of sea surface. Sampling was carried out usually in a daytime at 14:00 (Japanese Standard Time), to avoid contamination of a great deal of zooplankton, and to keep safety and reliability in operations. 38 samples were obtained along the cruise track of the R/V Ryofu Maru as in Fig. 2.

3. Sorting and measurement

The materials collected in the net were washed by sea water, gathered into the inner bag, and then transferred into a transparent jar for sorting. After the most of organisms such as zooplankton sunk, all the tars were separated by hand picking

* Operational plan in MaPPMoPP of IGOSS, published by Intergovernmental Oceanographic Commission (1974).

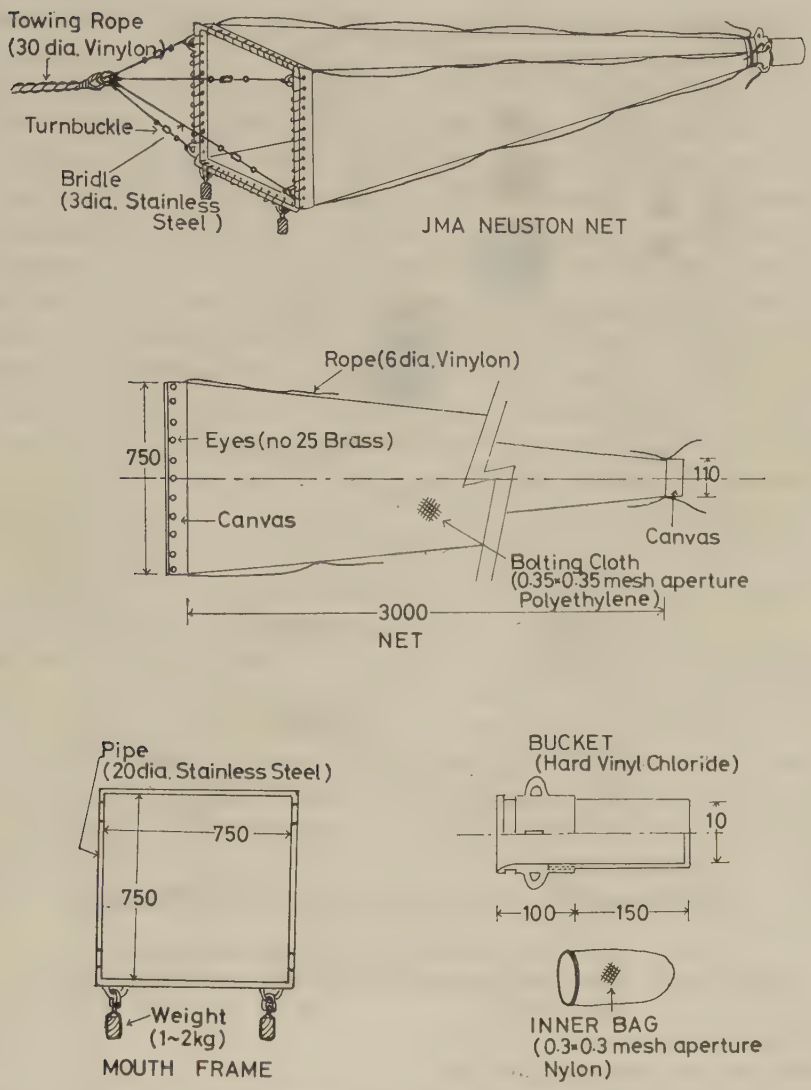

Fig. 1 Diagram of the JMA type neuston net.

from the mixture with the needles under the magnifier and put on the filter paper for removing water from the surface of tar. Then, tar separated was put into the weighing bottle and stored in the freezer of the vessel.

At laboratory on land, amount of tar was determined gravimetrically within the error of ± 0.1 mg. Finally, the concentration of floating tar was given as net weight

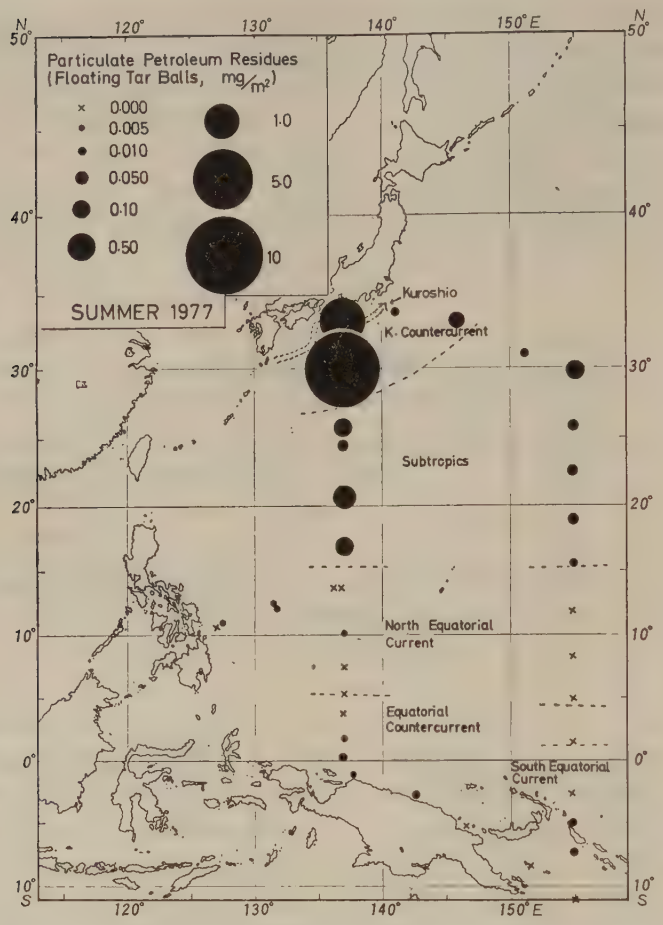

Fig. 2 Distribution of floating tar concentration (mg/m^2) and surface ocean currents in the western Pacific, summer 1977.

of tar (mg) per unit sea surface area (m^2).

The tar sticked on the net was washed with carbon tetrachloride (CCl_4). Amount of the tar in CCl_4 solution was weighed, if necessary, after evaporating of CCl_4.

4. Distribution of floating tar in the western Pacific

Although, numbers of data obtained is not enough to discuss the geographical distribution in the western Pacific in detail, it can be safely said that tar concentration of surface waters in the western Pacific is not uniform as shown in Fig. 2. There

exists a clear difference in tar concentration between the north and south region of the western Pacific.

High concentration of tar, ranging from 0.010 to 13.3 mg/m^2 with an average of 4.3 mg/m^2 appear in the Kuroshio region. Extremely high value, 3.0 and 13.3 mg/m^2, are found at the boundary between coastal water and the Kuroshio, and also at the periphery of the eddy which was cut off from the Kuroshio. The high concentration may be suggestive of somewhat the process of accumulation at the boundaries where the current system is rather complicated. Most tar lumps collected in the Kuroshio region are approximately 5–10 mm in diameter, and fresh, sticky and shiny in appearance. The samples collected in the surface water contains appreciable amount of neritic plankton, seaweed and miscellaneous plastics together with tar.

In the subtropical region, floating tar with concentration ranging from 0.008 to 0.35 mg/m^2 is lower than those in the Kuroshio region but higher than those in the southern region. In addition, a conspicuous regional variation is recognized in the subtropics. Namely, the concentration of tar in the western region along 137°E is higher than in the eastern region along 155°E, as listed in the Table 1. Judging from the appearance of tar collected, it can be said that tar in the eastern region is much weathered than that in the western region.

Trace of crumbled tar smaller than 1 mm in diameter was found in the sea water collected in regions of the North Equatorial Current, Equatorial Countercurrent and South Equatorial Current. These samples contain blue colored lives such as great numbers of Pontellid accompanying a few *Halobates, Porpita, Physalia* and *Velella.* Tar concentrations in these regions are ranging from 0.000 to 0.005 mg/m^2 with mean of 0.001 mg/m^2 along 137°E and east of the Philippines, while no tar was found along 155°E.

Also, in the neritic water of Papua New Guinea, floating tar is rarely found. The

Table 1. Summary of floating tar concentrations in the western Pacific, June–July 1977.

Regions		Range of concentration (mg/m^2)	Mean concentration (mg/m^2)
Kuroshio and Kuroshio Countercurrent		0.010–13.3	4.31
Subtropics	137°E	0.020–0.35	0.19
	155°E	0.008–0.18	0.050
North Equatorial Current and Equatorial Countercurrent	137°E	0.000–0.005	0.001
	155°E	0.000–0.000	0.000
Neritic water of Papua New Guinea		0.000–0.010	0.004

concentration is ranging from 0.000 to 0.010 mg/m^2 with mean of 0.004 mg/m^2. The samples collected there consist of phytoplankton, especially blooming *Trichodesmium*, Pontellid and trace of tar being resemble to carbonized matter.

It may be said from the distribution of floating tar and ocean currents in Fig. 2 that main source of tar in the western Pacific could be located in the north western margin of the western Pacific where the main tanker traffic is located. Namely, the concentration and size of floating tar decrease from the Kuroshio region toward eastern and southern regions. Also, dull and crumbly tar in the eastern and southern regions might indicate that tar have been presumably weathered, drifting from northern or northwestern region at where sticky and shiny tar is dominant. The Kuroshio, originated east of the Philippines, can transport the miscellaneous waste oils from the tanker traffic to the northeast. Likewise, tar, being weathered, is still drifted and diverged to various directions including the subtropical regions by the Kuroshio Countercurrent and monsoon.

5. Comparison with the North Atlantic

Although the level of petroleum pollution in the Kuroshio region is not so high as that in the Mediterranean Sea, but almost equal to those of the Gulf Stream, Gulf

Table 2. Summary of floating tar concentrations in the North Atlantic and adjacent seas.

Regions	Period	Range (mg/m^2)	Mean (mg/m^2)	Weight	Authors
Mediterranean Sea	1969	1.0–540*1	20.0*1	wet	Horn *et al.* (1970)
North western Atlantic	1969–1970	0.1–9.7	1.0	wet	Morris (1971)
Western North Atlantic	1971–1973			wet	McGowan *et al.* (1974)
Ocean station Bravo*2		0–0.003	0.000		
Charlie		0–1.83	0.12		
Delta		0–10.73	1.15		
Echo*2		0–21.62	2.64		
Gulf Stream system	1972–1973		0.05–4.8	dry	Sherman *et al.* (1974)
Gulf of Mexico	?	0–10	1.2	dry	Jeffery *et al.* (1974)
Caribbean Sea	?	0–4.51	0.47		
North Atlantic	1971–1974	0–91.8*3	0.57	dry	Levy & Walton (1976)
northern region (north of 45°N)			0.01		
between Greenland and Labrador			0.00		
southern region (15°N–45°N)			1.16		
Gulf stream			1.15		
Sargasso Sea			2.64		

*1 Original displacement volume was converted to wet weight by Morris (1971).
*2 Ocean station Bravo is located in the northern region of the North Atlantic and Echo is in the Sargasso Sea.
*3 Value 91.8 was observed in the Sargasso Sea in 1973.

of Mexico and Sargasso Sea which are located in or adjacent to the southern region in the North Atlantic (Table 2).

While, the tropical water in the western Pacific as well as northern region in the North Atlantic is not so polluted in regard to floating tar. Both regions have a very similar property to each other, because these are far from major population on land and the frequent maritime transportation including tankers. Therefore, these regions are almost free from tar pollution (Levy & Walton, 1976).

Monitoring of floating tar in the western Pacific is ongoing by Japan Meteorological Agency, to get further information on background level of oil pollution including its seasonal and regional change, in order to clarify the effects of ocean currents, weather conditions and human activities on the distribution of tar in the ocean.

Acknowledgements

The authors wish to acknowledge members of Oceanography Division, Captain K. Shirakawa and crew of R/V Ryofu Maru for their help in collection of sample in this survey. They also wish to acknowledge Dr. T. Suzuoki of Oceanography Division, Marine Department, for a critical reading of this manuscript and many valuable advices.

References

Horn, M. H., J. M. Teal and R. H. Backus (1970): Petroleum lumps on the surface of the sea. *Science* **168**, 245-246.

Japan Maritime Safety Agency (1977): Marine Safety White Paper. (in Japanese).

Jeffery, L. M., W. E. Pequegnat, E. A. Kennedy, A. Vos and B. M. James (1974): Pelagic tar in the Gulf of Mexico and Caribbean Sea. Marine pollution monitoring. Proc. Symp. Workshop Natl. Bur. Stand., Gaithersburg. Md., May 13-17, 1974. *Natl. Bur. Stand. Spec. Publ.* **409**, 233-235.

Komaki, Y. and Y. Morioka (1975): "Hopping Boy", a simple wood-framed neuston net. *Bull. Jap. Sea Reg. Fish. Res. Lab.*, **26**, 67-72.

Levy, E. M. and A. Walton (1976): High seas oil pollution, particulate petroleum residues in the North Atlantic. *J. Fish. Res. Board Can.*, **33**, 2781-2791.

Marumo, R. and K. Kamata (1973): Oil globules and their attached organisms in the East China Sea and Kuroshio area. *J. Oceanogr. Soc. Jap.*, **29**, 155-158. (in Japanese).

McGowan, W. E., W. A. Saner and G. L. Hufford (1974): Tar ball sampling in the western North Atlantic. Marine pollution monitoring. Proc. Symp. Workshop Natl. Bur. Stand., Gaithersburg, Md., May 13-17, 1974. *Natl. Bur. Stand. Spec. Publ.* **409**, 83-84.

Morris, *B. F.* (1971): Petroleum, tar quantities floating in the northwestern Atlantic taken with a new quantitative neuston net. *Science* **173**, 430-432.

Odate, S. and K. Hayashi (1973): The relationship between distribution of waste oil and distribution of fish eggs and larvae in the northwestern Pacific. *Bull. Jap. Soc. Fish. Oceanogr.*, **23**, 124-128 (in Japanese).

The Oceanographical Magazine, Vol. 30, Nos. 1-2. (1979)

SHERMAN, K., J. B. COLTON, R. L. DRYFOOS, K. D. KNAPP and B. S. KINNEAR (1974): Distribution of tar balls and neuston sampling in the Gulf Stream system. Marine pollution monitoring. Proc. Symp. Workshop Natl. Bur. Stand., Gaithersburg, Md., May 13-17, 1974. *Natl. Bur. Stand. Spec. Publ.* **409**, 243-245.

西太平洋における浮遊タールの分布

佐　野　　昭・佐　藤　亘　男・久　保　　直
(気象庁海洋気象部)

操作が簡単な気象庁型ニューストンネットを用いて，1977年6～7月の凌風丸の航海で西太平洋における浮遊タールの分布調査を実施した。タール濃度は黒潮域で最高で，亜熱帯海域がこれについでいたが，北赤道海流域，赤道反流域，パプア・ニューギニア沿岸域では痕跡程度であった。また，同一海流域内でも137°E 線上のほうが155°E 線上よりも高濃度であった。すなわち，浮遊タールは日本近海から南方または東方に遠ざかるにつれて減少する傾向があった。この傾向はタールの風化度にもあてはまり，日本近海では粘度がありつやのある黒色の試料が多かったが，東方または南方に遠ざかるにつれ，硬度を増し，かつ退色してゆく傾向があった。

The Oceanographical Magazine
Vol. 30, Nos. 1-2, pp. 55 to 60, March 1979

Visual observation on the floating pollutants in open ocean

Tetsuro SUZUOKI and Kiyoshi SHIRAKAWA
Japan Meteorological Agency

(Received January 8, 1979; accepted January 11, 1979)

Abstract: Visual observation on the floating plastics of JMA was preliminarily done in the western North Pacific during 1976-1978. The result shows that the floating plastics distribute all over the open sea. The contamination mainly occurs in the coastal region and spreads over the regions of the Kuroshio and its counter-current. Such a trend is found to be well repeated during the period of survey.

The level of pollution in the open ocean south of 20°N is estimated to be ~0.7 pieces/100 miles which may indicate the present background level of floating plastics.

This finding suggests that this kind of pollutant can be regarded as one of the useful parameters to indicate the behavior of floating pollutants in the marine environment.

It is, however, pointed out that there remains a serious problem for further extension of this type of survey. It is very difficult to obtain statistically valid and intercomparable data on account of unavoidable variability in the quality of data obtained by multi-ship surveys.

1. Introduction

Recently, on the surface of sea, beach and sea floor there is multitude of society's waste disposal that is not easily decomposed in either marine or non-marine environments. These are plastic-ware, plastic bags, glass-ware, metal objects and so far. Some of them, such as polystylene spheres and discs have been discarded from the manufacturing processes. Substantial portion of litter appears to come directly from ships.

It is time to take a measure for controlling of expanding pollution by the litters mentioned above. Statistically valid observation or sampling techniques are urgently needed to evaluate amounts and distribution of litters on the ocean surface—and also on the sea-floor—in order to assess the effect of litter upon various components of the ocean system.

Of great importance is to find out the parameters which are indicative of actual level of pollution and to assess the present situation of litter on the surface water of the ocean.

In this regard, the visual observation in MaPPMoPP/IGOSS(*) has been implemented internationally for oil slicks, floating petroleum residues and other floating pollutants on the sea surface.

After our preliminary surveys on this program, it is concluded that oil slicks are not feasible as an indicator of floating pollutants in the open ocean on account of its extremely low intensity which brings about difficulty in identification and quantitative estimation in visual observation on the sea surface.

Thus, a principal parameter in the survey presented here is limited to plastics such as polystylene form and plastic float which are easily distinguishable and thought to be one of the typical floating pollutants on the ocean surface. The survey was carried out on board the R/V Ryofu Maru in the western North Pacific during 1976–1978 in the framework of JMA's ongoing program on the background marine pollution monitoring in open ocean.

2. Results and discussion

Geographical distributions of floating plastics in visual observations during 1976–1978 are shown in Fig. 1(a)~(d). The numbers of sites where pollutants were found and the total numbers of pollutants in each day-time observation are given in these figures. It is seen from these results that the trend of lowering of pollution level with lowering of latitudal position appears. The total numbers of pollutants presented here, however, is not so quantitative. Although the observation time is fixed to only day-time, the cruise distance a day can not be constant on account of ship's frequent stopping for the observation such as hydrocasting, sample collection and so far.

For parameterization, all the data in figures are converted to be expressed in terms of linear density which are practically given by the ratio of total number of pollutant in day-time observation to actual cruise distance, that is, numbers of pieces/100 miles.

In order to get a general trend in the distribution of floating plastics the area covered was devided into six portions with 10° of latitudal span. The weighted means of the values obtained in each span are given in Table I. The ninth column and the bottom line in the table show the weighted mean in each of latitudal and longitudal span, respectively.

Distributions along two long meridional lines, 137°E and 155°E show that the density in northern part is higher than southern part. This trend appears independently of time, season and site of observations. As for latitudal distribution, in the region between the Kuroshio and 30°N the western sector (137°E) shows higher density than the eastern sector (155°E), while in the region between 30° and 20°N the

(*) Marine Pollution (Petroleum) Monitoring Pilot Project/Integrated Global Ocean Station Systems.

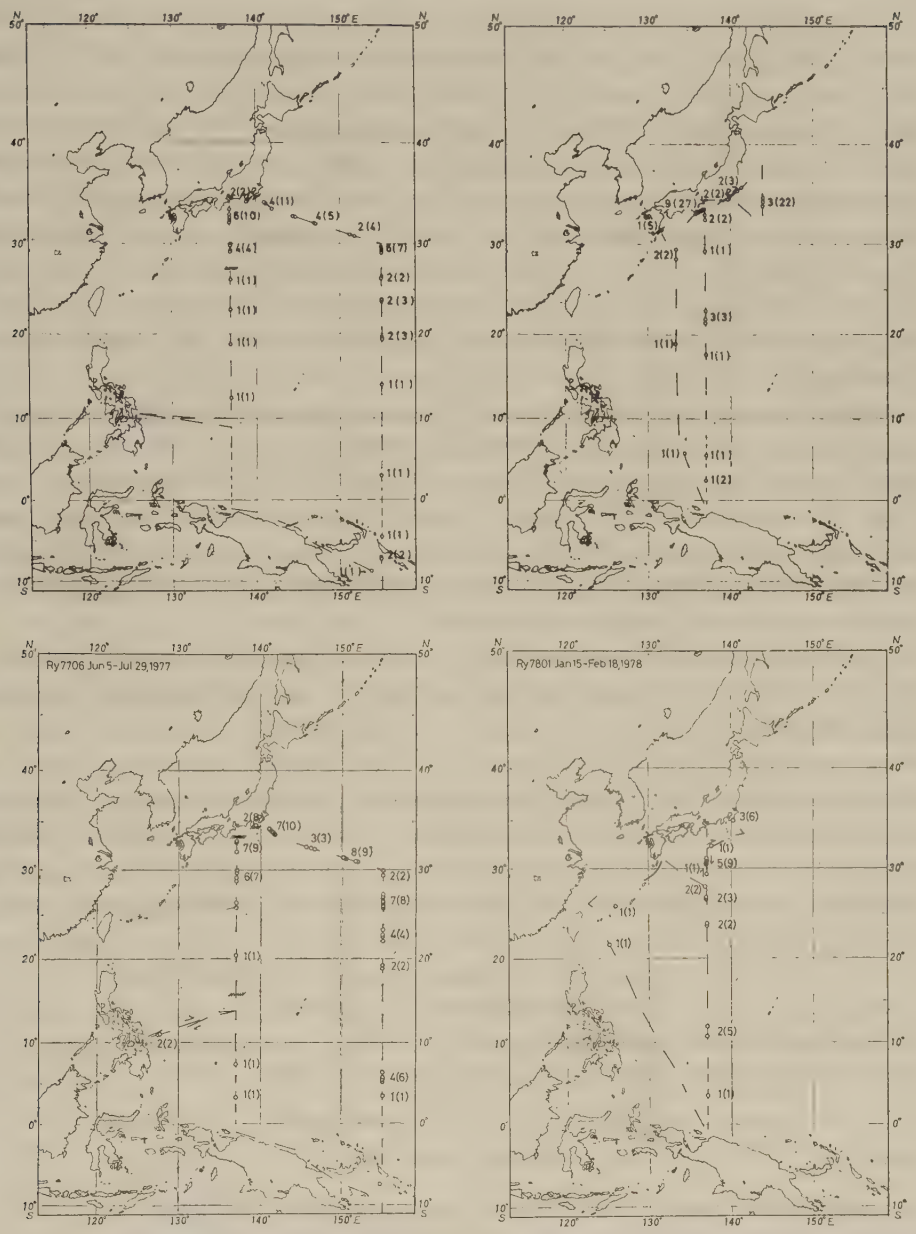

Fig. 1 Floating plastics (open circle) and oil slick (hatched area) in the regions of the western North Pacific. A bold line denotes the line where visual observations were performed in day-time. The number and that in parentheses denote the numbers of site where pollutants were found and the total numbers of pollutant in each day-time, respectively.

density on 155°E line is higher than that on 137°E line. On 135°E line the high density band with around 150 miles of width between the Kuroshio and 30°N was found while on 155°E line this high density band expands to around 600 miles of width—to around 20°N. Seasonal variations appeared only in the case of 137°E line. The density in the region between the Kuroshio and its countercurrent is higher in summer than in winter. In winter the region with relatively higher density seems to expand down to northern region of the North Equatorial current. This finding are well reproduced during 3 years for 1976–1978 as seen in Table I, and may reflect that the south-eastward transportation of floating plastics is predominant in winter. The coastal sector shows generally very high density with very wide range of fluctuation.

Average level of pollution by plastics in whole western North Pacific is approximately estimated to be 2.3 pieces/100 miles with the range of 0.6–2.7 except the region of near-coast. Moreover, the regions south of 20°N including southern half of the subtropics, the North Equatorial Current, the Equatorial Countercurrent and South Equatorial Current show the lower contamination level of 0.6~0.7 pieces/100 miles. This might indicate the present background level of floating plastics in the open ocean of the western North Pacific.

It should be noted that these litters distribute heterogeneously over the wide area of open ocean and that there exists not so distinctive seasonal change in the trend of the distribution.

The density distribution in the coastal area is reasonably understood when the input of the disposal from land to ocean environment is taken into account. However, the relatively dense distribution of these litters in the region southeast of Honshu Island probably does not mean that the source of the pollutant is mainly located around this region. It is more likely that these litters come from the pacific coastal

Table 1. Distribution of the floating plastics in the Western Pacific.
(unit: numbers of plastics/100 miles)

Year	1976		1977	1977	1977		1978		Currents &
Season	summer		winter	spring	summer		winter	average	waters
	137°E	155°E	137°E		137°E	155°E	137°E		
coastal		6.0		8.0	75	40		30	31.8	
coastal–30°N	8.3	4.0		5.0	3.8	8.2	4.8	3.3	5.3	Kuroshio & its countercurrent
30°N–20°N	1.8	3.3		1.0	4.5	2.4	4.5	1.6	2.7	Subtropic waters
20°N–10°N	0.6	1.2		0.3	—	0.0	0.6	1.5	0.7	North equatorial current
10°N– 0°N	0.0	0.3		0.5	—	0.6	2.0	0.2	0.6	Equatorial counter current
0°N–10°S	—	1.0		—	—	—	0.4	—	0.7	South equatorial current
average	2.7	2.0		1.7		2.8	2.5	1.7		

region, as the society's discard accompanied with development and advancement in human activity on land or near-shore regions.

The patterns of litter distribution may closely related to over-all oceanic condition in terms of ocean current system and wind system such as monsoon in the western North Pacific. For instance, though the floating plastics are abundant in the regions of the Kuroshio, its countercurrent and the northern part of subtropics, relatively few floating plastics are found in the region of the North Equatorial current which is far from highly industrialized region on land.

Types and characteristics of pollutants monitored in present survey are limited to floating plastics with very low specific gravity compared with the sea water and with high resistance against chemical or mechanical decomposition in the ocean environment. Other floating litters with the properties similar to floating plastics will behave in same manner as the floating plastics. Accumulation of such kinds of pollutants in an specified region may provide new echonics for marine organisms there and hence alter the structure of marine community in future.

In our present study, visual observation was performed by couples of specially trained navigators on board the R/V Ryofu Maru so as to minimize the variability in the way of each observation, as a result of which we could describe semi-quantitatively the distribution of floating plastics. It is, however, doubtful that statistically valid and intercomparable data can be tentatively obtained in world wide survey, because wide spectrum of data qualities due to variability in the way of observation should be expected when the observation is done by means of various kinds of ships such as research vessel, commercial ship, fishing boat and so far. For instance, the probability in detection of pollutants in visual observation is critically affected by the size and shape of the ships—the height and position of observation platform on board—, and personal difference in visual observation. In this regard, care should be taken in further extension of this kind of observation by multi-ship system.

It is pointed out that further data accumulations provide more rigid statistical information which could be useful in describing the behavior of floating substances in marine environment in connection with a general oceanographic condition.

Acknowledgements

Thanks are due to the members of oceanography division and also officers and crew of the R/V Ryofu Maru, Marine Department, Japan Meteorological Agency for collecting the data on board throughout the present work.

The Oceanographical Magazine, Vol. 30, Nos. 1-2. (1979)

外洋における浮遊汚染物質の目視観測

鈴置哲朗・白川潔
(気象庁海洋気象部)

1976年から1978年にわたって西太平洋海域における浮遊汚染物質（主としてプラスチックス）の目視観測を凌風丸により実施した。その結果，これらの汚染物質は沿岸から外洋全域にわたって存在し，高レベル域は沿岸から黒潮反流域まで及び，20°N 以内では比較的低レベルであることが分った。この傾向は季節等に無関係に観測期間中再現された。

以上の結果から，この種の汚染物質は海洋環境における浮遊性汚染物質の挙動を知るための有力な指標になり得ると考えられる。

しかしながら，この種の調査を多船によって行う場合，それぞれの観測資料の質に関する多様性が予想されるので，全地球的な統計資料を得るには充分注意を払う必要がある。

The Oceanographical Magazine
Vol. 30, Nos. 1-2, pp. 61 to 74, March 1979

Fluorescing materials in marine environment and petroleum pollution

I. Analytical method and preliminary report of the result

Koji SHIGEHARA, Kan KIMURA, Jun-ichi OHOYAMA, and Naoshi KUBO
Japan Meteorological Agency

(Received January 8, 1979; revised January 16, 1979; accepted January 16, 1979)

Abstract: Concentration of fluorescing materials in surface seawater of the western Pacific and nearby waters was determined by fluorescence spectrophotometry using a carbon tetrachloride extraction, for monitoring of marine pollution by petroleum.

The sampling and analytical methods were specially designed and modified so as to reduce contamination. The accuracy of the method is obtained to be within ±2% or 3 ng chrysene equivalents per kg of seawater sampled (ng chr./kg). A result of testing the method reveals that the fluorescence spectrophotometry must be carefully applied for getting the intercomparable data in each laboratory.

Seasonal or regional variation in the concentration is not clear except the Eastern China Sea. Minimum concentration in each region except the Eastern China Sea is almost the same, that is, 50 ng chr./kg. This value might indicate a background level of fluorescing materials in these regions.

The data obtained by the present method are useful in monitoring some portions of probably non-biogenic polynuclear aromatic hydrocarbons which are one of the toxic materials in the marine environment.

1. Introduction

Recently it is noted that marine pollution by petroleum is probably spreading over the open ocean from coastal region. Many studies on early behavior of released petroleum and chemical dispersant for oil spills and their effects in marine environment have been reported (comprehensive reports have been given by HOULT (1969), NELSON-SMITH (1972), BARKER (1976), and TSUDA (1976)). These studies have been, however, focused on the higher level of petroleum pollution owing to accident such as wreck of a tanker. On this account, our knowledge with respect to concentrations, distribution, fate, and ecological effects of petroleum hydrocarbons in the open ocean is still quite poor. Therefore, it is really important to grasp exactly the present background level of the pollution in the open ocean. From this point of view, "IGOSS* Marine Pollution (Petroleum) Monitoring Pilot Project" (MaPPMoPP) has been

* Integrated Global Ocean Station System, IOC/WMO.

carried out since 1975, for the purpose of global survey on the present level of petroleum concentrations in sea surface. The Pilot Project include the following items: the observation of visual oil slicks and other floating pollutants, and measurement of the concentrations of the petroleum residues (floating tar balls) and the dissolved and/or dispersed petroleum hydrocarbons.

It is well known that hydrocarbons in marine environment àre consist of petroleum and recent biogenic hydrocarbons, such as paraffins, olefins cycloparaffins, aromatic and polynuclear aromatic hydrocarbons, etc. Usually, it is required to use a refined technique such as a gas chromatography, a mass spectrometry, or a combined gas chromatography—mass spectrometry in order to distinguish petroleum from recent biogenic hydrocarbons. However, the polynuclear aromatic hydrocarbons, not being produced in recent marine environment, can be simply determined by fluorescence spectrophotometric method without distinguishing petroleum from recent biogenic hydrocarbons. Therefore, the Pilot Project has recommended the fluorescence spectrophotometry using a carbon tetrachloride extraction for determination of dissolved and/or dispersed petroleum hydrocarbons (LEVY, 1971) provided that polynuclear aromatic hydrocarbons are representative of total fossil hydrocarbons in terms of concentration.

Our principal concerns in present study are to test the methodology used in the Pilot Project, and to establish a technique appropriate for the determination of the petroleum hydrocarbons concentration in the open ocean.

2. Experimentals

2.1 Reference materials and reagents

Reference materials used for testing the method were chrysene (benzo [*a*] phenanthrene) and API (American Petroleum Institute) reference oils, which were Kuwait crude oil, South Louisiana crude oil, Bunker C oil, and No. 2 fuel oil. Chrysene used was purified by recrystallization from its benzene solution. Though carbon tetrachloride used for extraction was fluorophotometrically pure, those other than "Dotite Luminasol®" were purified by redistillation. Chromatography grade *n*-hexane of Wako Pure Chemical Industries was used without purification since the solvent had no fluorescence within the range of wave-length used in our fluorescence spectrophotometry.

2.2 Sampling and analytical procedures

Sampling volume of seawater was 1 *l* instead of 3 *l* by the MaPPMoPP Manuals (UNESCO, 1974, 1976). Twenty milliliters of carbon tetrachloride were placed in a

clean bottle having a volume of 1.25 *l*. The bottle was sealed with a screw cap having a Teflon linear. These preparations were carried out in the laboratory on land. Before a sample was taken, the bottle was placed in a weighted Pylen® net and the cap was removed. While the ship was still moving slowly forward, the assembly was thrown overboard into the sea from the bow as far away as possible. The bottle was filled with seawater at 1 m depth or shallower. Upon retrival, some excess water was spilled, and sample volume was adjusted to 0.8–1 *l*. After sealing the bottle, the bottle was shaken several times by hands and was stored. Accurate volume of seawater sampled was measured after carbon tetrachloride extraction on land laboratory.

Though our procedure was essentially the same as that given by the MaPPMoPP Manuals (UNESCO, 1974, 1976), some modifications in practical use were made so as to reduce contamination. A scheme of the modified analytical procedure was shown in Fig. 1. The bottle containing seawater and carbon tetrachloride was shaken for ten minutes by shaking apparatus. The carbon tetrachloride was transferred by a

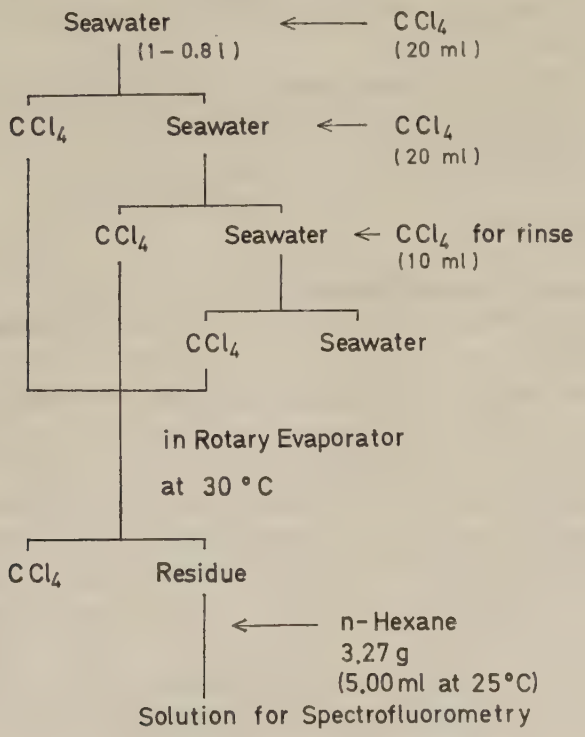

Fig. 1 A scheme for extraction.

pipette to a 100 ml flask having transparently ground joint of standard taper. This extraction procedure was repeated again. The flask containing 50 ml of the carbon tetrachloride solution was attached to a rotary evaporator in a clean hood, and the solvent was gently evaporated under reduced pressure at 30°C. Residual vapor in the flask was completely removed by keeping the flask up-side down in the clean hood. A known amount of *n*-hexane (usually 5.00 ml) was poured into the flask, which was sealed with a glass stopper. Then, the flask was shaken slowly to solve the extract sticking on inside wall.

n-Hexane solutions of reference materials such as chrysene and API oils were prepared in each reagent bottles by gravimetric method using micro or ultramicro balance throughout all the procedures of preparation, for the purpose of preventing contamination. The solution were stored in dark under refrigeration.

Fluorescence spectrophotometry was carried out by using a Hitachi Model 512 fluorescence spectrophotometer with 1 cm quartz cells. Measurement conditions of the spectrofluorometry were as follows: 310 nm of wave-length and 20 nm of slit-width for excitation, and 362 nm of wave-length and 10 nm of slit-width for emission. The sensitivity of the fluorescence spectrophotometer was 0.2 μg/kg for *n*-hexane solution of chrysene.

Fluorescence intensity by contaminants in reagents used and/or contamination throughout all the procedure (from washing of the sampling bottle to the fluorometry) was measured as a blank.

3. Results and discussion

3.1 Standard material and calibration

Table 1 shows that fluorescence intensities of solutions of the reference materials

Table 1. Fluorescence intensities (arbitrary unit) of solution of the reference materials.

Slit-width	10 nm		20 nm	
Concentration	0.5 mg/kg	3 mg/kg	0.5 mg/kg	3 mg/kg
Chrysene	7.52	40.8	21.9	126
API Kuwait Crude Oil	0.96	6.00	4.02	25.1
API South Louisiana Crude Oil	1.67	10.7	7.03	45.7
API Bunker C Oil	5.04	31.5	21.3	132
API No.2 Fuel Oil	0.24	1.43	1.33	7.06

Excitation wave-length: 310 nm (slit-width: 20 nm)
Emission wave-length: 360 nm

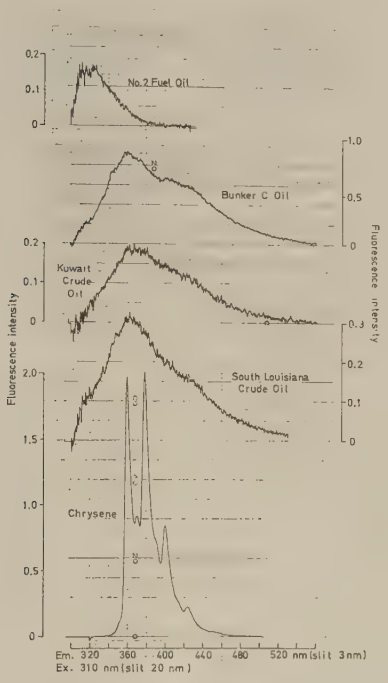

Fig. 2 Emission spectra of the reference materials.
Excitation wave-length: 310 nm (slit-width: 20 nm)
Emission slit-width: 3 nm

are quite different each other in spite of the same concentration. These are caused by differences in concentrations of fluorescing materials among the reference materials involved, because the concentrations which are measured by fluorescence spectrophotometry are not concentrations of total petroleum hydrocarbons but those of fluorescing materials, which are mainly composed of polynuclear aromatic hydrocarbons. Figure 2 shows that emission spectra of *n*-hexane solutions of the reference materials are also different each other. The fluorescing materials among the reference materials involved are different in composition as well as in total concentration.

Thus, the concentration and the composition of polynuclear aromatic hydrocarbons in various crude and fuel oils show very wide variability. Besides, the petroleum in the marine environment consist of various type and grade of oils, and its composition is probably altered by evaporation or degradation after its input into the marine environment. As oils measured in present seawater are no longer crude oil, the expression in terms of crude oil or fuel oil equivalent give no rational meanings, but make a serious trouble in intercomparison. Thus, chrysene is chosen as the

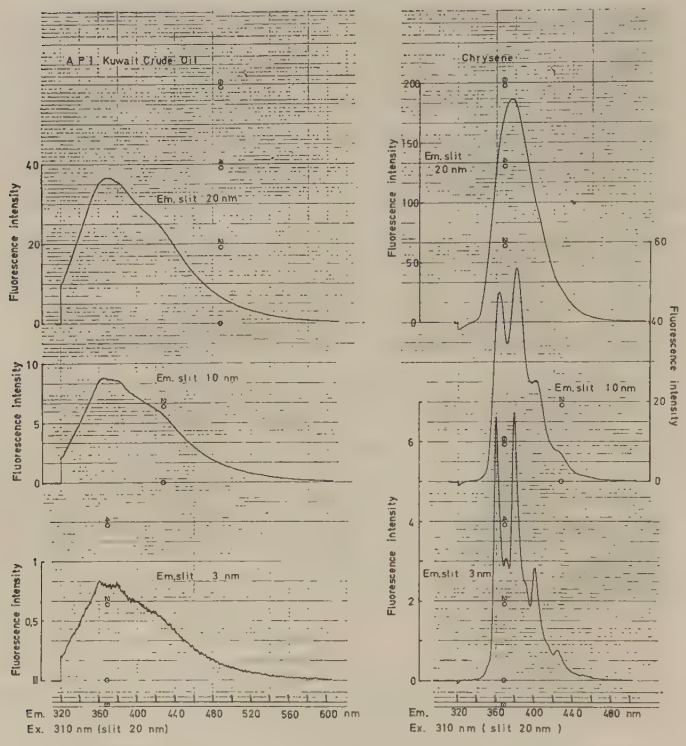
A P I Kuwait Crude Oil
Em. slit 20 nm
Em. slit 10 nm
Em. slit 3 nm
Fluorescence intensity
Em. 320 360 400 440 480 520 560 600 nm
Ex. 310 nm (slit 20 nm)
Chrysene
Em. slit 20 nm
Em. slit 10 nm
Em. slit 3 nm
Fluorescence intensity
Em. 320 360 400 440 480 nm
Ex. 310 nm (slit 20 nm)

Fig. 3 Emission spectra of chrysene and API Kuwait crude oil on the various emission slit-widths.
Excitation wave-length: 310 nm (slit-width: 20 nm)

standard material, because it is one of the most typical polynuclear aromatic hydrocarbons included in petroleum and enable to obtain as a chemically pure crystal in everywhere.

Excitation and emission spectra of reference materials have been measured by using three sort of slit-width (3, 10, and 20 nm). From these spectra, it is clarified that the emission spectrum is not affected by the excitation slit-width, and that the optimum wave-length and slit-width for excitation are 310 nm and 20 nm respectively. On the other hand, a spectrum of emission on 20 nm slit-width is different from the others, especially in case of chrysene, as shown in Fig. 3. Judging from the spectrum and sensitivity, 362 nm and 10 nm are selected as optimum wave-length and slit-width for emission respectively.

Table 2 shows that the ratio of the fluorescence intensity of the chrysene solution to that of the Kuwait crude oil solution is seriously affected by the slit-width. In

Table 2. The ratios of fluorescence intensity of chrysene solution to that of crude oil solution on the various emission slit-widths.

Slit-width	3 nm	10 nm	20 nm
Chrysene	21.1	150	434
API Kuwait Crude Oil	2.71	29.0	121
Chrysene / Kuwait Crude Oil	7.8	5.2	3.6

Concentration: 10 mg/*l* (15.27 mg/kg)
Excitation wave-length: 310 nm (slit-width: 20 nm)
Emission wave-length: 360 nm

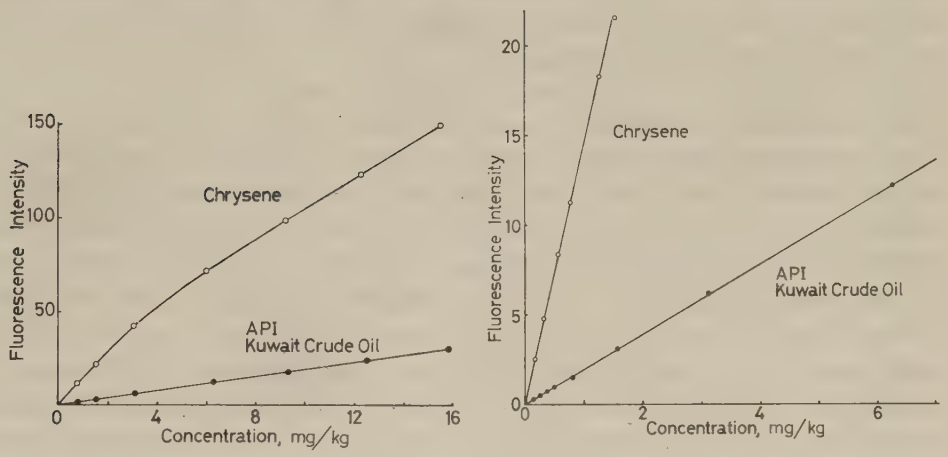

Fig. 4 Calibration curves of n-hexane solutions of chrysene (○) and API Kuwait crude oil (●).
Excitation wave-length: 310 nm (slit-width: 20 nm)
Emission wave-length: 362 nm (slit-width: 10 nm)

order to get the values intercomparable among laboratories, slit-widths for excitation and emission should also be strictly fixed to this type of measurement, in addition to wave-lengths which are designated in the MaPPMoPP Manuals (UNESCO, 1974, 1976).

Figure 4 shows calibration curves of *n*-hexane solutions of chrysene and API Kuwait crude oil measured under the conditions described above. Fluorescence intensity of the Kuwait crude oil solution is linear against concentration in the range from zero to 16 mg/kg (Fig. 4a). On the other hand, the linear relation is only appeared in the concentration below 1 mg/kg for the chrysene solution.

In the case of the concentration less than 1 mg chrysene equivalent/kg (Fig. 4b), the ratio of the fluorescence intensity of the chrysene solution to that of the crude oil solution is a constant, 7.7_2, which can be straightforwardly used as a conversion coefficient. In the case of the concentration higher than 1 mg chrysene equivalent/kg, however, the conversion coefficient can be obtained by preparing an empirical concentration—relative intensity curve for each of chrysene—the crude oil pairs over the probable concentration range expected for the measurement.

Up to now, various kinds of reference standards in the fluorescence spectrophotometry have been used for the determination of petroleum hydrocarbons concentration. On the basis of the relations given in Fig. 4a and b, we can obtain the empirical relation between the concentration and relative fluorescence intensity. By using this relation, we can convert the values of chrysene equivalent into those of the crude oil equivalent and *vice versa*.

3.2 Evaluations of analytical procedure and error

Loss of solute in the process of solvent evaporation at 30°C has been tested by using the Kuwait crude oil and chrysene, of which recoveries are found to be 95.5% (standard deviation, σ, is 1.0%) and 100.0% ($\sigma=0.9\%$), respectively. Loss of the Kuwait crude oil found here is probably due to the loss of lighter components of the oil with higher vapor pressure. This finding suggests that there is no loss of hydrocarbons extracted from natural seawater on the solvent evaporation process. It is safely presumed that these fractions have been evaporated under the temperature condition in natural sea surface. Loss of solute in the whole processes including solvent extraction and solvent evaporation has been tested by using the Kuwait crude oil, of which recovery is found to be 89.9% ($\sigma=1.0\%$). Consequently, the recovery of reference oil mainly on the solvent extraction is estimated to be about 94% for the Kuwait crude oil. We confirm that carbon tetrachloride which has been adopted by the MaPPMoPP Manuals (UNESCO, 1974, 1976) is appropriate for the extraction, although KEIZER and GORDON (1973) have reported that carbon tetrachloride is less suitable as an extraction solvent for this analysis because of low recovery of a fuel oil on whole processes.

The blank value has been determined on every cruise. The values on the same cruise are consistent with each other and the standard deviation is not over a value of 1.2 ng chrysene equivalents per kg of seawater sampled (ng chr./kg).

The results described above lead us the conclusion that the concentration measured by our procedure is accurate within 2% of relative error and within 3 ng chr./kg of absolute error with the 95% confidence level.

In the intercomparison exercise for MaPPMoPP, it has been demonstrated that

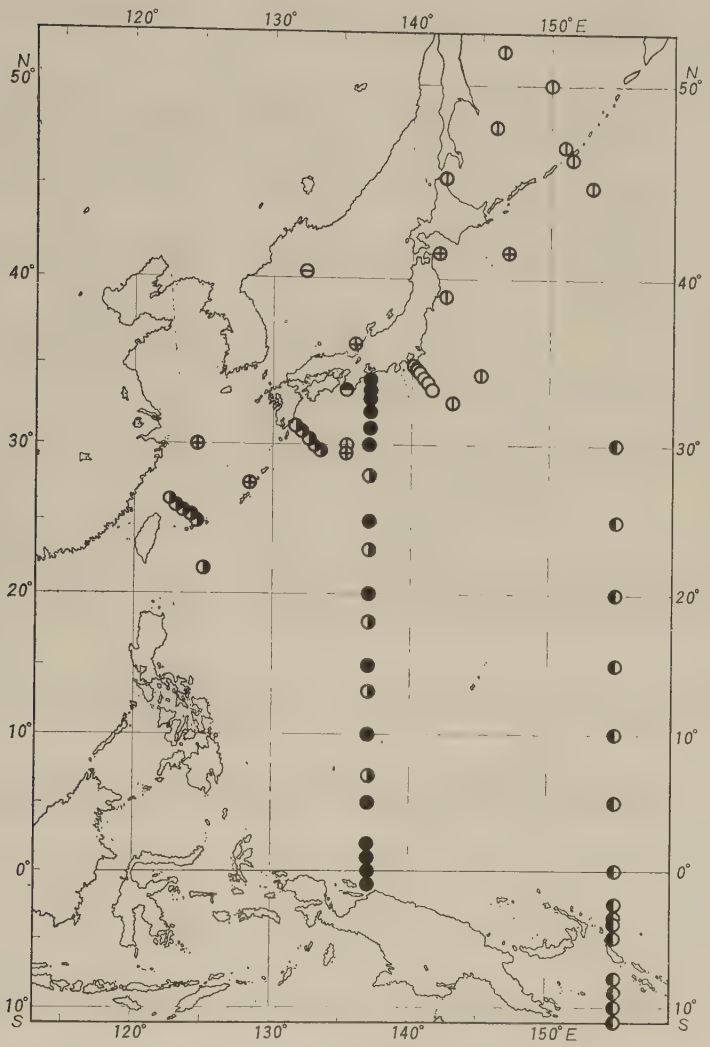

Fig. 5 Location of the sampling station.

○: All seasons (from Spring 1977 to Spring 1978);
◐: Summer 1977;
●: Summer 1977 and Winter 1978;
⊕: Autumn 1977;
◓: Autumn 1977, Winter 1978, and Spring 1978;
◑: Winter 1978;
⊕: Winter 1978 and Spring 1978;
⊖: Spring 1978.

Table 3. Concentration of the fluorescing materials in the surface seawater.

Station No.	Date Day	Mo.	Yr.	Time Hr.	Min.	Position Lat.	Long.	Temp. °C	Salinity ‰	Fluo. Mat. ng chr./kg
Ryofu Maru										
Ry 4997	8	5	1977	19	35	34°56′N	140°14′E	15.3	34.493	329
Ry 4998	8	5	1977	20	50	34 45	140 24	16.6	34.637	1.81×10^3
Ry 4999	9	5	1977	3	35	34 32	140 35	19.1	34.632	93
Ry 5000	9	5	1977	6	30	34 10	140 54	21.6	34.677	122
Ry 5001	9	5	1977	10	50	33 49	141 16	20.0	34.762	109
Ry 5002	9	5	1977	18	00	33 32	141 30	20.0	34.787	143
Ry 5003	4	6	1977	21	10	34 58	140 15	20.0	34.476	170
Ry 5004	5	6	1977	2	45	34 34	140 44	23.7	34.617	118
Ry 5005	5	6	1977	8	12	34 08	140 53	22.4	34.756	55
Ry 5006	5	6	1977	11	48	33 52	141 11	22.6	34.664	120
Ry 5007	5	6	1977	15	40	33 30	141 30	22.4	34.754	81
Ry 5008	8	6	1977	9	03	30 01	154 59	21.5	34.751	75
Ry 5013	9	6	1977	20	45	25 01	154 59	25.9	34.914	96
Ry 5018	11	6	1977	9	20	20 01	155 01	28.3	35.200	101
Ry 5023	12	6	1977	18	20	14 59	155 02	28.4	35.105	143
Ry 5028	14	6	1977	2	40	10 00	155 00	28.4	34.335	69
Ry 5038	15	6	1977	20	30	4 59	154 58	29.3	34.150	75
Ry 5048	18	6	1977	5	00	0 01	155 01	29.4	34.320	151
Ry 5053	20	6	1977	12	40	2°31′S	155°00′E	29.9	34.475	94
Ry 5055	21	6	1977	1	00	3 30	155 00	29.3	34.398	131
Ry 5056	21	6	1977	4	35	4 00	155 00	29.5	34.488	99
Ry 5058	21	6	1977	14	20	5 00	155 00	29.3	34.401	320
Ry 5059	28	6	1977	18	00	7 59	154 59	28.4	34.438	86
Ry 5060	29	6	1977	0	35	9 00	155 00	28.2	34.607	86
Ry 5061	29	6	1977	7	25	10 00	155 00	27.6	34.615	105
Ry 5062	29	6	1977	14	20	11 00	155 01	26.8	34.679	65
Ry 5063	3	7	1977	18	10	1 00	137 00	28.9	34.522	55
Ry 5065	4	7	1977	5	50	0 03	137 00	29.1	34.073	250
Ry 5067	4	7	1977	21	35	0°59′N	137°00′E	28.7	33.874	60
Ry 5069	5	7	1977	10	45	1 59	137 00	28.9	34.093	148
Ry 5075	7	7	1977	3	15	5 00	136 59	28.8	33.947	69
Ry 5083	9	7	1977	7	00	9 59	137 02	29.2	34.315	59
Ry 5089	22	7	1977	23	20	15 00	137 01	29.2	34.685	86
Ry 5094	24	7	1977	7	30	20 00	137 00	29.6	34.526	86
Ry 5099	25	7	1977	16	30	25 02	137 00	29.3	34.552	48
Ry 5104	27	7	1977	16	00	30 01	137 00	28.6	34.195	103
Ry 5105	27	7	1977	23	10	31°00′N	136°58′E	28.7	34.398	148
Ry 5106	28	7	1977	4	40	32 00	137 01	29.1	34.464	130
Ry 5107	28	7	1977	9	50	32 39	137 01	29.4	34.448	142
Ry 5108	28	7	1977	14	30	33 26	137 04	29.6	34.394	125
Ry 5109	28	7	1977	18	10	34 00	137 01	27.9	34.245	86
Ry 5110	10	10	1977	18	15	45 30	142 30	10.8	32.371	55
Ry 5128	13	10	1977	23	00	48 01	146 01	9.4	32.426	75
Ry 5141	16	10	1977	14	50	50 01	150 02	8.8	32.219	98
Ry 5148	18	10	1977	8	00	51 27	146 33	6.5	31.989	220
Ry 5153	19	10	1977	23	05	47 01	151 00	7.5	32.689	131
Ry 5154	20	10	1977	4	20	46 30	151 29	8.4	32.623	120
Ry 5156	20	10	1977	19	45	45 00	153 01	6.4	32.698	136
77-10-A	29	10	1977	14	00	38 53	142 31	——	——	83
77-10-B	30	10	1977	14	00	34 21	144 55	——	——	56
77-10-C	11	11	1977	14	05	32 41	143 01	——	——	225
Ry 5157	13	11	1977	19	10	34 59	140 13	22.3	34.428	100
Ry 5158	13	11	1977	22	00	34 46	140 26	23.9	34.495	195
Ry 5159	14	11	1977	1	06	34 32	140 37	23.9	34.449	177
Ry 5161	14	11	1977	9	29	33 52	141 09	22.6	34.484	285
Ry 5162	14	11	1977	15	05	33 32	141 26	22.3	34.472	128
Ry 5163	15	1	1978	12	28	34 00	137 00	18.9	34.669	162
Ry 5164	15	1	1978	17	06	33 20	136 57	18.8	34.683	272
Ry 5165	15	1	1978	22	08	32 40	137 00	18.1	34.599	190
Ry 5166	16	1	1978	4	15	32 01	136 59	18.7	34.643	154
Ry 5167	16	1	1978	11	00	31 00	137 00	18.4	43.611	148
Ry 5168	16	1	1978	17	20	30 02	137 05	21.0	34.724	133
Ry 5170	17	1	1978	6	10	28 01	136 59	21.2	34.630	124
Ry 5173	18	1	1978	1	00	25 01	137 01	24.7	35.132	137
Ry 5175	18	1	1978	13	10	23 00	137 00	25.6	34.939	162
Ry 5178	19	1	1978	7	30	20 01	137 00	25.9	34.829	131
Ry 5180	19	1	1978	20	10	17 58	137 05	26.7	34.805	157
Ry 5183	20	1	1978	13	40	15 00	137 00	27.9	34.796	208
Ry 5185	21	1	1978	1	40	13 00	137 00	27.4	34.644	96
Ry 5188	21	1	1978	19	15	10 00	136 59	27.8	34.255	50
Ry 5192	22	1	1978	18	10	7 00	137 00	27.9	34.540	74

Station No.	Day	Date Mo.	Yr.	Time Hr.	Min.	Position Lat.	Long.	Temp. °C	Salinity ‰	Fluo. Mat. ng chr. eq./kg
Ryofu Maru										
Ry 5196	23	1	1978	20	50	5°01′N	137°01′E	28.0	34.412	111
Ry 5202	25	1	1978	7	20	2 01	137 01	28.7	34.304	439
Ry 5204	25	1	1978	19	40	1 00	137 02	28.6	34.340	347
Ry 5206	26	1	1978	7	10	0 01	137 00	28.6	34.183	84
Ry 5208	26	1	1978	22	00	1°00′S	137°00′E	28.6	34.191	117
78-2-01	1	2	1978	15	12	21°46′N	125°01′E	——	——	68
Ry 5209	5	2	1978	18	00	25 00	124 29	22.2	34.860	305
Ry 5210	5	2	1978	21	30	25 20	124 01	23.3	34.809	1.63×10^3
Ry 5211	6	2	1978	1	40	25 40	123 30	24.0	34.849	1.07×10^3
Ry 5212	6	2	1978	5	25	26 00	123 00	24.0	34.825	472
Ry 5213	6	2	1978	9	00	26 20	122 30	20.9	34.785	336
Ry 5221	12	2	1978	20	35	31 10	131 30	17.4	34.721	59
Ry 5222	12	2	1978	23	35	30 49	131 55	21.3	34.797	138
Ry 5223	13	2	1978	9	30	30 20	132 31	21.0	34.809	102
Ry 5224	13	2	1978	15	25	29 59	132 55	20.2	34.776	113
Ry 5225	13	2	1978	20	00	29 38	133 20	20.1	34.779	75
Ry 5233	17	2	1978	7	45	33 31	141 31	18.2	34.764	140
Ry 5234	17	2	1978	12	50	33 50	141 12	17.8	34.728	191
Ry 5235	17	2	1978	19	48	34 12	140 53	17.9	34.751	70
Ry 5236	18	2	1978	1	50	34 32	140 35	18.1	34.763	110
Ry 5237	18	2	1978	6	05	34 45	140 23	18.2	34.784	99
Ry 5238	18	2	1978	9	15	34 55	140 13	17.6	34.751	77
Ry 5239	10	5	1978	7	40	33 30	141 30	20.5	34.833	44
Ry 5240	10	5	1978	9	30	33 50	141 12	19.3	34.807	80
Ry 5241	10	5	1978	14	00	34 09	140 56	21.1	34.803	49
Ry 5242	10	5	1978	20	05	34 38	140 40	21.5	34.781	360
Ry 5243	11	5	1978	0	40	34 49	140 30	19.2	34.651	228
Ry 5244	11	5	1978	6	55	34 56	140 11	17.6	34 585	108
Kofu Maru										
Ko 2716	8	2	1978	11	10	41°28′N	142°02′E	6.2	33.576	111
Ko 2721	10	2	1978	4	48	41 32	146 58	3.7	33.439	232
Ko 2741	22	4	1978	21	15	41 28	142 00	4.8	33.329	175
Ko 2746	23	4	1978	23	19	41 30	147 00	2.6	33.053	70

Station No.	Day	Date Mo.	Yr.	Time Hr.	Min.	Position Lat.	Long.	Temp. °C	Salinity ‰	Fluo. Mat. ng chr./kg
Shumpu Maru										
Sh 1204	23	9	1977	1	50	33°29′N	135°14′E	27.3	34.453	197
Sh 1211	24	9	1977	13	20	29 58	135 16	28.9	34.489	243
Sh 1248	17	2	1978	17	25	33 30	135 15	16.1	34.722	146
Sh 1256	21	2	1978	10	35	29 29	135 15	20.5	34.829	276
Sh 1273	30	4	1978	13	45	33 32	135 15	19.0	34.711	636
Sh 1281	2	5	1978	13	25	29 18	135 15	21.4	34.776	433
Chofu Maru										
Ch 0961	12	2	1978	12	07	30°00′N	124°30′E	13.5	34.212	341
Ch 0972	14	2	1978	3	06	27 30	128 15	21.4	34.807	416
Ch 1005	30	4	1978	20	01	27 30	128 14	22.8	34.752	199
Ch 1016	2	5	1978	10	55	30 00	124 31	15.7	33.033	285
Seifu Maru										
Si 2339	24	2	1978	13	30	36°09′N	135°50′E	10.9	34.201	157
Si 2358	8	5	1978	20	01	36 09	135 52	15.1	34.609	298
Si 2367	10	5	1978	15	35	40 21	132 44	9.2	34.081	298

our analytical procedure above described are precise. Our results of analysis of unknown sample for the intercomparison exercise is 97.3±2.2% against the expected value (ZSOLNAY, 1978).

3.3 Concentration of fluorescing materials in surface seawater

Sampling was carried out from May 1977 to May 1978 on board the research vessels (Ryofu Maru, Kofu Maru, Shumpu Maru, Chofu Maru, and Seifu Maru) which belong to the Japan Meteorological Agency. Location of the sampling stations is shown in Fig. 5. The concentration of fluorescing materials in surface seawater is listed in Table 3 together with the pertinent data such as water temperature and salinity.

The average and the range of the concentration in each of regions and seasons are listed in Table 4. Though extremely high values of $305-1.63\times10^3$ ng chr./kg have been obtained in winter of the Eastern China Sea, the values of fluorescing materials concentration in each regions and seasons except in winter of the Eastern China Sea are found to be range from 44 to 636 ng chr./kg.

Judging from comparatively wide fluctuation of concentration in each of regions

Table 4. The average and the range of fluorescencing materials concentrations in the surface seawater.

Season & year	Region	No. of sample	Concentration, ng chr./Kg	
			Average	Range
Summer, 1977	Pacific			
	Seas adjacent to Japan(1)	11	116	55−148
	Open ocean(2)	11	82	48−143
	Seas adjacent to New Guinea island(3)	13	127	55−320
Winter, 1978	Pacific			
	Seas adjacent to Japan(1)	21	143	59−276
	Open ocean(2)	11	120	50−208
	Seas adjacent to New Guinea island(3)	4	247	84−439
Autumn, 1977	Pacific			
	Seas adjacent to Japan(1)	12	162	56−285
Spring, 1978	Pacific			
	Seas adjscent to Japan(1)	10	218	44−636
Autumn, 1977	The Sea of Okhotsk	5	116	55−220
Autumn, 1977	The Eastern China Sea	2	60	60
Winter, 1978	The Eastern China Sea	7	652	$305-1.63\times10^3$
Spring, 1978	The Eastern China Sea	2	242	199−285

(1) The Kuroshio and north of the Kuroshio
(2) From the Kuroshio Countercurrent to Equatorial Countercurrent
(3) South of Equatorial Countercurrent

and seasons as shown in Table 4, a seasonal or regional variation of fluorescing materials concentration appears not so clearly as that of floating tar balls which has been reported by SANO *et al.* (1979), except the Eastern China Sea. Further, no correlation in concentration between the fluorescing materials and the floating tar balls is found. These findings might suggest the difference in their main sources and behavior in the marine environment.

It is to be noted that minimum concentration in each group (shown in Table 4) except the Eastern China Sea is in narrow range: 44–59 ng chr./kg, though maximum value in each group is widely fluctuated and affects largely to the average value. This might indicate that the value of 50 ng chr./kg is a background level of fluorescing materials in these regions. In this moment, it is not clear either the extremely high values found in the Eastern China Sea are seasonal or accidental.

Although the concentration of fluorescing materials in seawater have also been reported by CRETNEY and WONG (1974) (50°N, 145°W), by GORDON and KEIZER (1974) (Halifax-Bermuda), and by the Hydrographic Department (1977, 1978) (coastal region of Japan), their values can not be directly compared with ours because of difference in measurement condition, solvent for extraction, and/or standard material.

Although the material determined by the fluorescence spectrophotometry is a portion of fluorescing materials, it can not be secured that the fluorescing materials can be straightforwardly regarded as petroleum originated ones, unless more sophisticated technique such as a gas chromatography, a mass spectrometry, or a combined gas chromatography—mass spectrometry is applied. As described above, however, the data obtained by well defined fluorescence spectrophotometry is worth using only as a parameter for monitoring some portions of probably non-biogenic polynuclear aromatic hydrocarbons which are one of the toxic materials in the marine environment.

Acknowledgements

The authors are greatly obliged to Mr. Tsutomu AKIYAMA, Director of the Technical Department, the Sendai District Meteorological Observatory for his kind advice and encouragement. They also express their hearty thanks to Dr. Tetsuro SUZUOKI of the Marine Department for his earnest discussion and critical reading of this paper. Thanks are also due to the members of the Marine Department; to the members of the Oceanographical Sections of the Hakodate, the Kobe, the Nagasaki, and the Maizuru Marine Observatories; to officers and crew of the R/Vs Ryofu Maru, Kofu Maru, Shumpu Maru, Chofu Maru, and Seifu Maru for collecting the samples.

The authors are also indebted to Professors Jerry M. NEFF and Takashi ICHIYE of Texas A&M University for getting the API reference oils.

References

BARKER, J. M., ed. (1976): Marine Ecology and Pollution. Applied Science Publishers, Ripple Road, 566 pp.

CRETNEY, W. J. and C. S. WONG (1974): Fluorescence monitoring study at Ocean Weather Station "P". Marine Pollution Monitoring (Petroleum), NBS Spec. Publ. **409**, 175-177.

GORDON, D. C. Jr. and P. D. KEIZER (1974): Hydrocarbon concentrations in seawater along the Halifax-Bermuda section: Lessons learned regarding sampling and some results. *ibid.*, 113-115.

HOULT, D. P., ed. (1969): Oil on the Sea. Plenum Press, N.Y., 114 pp.

KEIZER, P. D. and D. C. GORDON, Jr. (1973): Detection of the amounts of oil in sea water by fluorescence spectroscopy. J. Fish. Res. Board Canada, **30**, 1039-1046.

LEVY, E. M. (1971): The presence of petroleum residues off east coast of Nova Scotia, in the Gulf of St. Lawrence River. Water Res., **5**, 723-733.

Hydrographic Department (1977): Report on Marine Pollution Surveys (No. 3), Results of Survey in 1975. Hydrographic Department, Maritime Safety Agency, Japan, 56 pp.

Hydrographic Department (1978): Report of Marine Pollution Surveys (No. 4), Results of Survey for 1976. Hydrographic Department, Maritime Safety Agency, Japan, 60 pp.

NELSON-SMITH, A. (1972): Oil Pollution and Marine Ecology. Paul Elek, London, 260 pp.

SANO, A., N. SATO, and N. KUBO (1979): Floating particulate petroleum residues, tar balls, in the western Pacific. Oceanogr. Mag., **30**, 47-54.

TSUDA, S., ed. (1976): Behavior of released fuel oil in seawater and its effects (in Japanese). Report of the Co-operative research, Ministry of Education, Science, and Culture, 220 pp.

UNESCO (1974): Operational plan for the Pilot Project on Marine Pollution Monitoring under the framework of IGOSS. UNESCO.

UNESCO (1976): Guide to operational procedures for the IGOSS Pilot Project on Marine Pollution (Petroleum) Monitoring. UNESCO, 50 pp.

ZSOLNAY (1978): Internal report for IGOSS Pilot Project on Marine Pollution (Petroleum) Monitoring—standardization of measurement of dissolved/dispersed constituents from petroleum pollution. IOC-WMO/MAPPMOPP—II/12.

海洋におけるけい光物質と石油汚染

Ⅰ．分析方法の検討と測定結果

重原好次・木村　完・大山準一・久保　直

(気象庁海洋気象部)

石油による海洋汚染調査の目的で，西部太平洋および隣接海の表面海水中のけい光物質濃度を，四塩化炭素抽出—分光けい光法により測定した。

試料の汚染をできる限り少なくするために，試料の採取方法および分析方法を検討し，改良した。本方法によれば，海水中のけい光物質は，±2％あるいは±3 ng クリセン当量/kg 海水(ng chr./kg)の精度で測定できる。測定方法の検討の結果，研究室間で相互比較が可能な測定値を得るためには，分光けい光法の測定条件は細部にわたって統一されなければならないことがわかった。

東シナ海を除いては，けい光物質濃度の海域あるいは季節による変動は明らかでない。東シナ海を除く各海域の最低値は，ほとんど等しい。このことから，この 50 ng chr./kg という値が，これらの海域における，けい光物質のバックグラウンドレベルであるといえよう。

測定条件を詳細に規定した分光けい光法による精度の高い測定値は，非生物起源の海洋汚染物質である多環芳香族炭化水素を監視するために有用である。

The Oceanographical Magazine
Vol. 30, Nos, 1-2, pp. 75 to 84, March 1979

NOTE

The normals of monthly mean sea surface temperature in the western North Pacific

Oceanography Division
Japan Meteorological Agency
(Received January 5, 1979; accepted January 11, 1979)

The normals of monthly mean sea surface temperature in the western North Pacific Ocean were prepared based upon the Ten-Day Marine Report from 1951 through 1975. The objective of this note is to present the newly computed normals.

Since 1946 the Japan Meteorological Agency has been routinely issued the Ten-Day Marine Report to provide current oceanic information in the western North Pacific to various users such as the fishery industries, oceanographical and meteorological scientists. Although the Ten-Day Marine Report contains the sea surface current and subsurface temperature charts, the most important and basic one is the chart of ten days mean sea surface temperature. This chart has been prepared by compiling the sea surface temperature data from oceanographic research vessels, merchant ships, fishing boats and airplanes. Recently, the sea surface temperature derived from the infrared observations from the G.M.S. "Himawari", which is a geostational meteorological satellite of Japan launched above the equator at 140°E, has also taken into consideration for the analysis.

The thermal field is contoured with the interval of one degree centigrade. Before July 1956 the analysis was taken based upon the individual temperature data during ten days and thereafter the temperature reduced to means for one degree rectangles has been treated in preparation the chart instead of the original data. The area of analysis was initially limited in the seas adjacent to Japan bounded by latitude 21°N to 47°N and latitude 118°E to 165°E. The expansion of the analysis area was intended at several times. Namely, during the period from April 1956 through June 1959 the coverage was from 7°N to 50°N in latitude and from 115°E to 180° and during the period from July 1959 through December 1969 it was ranged from 10°N to 53°N in latitude and from 115°E to 180° in longitude, respectively. Recently, the chart is covered the waters from 10°N to 53°N in latitude and 110°E to 180° in longitude.

Oceanography Division: Normals of Monthly Mean Sea Surface Temperature

The normals of monthly mean sea surface temperature presented here were calculated on the basis of the data derived from the abovementioned charts. In this investigation the statistics were carried out for the area bounded by latitude 10°N to 53°N and longitude 110°E to 180°, and for the period of 25 years from 1951 through 1975.

First, monthly mean sea surface temperature was determined as an arithmetric average of ten days mean. The individual ten days mean sea surface temperature was estimated at the center of one degree square of latitude and longitude. The estimation was made subjectively for the nearest 1°C with the exception of the nearest 0.1°C in 1975. However, the monthly mean was regarded as missing for the square in which two or more ten days means were not available. The normals of monthly mean were obtained as arithmetric average of the monthly means equally weighted of 15 or more years' duration. The average obtained from the monthly means for duration less than 15 and more than 4 years were treated merely as reference value. The normal of annual mean sea surface temperature was determined as the average of the normals from January through December. The annual range of the normals of monthly means was sought on the basis of the normals of twelve months.

The isotherm charts of each normal and the annual range are given in figures. The isotherm line based upon the reference values are indicated in dot line.

The similar sort of normals has been prepared for the period from 1951 through 1960 and the period from 1956 through 1970. The former normals were limited in the seas adjacent to Japan (Masuzawa *et al.*, 1962). Although the latter one was intended to cover the same waters to the present one, the normals were not given for the Sea of Okhotsk and the Sea of Japan (Japan Meteorological Agency, 1975). The newly prepared normals have been used as the reference to provide the anomaly chart of the monthly mean sea surface temperature on the Ten-Day Marine Report since 1979.

The preparation of the new normals presented here were carried out by Messrs Iwao Nishimori and Koichi Nagasaka in the Oceanography Division of the Marine Department and their service is appreciated.

References

Masuzawa, J., T. Tsuchida and T. Inoue (1962): The monthly mean sea-surface temperature in the Northwestern Pacific Oceanographical Magazine, **13** No. 2, 77-87.

Japan Meteorological Agency (1975): Oceanographic Atlas of the Northwestern Pacific, **1**, Monthly normal of sea surface temperature, 1956-1970. JMA, pp. 90.

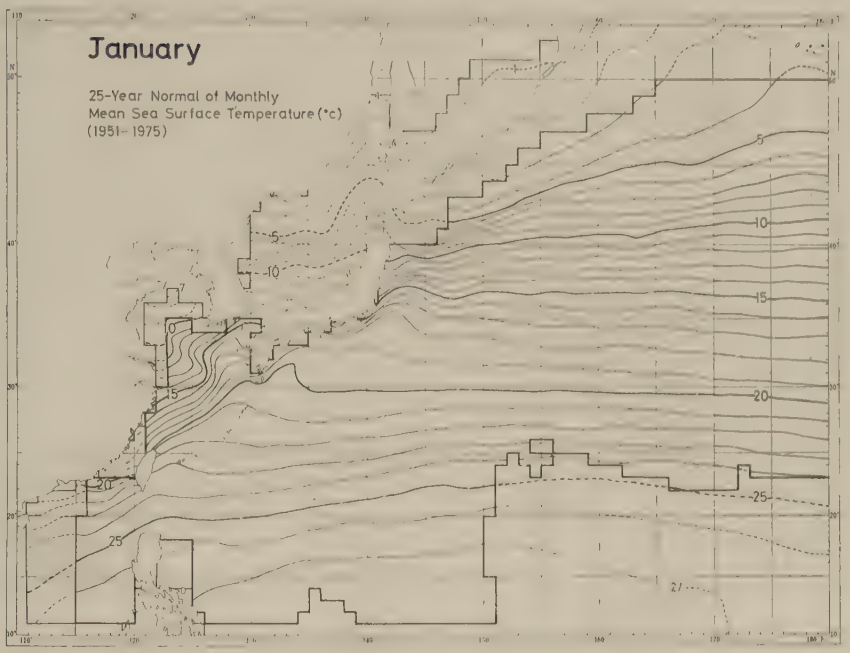
January
25-Year Normal of Monthly
Mean Sea Surface Temperature (°c)
(1951-1975)
5
10
15
20
25
27

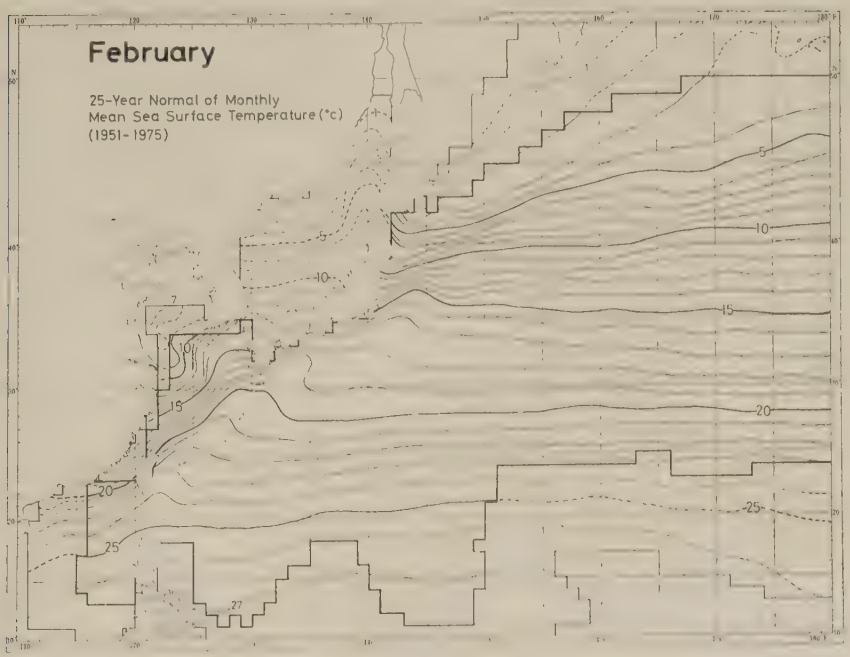
February
25-Year Normal of Monthly
Mean Sea Surface Temperature (°c)
(1951-1975)
5
10
15
20
25
27

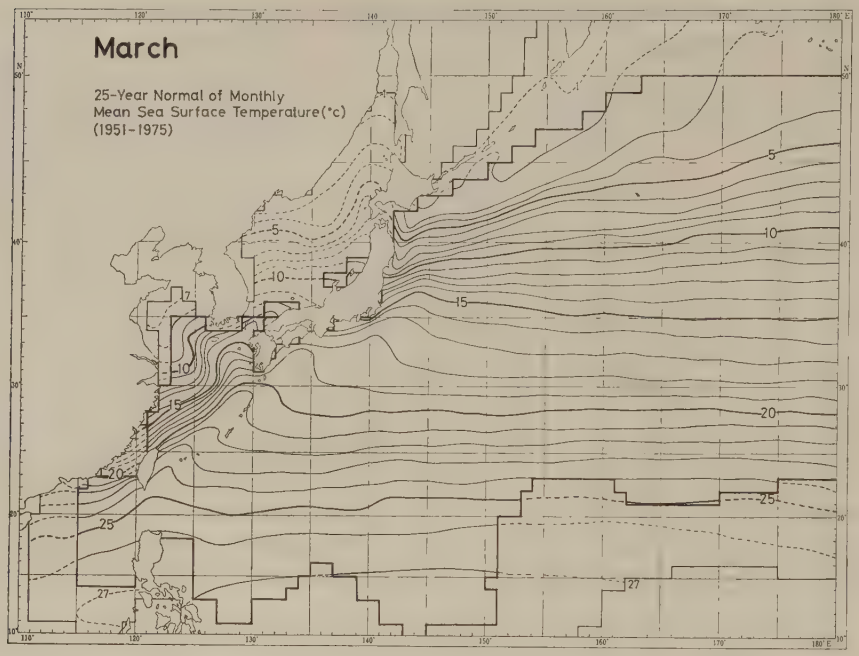
March
25-Year Normal of Monthly
Mean Sea Surface Temperature (°c)
(1951-1975)
5
10
15
20
25
27

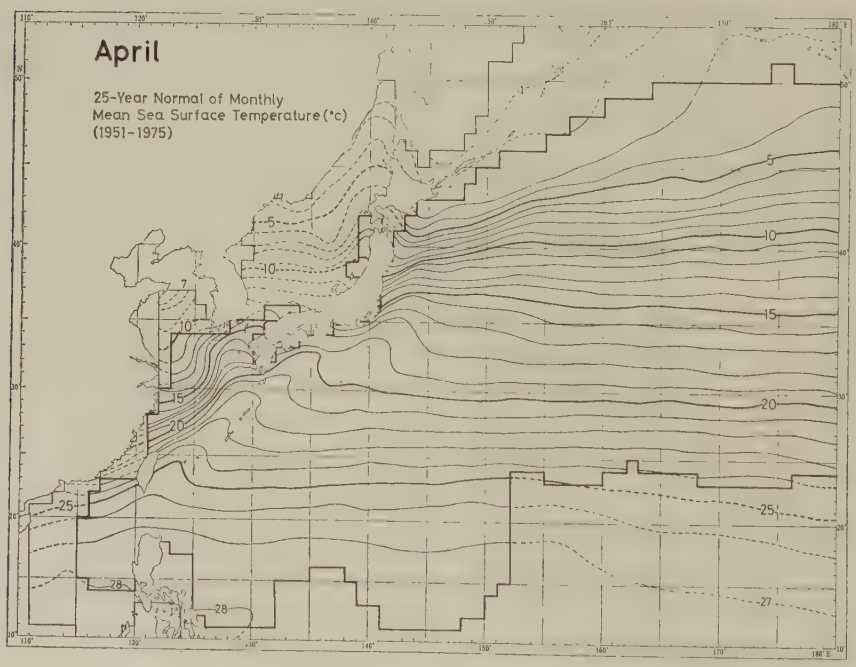
April
25-Year Normal of Monthly
Mean Sea Surface Temperature (°c)
(1951-1975)
5
10
15
20
25
27
28

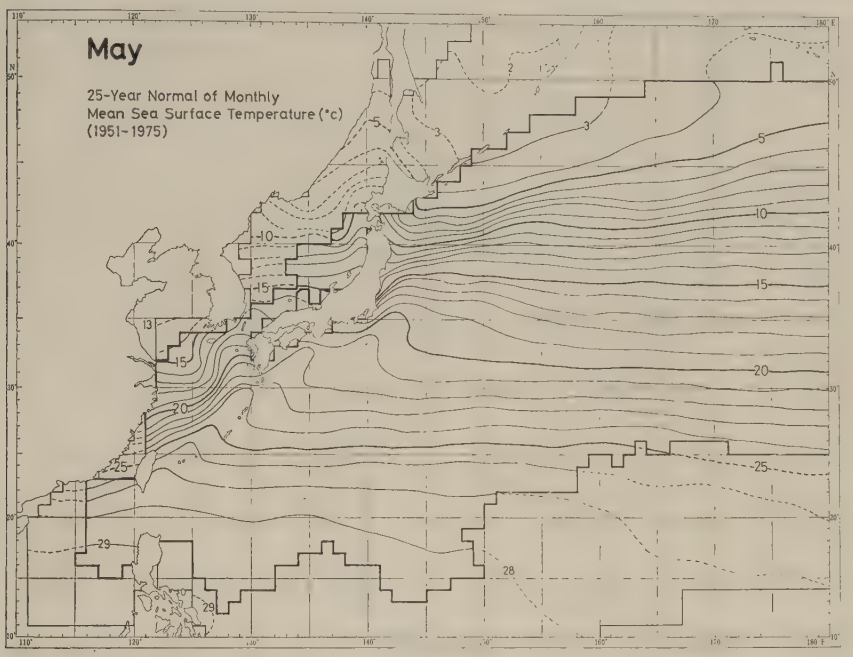
May
25-Year Normal of Monthly
Mean Sea Surface Temperature (°c)
(1951-1975)

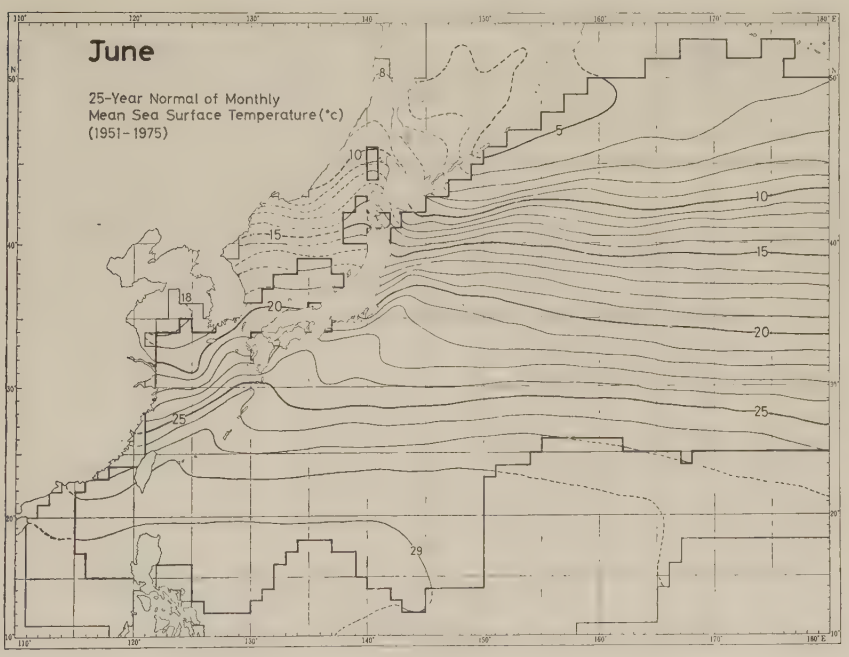
June
25-Year Normal of Monthly
Mean Sea Surface Temperature (°c)
(1951-1975)

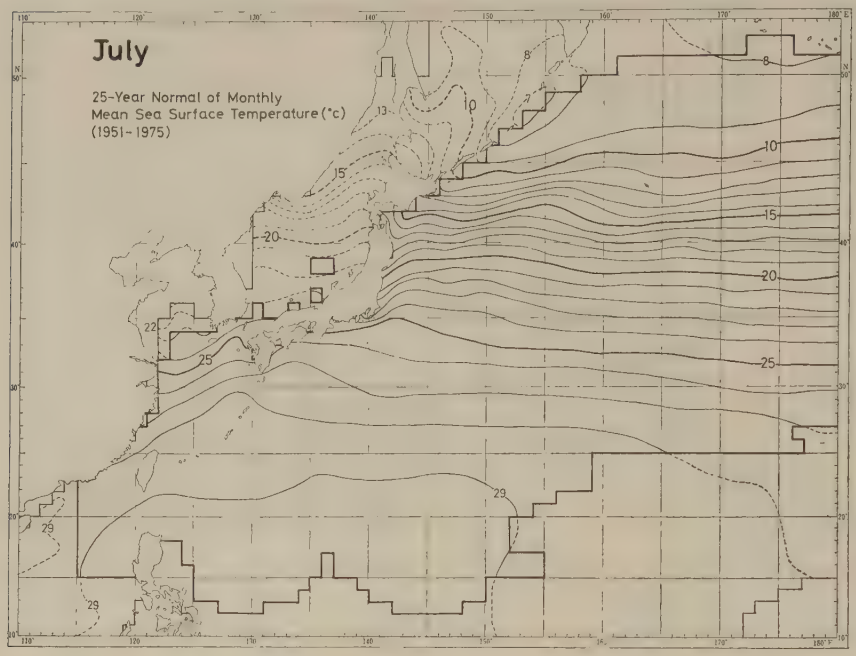
July
25-Year Normal of Monthly
Mean Sea Surface Temperature (°c)
(1951-1975)

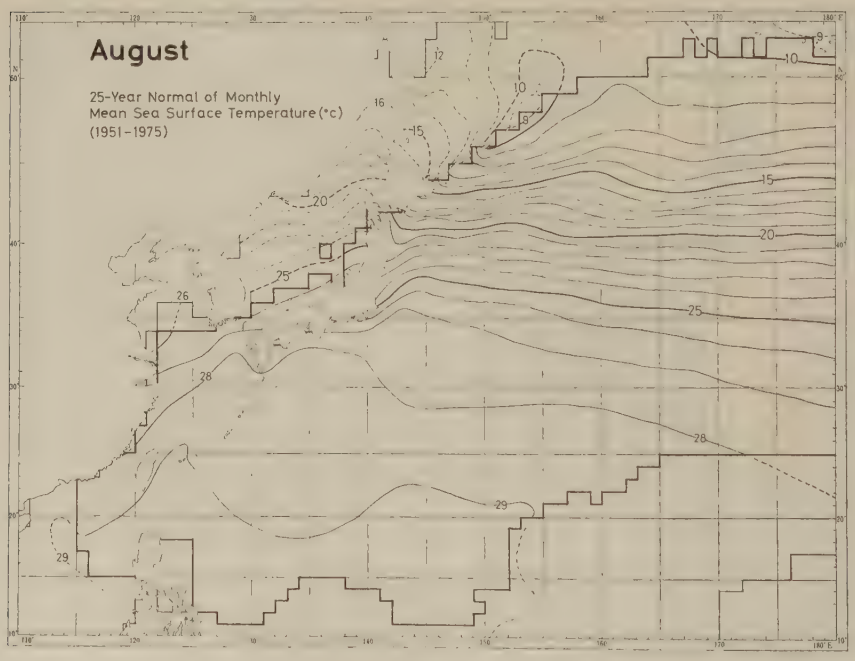
August
25-Year Normal of Monthly
Mean Sea Surface Temperature (°c)
(1951-1975)

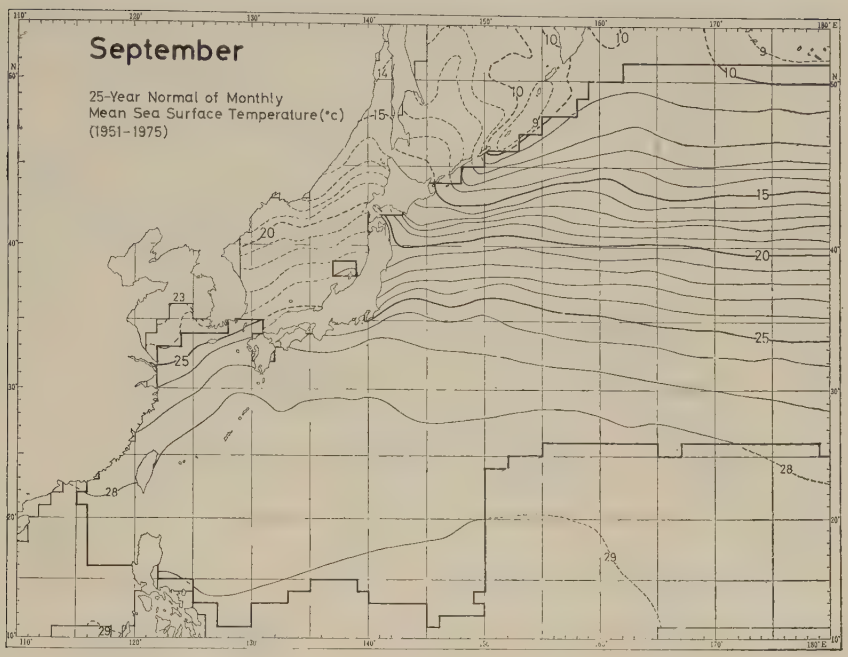
September
25-Year Normal of Monthly
Mean Sea Surface Temperature (°c)
(1951-1975)

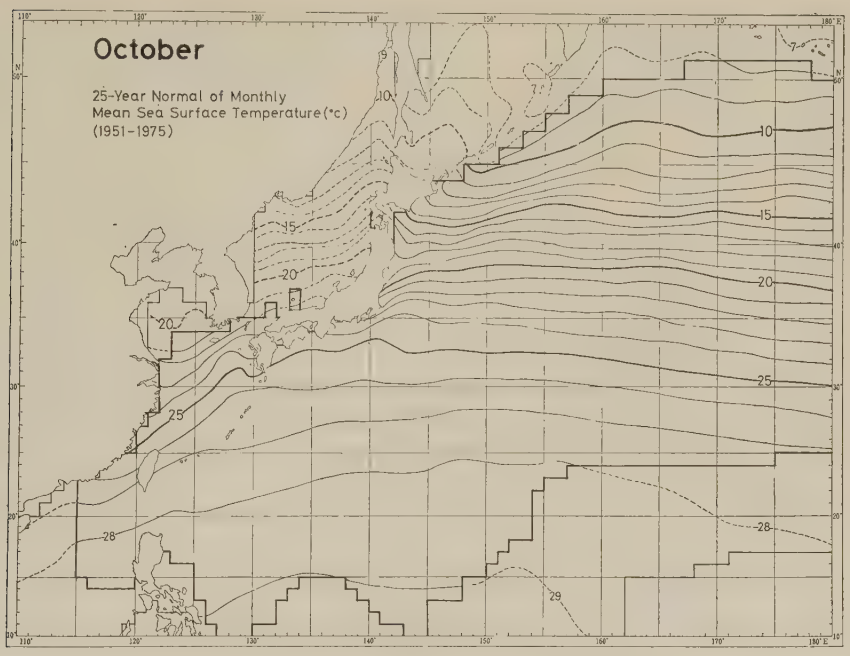
October
25-Year Normal of Monthly
Mean Sea Surface Temperature (°c)
(1951-1975)

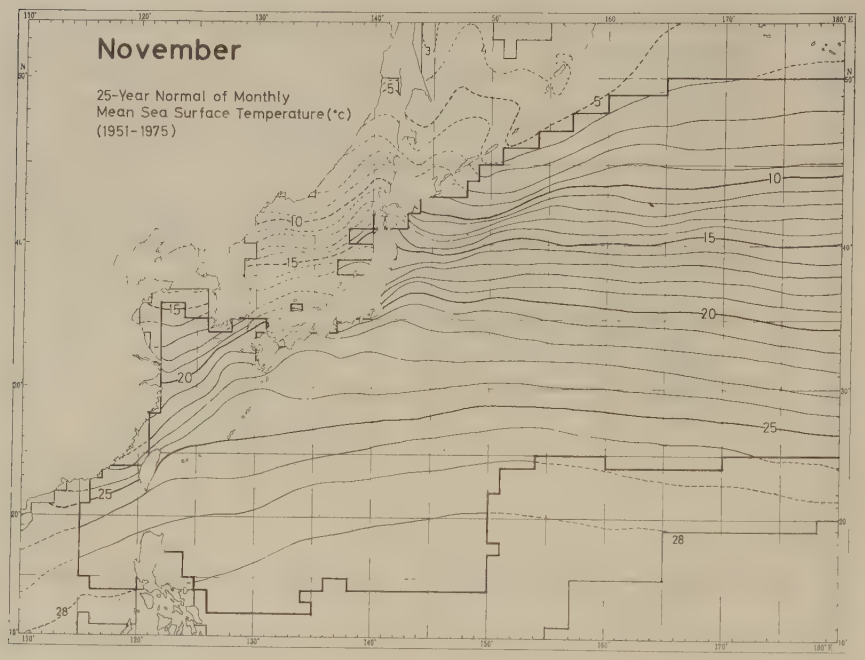
November
25-Year Normal of Monthly
Mean Sea Surface Temperature (°c)
(1951-1975)
5
10
15
20
25
28

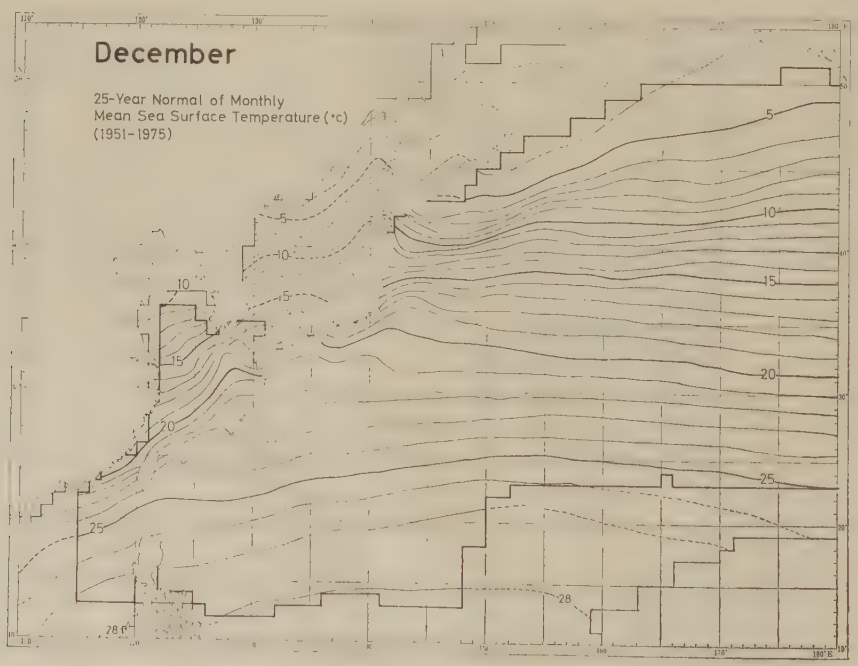
December
25-Year Normal of Monthly
Mean Sea Surface Temperature (°c)
(1951-1975)
5
10
15
20
25
28

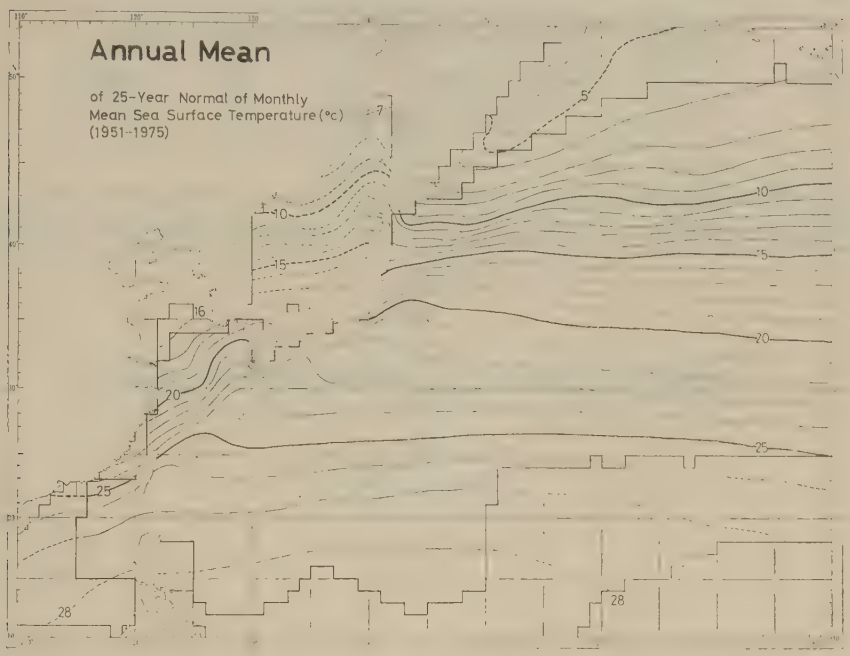
Annual Mean
of 25-Year Normal of Monthly
Mean Sea Surface Temperature (°c)
(1951-1975)

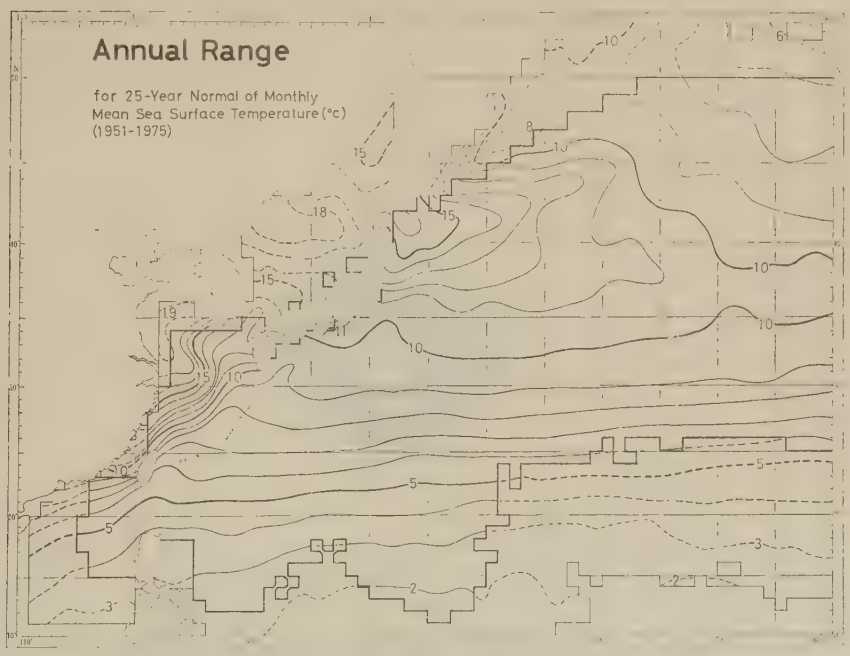
Annual Range
for 25-Year Normal of Monthly
Mean Sea Surface Temperature (°c)
(1951-1975)

Oceanography Division: Normals of Monthly Mean Sea Surface Temperature

西部北太平洋における海面水温の月別累年平均値

気象庁海洋気象部海洋課

気象庁全国海況旬報に掲載されている旬平均海面水温図をもとに，25年間（1951～1975年）の月別海面水温累年平均値を求めた。対象海域は 10°～53°N・110°E～180° で緯経度1度桝目毎に統計した。

気象庁

欧文海洋報告

第 30 巻

THE OCEANOGRAPHICAL MAGAZINE

Vol. 30

Published by the Japan Meteorological Agency

March, 1979

CONTENTS

SHUTO, K.: The flow conditions of the Kuroshio in the vicinity of Cape Shionomisaki 1

KONAGA, S., K. NISHIYAMA, A. WATANABE and H. SAITO: Short term fluctuations of current velocities near Oshima Island, Izu District, Japan 15

ISOZAKI, I.: On the seiches of Habu-harbor 31

SANO, A., N. SATOH and N. KUBO: Floating particulate petroleum residues, tar balls, in the western Pacific 47

SUZUOKI, T. and K. SHIRAKAWA: Visual observation on the floating pollutants in open ocean 55

SHIGEHARA, K., K. KIMURA, J. OHOYAMA and N. KUBO: Fluorescing materials in marine environment and petroleum pollution. I. Analytical method and preliminary report of the result 61

Note

Oceanography Division, Japan Meteorological Agency: The normals of monthly mean sea surface temperature in the western North Pacific 75

昭和54年3月31日　発行

編集兼発行者　気象庁
東京都千代田区大手町1の3の4

印刷者　青木俊夫

印刷所　昌美印刷株式会社
東京都千代田区飯田橋2の6の1